ISVER Annual Meeting 2026

הכנס השנתי ה- 46

האגודה הישראלית
לחקר העין והראיה

יום חמישי | 23.4.2026

מלון דניאל, הרצליה

ISVER
האגודה הישראלית לחקר העין והראיה
Israel Society For Vision & Eye Research
ARVO
CHAPTER AFFILIATE

PROGRAM & ABSTRACTS

46th Annual Meeting

Daniel Hotel, Herzliya

April 23th 2026

תכנית מדעית ותקצירים

הכנס השנתי ה- 46 של
האגודה הישראלית לחקר העין והראיה

מלון דניאל, הרצליה

23 באפריל 2026

יו"ר האגודה:

פרופ' מיכל קרמר

הוועדה המדעית:

ד"ר הדס בן-אלי, פרופ' דינה צור, ד"ר קלאודיה יהלום

שיפוט תקצירים:

פרופ' סאמר ח'טיב, פרופ' דינה צור, פרופ' רובי שלום-פוירשטיין,
פרופ' שירי סודרי, ד"ר הדס בן-אלי

ארגון התכנית המדעית:

פרופ' מיכל קרמר, ד"ר הדס בן-אלי

הפקת הכנס:

IN STYLE Events

ISVER Annual Meeting 2026

הכנס השנתי ה- 46

האגודה הישראלית לחקר העין והראיה

יום חמישי | 23.4.2026

מלון דניאל, הרצליה

ISVER
האגודה הישראלית לחקר העין והראיה
Israel Society For Vision & Eye Research
ARVO CHAPTER AFFILIATE

Our thanks and appreciation to the supporting companies

PLATINUM

Roche

GOLD

abbvie

astellas

BAYER

לראות
העמותה לחקר בריאות העין ומניעת עיוורון בישראל (ע"ר)

SILVER

אלפא נטו בע"מ
Alpha Net Ltd

Blueprint Genetics

G.S Optixx
ג.ש אופטיקס

IOS
האיגוד הישראלי לרפואת עיניים
ISRAEL OPHTHALMOLOGICAL SOCIETY

MEDTECHNICA
a partner for life

מדיטק
בריאות מתקדמת אלין

peripherex

REVITAL VISION

tixel

סלע
סוכנות לביטוח
מבית מיטב

יושבי ויושבות הראש של האגודה הישראלית לחקר העין והראיה
CHAIRPEOPLE OF THE ISRAEL SOCIETY FOR VISION AND EYE RESEARCH

Prof. Elaine Berman	1979-1982	פרופ' איליין ברמן ז"ל
Prof. Michael Belkin	1983-1985	פרופ' מיכאל בלקין
Prof. Saul Merin	1986-1989	פרופ' שאול מרין ז"ל
Prof. Shabtay Dikstein	1990-1993	פרופ' שבתאי דיקשטיין
Prof. Fabian Abraham	1994-1996	פרופ' פביאן אברהם ז"ל
Prof. Ido Perlman	1997-1999	פרופ' אידו פרלמן
Prof. Jacob Pe'er	2000-2003	פרופ' יעקב פאר
Prof. Ahuva Dovrat	2004-2006	פרופ' אהובה דברת ז"ל
Prof. Mordechai Rosner	2007-2009	פרופ' מרדכי רוזנר
Prof. Eyal Banin	2010-2012	פרופ' איל בנין
Prof. Avi Solomon	2012-2015	פרופ' אבי סלומון
Prof. Dror Sharon	2015-2018	פרופ' דרור שרון
Prof. Itay Chowers	2019-2021	פרופ' איתי חוברס
Prof. Shahar Frenkel	2021-2024	פרופ' שחר פרנקל
Prof. Michal Kramer	2024	פרופ' מיכל קרמר

חברי וחברות ועד האגודה הישראלית לחקר העין והראיה

BOARD MEMBERS OF THE ISRAEL SOCIETY FOR VISION AND EYE RESEARCH

Prof. Michal Kramer - Chairperson	פרופ' מיכל קרמר - יו"ר
Dr. Samer Khateb	ד"ר סאמר ח'טיב
Prof. Dinah Zur	פרופ' דינה צור
Prof. Shiri Soudry	פרופ' שירי סודרי
Ms. Sapir Shalom	גב' ספיר שלום
Dr. Hadas Ben-Eli	ד"ר הדס בן-אלי
Dr. Claudia Yahalom	ד"ר קלאודיה יהלום
Dr. Reut Ifrah	ד"ר רעות יפרח
Prof. Ruby Shalom-Feuerstein	פרופ' רובי שלום-פוירשטיין
Treasurer - Dr. Samer Khateb	גזבר - ד"ר סאמר ח'טיב
Association's auditor - Prof. Haim Levi	מבקר העמותה – פרופ' חיים לוי

מלגות לחוקרים צעירים

מענקי מלגות השתתפות ב ARVO למחברי העבודות המצטיינות 2025, ניתנו באדיבות עמותת "לראות" והאיגוד הישראלי לרפואת עיניים

לראות

העמותה לחקר בריאות העין
ומניעת עיוורון בישראל (ע"ר)

האיגוד הישראלי לרפואת עיניים
ISRAELI OPHTHALMOLOGICAL SOCIETY

AWARA WINNERS (Alphabetical Order)

Adi Kramer

Cell-Free DNA Methylation in Aqueous Humor

The Faculty of Medicine, Department of Ophthalmology, Hadassah-Hebrew University Medical Center, The Hebrew University of Jerusalem, Jerusalem, Israel

Rotem Mizrahi

Effect of Systemic Immune Status on Disease Progression in the Fam161a Knock-out Mouse Model of Retinitis Pigmentosa

Center for Retinal and Macular Degenerations, Department of Ophthalmology, Hadassah-Hebrew University Medical Center, Jerusalem, Israel

Gharam Yassen

miR-184/ATF3 Axis is Required for the Maintenance of Active Limbal Stem Cell State and Corneal Homeostasis

Department of Genetics & Developmental Biology, The Rappaport Faculty of Medicine & Research Institute, Technion Integrated Cancer Center, Technion – Israel Institute of Technology, Haifa, Israel

ARVO CHAPTER AFFILIATE

העמותה לחקר בריאות העין
ומניעת עיוורון בישראל (ע"ר)

<u>80%ממקרי העיוורון ניתנים למניעה באמצעות איתור מוקדם וטיפול מתאים</u>

עמותת "לראות", הוקמה ב-2006, במטרה למצוא מרפא למחלות עיניים הגורמות לעיוורון ולהקטין את מספר החולים. העמותה פועלת להעלאת המודעות לחשיבותן של בדיקות ראייה סדירות, למניעת התפתחות מחלות עיניים ואיתור פגמים.

<u>בעלי תפקידים בעמותת לראות</u>
נשיא העמותה: פרופ' מרדכי שני; **יו"ר העמותה:** מר אוהד להב; **מנכ"לית העמותה:** גב' נדין הולנדר.
יו"ר המועצה המדעית: פרופ' דרור שרון.
חברי הועד המנהל: פרופ' אדו פרלמן, פרופ' איתי חוברס, פרופ' אריה סולומון, פרופ' אירית בכר , פרופ' ענת לוינשטיין, פרופ' חנא גרזוזי, פרופ' יעקב פאר, פרופ' אהוד אסיה, פרופ' דרור שרון, פרופ' יאיר מורד, פרופ' חני ורבין, ד"ר רונית לוינגר, מר מרק עמוס, ד"ר ניר ארדינסט.

<u>פרויקטים נבחרים של עמותת לראות</u>

- **בדיקות עיניים בקהילה ובמקומות העבודה:**

עשרות אלפי קשישים בישראל, מקבלים את הידרדרות ראייתם, לעיתים עד לכדי עיוורון, כגזירת גורל. הם לא מודעים לכך שבמקרים רבים, ניתן להציל ולשפר משמעותית את ראייתם ואת איכות חייהם, בזכות הרפואה המשוכללת והמתקדמת של היום.
עמותת "לראות" מביאה את המרפאה לסביבתם הקרובה של הקשישים: לבתי אבות, למרכזי יום, למתנסי"ם או לביתם הפרטי, שם אנו עורכים ימי בדיקות מרוכזים, בכל הארץ. תוצאות הבדיקה מועברות בטכנולוגיה חדישה ומשוכללת לרופא/ה מומחה/ית, אשר מאבחנים את הבעיה ומצילים קשישים מעיוורון מיותר. בשנת 2025 בדקנו 1,561 נבדקים, כמחצית מהם נזקקו למעקב והמשך טיפול.

- **מניעת עיוורון בדור הבא:**

מטרת הפרויקט היא הנגשת ידע והשפעה על קהל היעד הרלוונטי (צעירים מגיל 17-35 וכן הורים לילדים בגילים אלו, מקרב משפחות אשר בקרבן אובחנה נשאות של גן RP) באופן שיביא לצמצום משמעותי של היקף הילודים, אשר נושאים גן דומיננטי הגורם לעיוורון ויקטין את הסיכוי להעברת הגן לדורות הבאים, באמצעות חומרי הדרכה קליטים ומובנים לציבור הרחב. עד כה נערך כנס בנושא והופק סרטון הסבר.

- **הנגשת מידע ויעוץ רפואי:**

עמותת לראות מחויבת להעלאת מודעות לבריאות העין ומניעת עיוורון ולהנגשת מידע רפואי מקצועי, מעודכן ומהימן. באתר העמותה וברשתות החברתיות ניתן למצוא מידע רב אודות מחלות עיניים, כולל פורומים מקצועיים, בהם אפשר לשאול כל שאלה ולקבל תשובה מפי רופא/ה מומחה. פורומים לדוגמה: מחלות עיניים אצל ילדים, ראיה ירודה, גידולי עיניים ועוד.

- **קבוצות מחקר בנושא מחלות רשתית, מחקר חדשני בתאי גזע ומועצה מדעית:**

כחלק ממאמץ לאומי לשיפור בריאות העין ומניעת עיוורון בישראל, עמותת לראות מובילה את הקמתן וניהולן של שתי קבוצות חוקרים שונות, לצורך קידום ופיתוח המחקר בארץ וכן מועצה מדעית מקיפה, הכוללת חוקרים מכל התחומים אשר מובילים מחקר חדשני בנושאים הנ"ל.

- **חודש המודעות:**

מדי שנה, בחודש דצמבר, עמותת יוצאת בקמפיין ארצי להעלאת מודעות לבעיות שונות הקשורות בראייה ועיוורון. השנה עסקנו במחלות רשתית של העין והגענו, באמצעות קמפיינים ממומנים בטלוויזיה, בפרינט ובדיגיטל, לעשרות אלפי אנשים חדשים, במטרה להעלות מודעות ולמנוע עיוורון.

<u>בקרו אותנו:</u>
פייסבוק || אינסטגרם || יוטיוב || אתר

נדין הולנדר
מנכ"לית העמותה
nadine@eyes.org.il

.....
חברי ועד מנהל: פרופ' ארי ברזילי, פרופ' דב ויינברגר, פרופ' אלי חזום, פרופ' ענת לוינשטיין, פרופ' חנא גרזוזי,
פרופ' יעקב פאר, פרופ' אהוד אסיה, פרופ' אידו פרלמן, פרופ' דרור שרון, פרופ' יאיר מורד, פרופ' אבי סלומון, ד"ר חני ורבין,
ד"ר רונית לוינגר, ד"ר יפית שטרק, גב' איריס שפיגל, מר מרק עמוס, ד"ר ניר ארדינסט, מר יאיר שפר, מר אשר גרינבאום
.....
www.eyes.org.il טלפון: 09-9518475 פקס: 153-9-9518475 רח' אוריאל אופק 10, הרצליה

Keynote Speaker

Prof. Ofer Yizhar

Neurons See the Light: New Tools for Studying and Treating the Nervous System

Thursday, April 23rd, 2026 at 13:45

Ofer Yizhar is an associate professor at the Weizmann Institute of Science in Israel. He received his PhD from the Tel Aviv University and conducted his postdoctoral research at Stanford University, where he developed new optogenetic tools for studying neural circuits. His lab develops neurotechnology for studying the brain, and uses a combination of optical, electrophysiological and behavioral techniques to understand the brain circuits involved in memory, decision making and social behavior. In the last few years, the lab has been focused on tools for silencing neurons, and specifically for optogenetic silencing of synaptic transmission. Tools created by the lab have been widely adopted by labs worldwide and used in a wide range of animal models and experimental paradigms. He was elected a full member of EMBO in 2022, and a Schaefer Research Scholar (Columbia University) in 2023.

ISVER 2026

Abstract Booklet – Table of Contents

AI

First Name	Last Name	Abstract Title
Alon	Moore Galindo	A Large Comprehensive Comparison of Large Language Models on Ophthalmology Board Exams
Nir	Avisar	AI-Based Structure–Function Analysis for a Novel Visual Field Reliability Index
Daniel	David	The Use of Artificial Intelligence Based Chat Bots in Ophthalmology Triage
Elad	Eilon	Systemic prostacyclin analogues in pulmonary hypertension are associated with reduced risk of age-related macular degene...
Hanna	Moalem	Identification and localization of myopic macular neovascularization using deep learning
Amit	Lejtman	Deep Learning-Based Localization and Classification of Retinal Anomalies on Fundus Images
Ori	Mekiten	Prediction of axial length from macular OCT images using artificial intelligence
Razan	Saadi	Evaluating ChatGPT's Accuracy in Recommending Surgical Intervention for Epiretinal Membrane: A Comparison with Expert Op...
Shai	Dushnitzky	Words Have Meaning: How Commercial LLMs are Fooled by Report Labels
Ben	Mizrahi	Drusen Subtypes as Biomarkers in Neovascular AMD: Insights from Volumetric AI-OCT Analysis
Eitan	Livny	Early Detection of Keratoconus Using Corneal Tomography Image Analysis by GPT-4o
Lena Ilanit	Trifonov	Machine learning to predict outcomes of anti-VEGF treatment for neovascular age-related macular degeneration
Ygal	Rotenstreich	Towards Non-Invasive Blood Count Using a Deep Learning Pipeline from Bulbar Conjunctiva Videos

● Anterior segment | Cataract | Cornea

First Name	Last Name	Abstract Title
Alon	Tiosano	Corneal power estimation from anterior corneal surface images using artificial intelligence
Arige	Gideon Abou Said	Automated detection of the Annular Dark Shadow for early identification of keratoconus using image-processing
Timna	Leshchinski	Phacoemulsification in patients with ocular cicatricial pemphigoid (OCP/MMP)
Efrat	Netanya	Reproducibility and Within-Subject Variability of the Dry Eye Analyzer in Young Adults With and Without Dry Eye Symptoms...
Ayala	Katzir	A Novel Method of Video Recording Ophthalmic Surgical Procedures Using the Smartphone
Zipora	Boim	Comparison of Patient-Reported Outcome Measures (PROMs) Following Cataract Surgery at Hadassah Medical Center
Reut	Ifrah	Association Between Contact Lens Type and Dry Eye Outcomes in Keratoconus
Shira	Hadad-Porat	Immune Regulation of the Limbal Stem Cell Niche by Dendritic and γδ T Cells
Yamit	Cohen-Tayar	Predicting keratoconus progression using machine learning analysis of tomographic images
Gharam	Yassen	The miR-184/ATF3 Axis Controls Active Limbal Stem Cell Identity and Corneal Epithelial Renewal

● Genetics

First Name	Last Name	Abstract Title
Efrat	Shavit Stein	TRIACK, A NOVEL IRREVESIBLE HIGH POTENCY THROMBIN PATHWAY MODULATOR IN EYE DROPS PENETRATES TO MURINE AND PIG RETINA
Eliane	Rozanes	Family Planning in Genetic Optic Atrophies in Israel, a Case Series and a Discussion of Ethical Considerations
Johanna	Valensi	Genetic Diagnosis of Inherited Retinal Diseases Improved by Whole Genome Sequencing
Manar	Salameh	A Knock-In Mouse Model for the Human TRPM1-p.Lys294* Mutation as the Cause of Congenital Stationary Night Blindness
Nina	Schneider	TRPM1 p.K294*: A Dual-Effect Mutation and Implications for Developing Targeted Therapies
Rabea	Misherki	A p63 point mutation impairs limbal stem cell and niche function that is rescued by the small moleculePRIMA-1Met (APR-2...

Rotem	Mizrahi	Probing the Molecular Mechanisms Underlying the Protective Role of Systemic Immunity in the Fam161a Knock-out Mouse Mode...
Sandeep	Sarma	A UGA stop codon suppressor tRNA therapy for gene-agnostic treatment of inherited retinal diseases
Alaa	Saleh	Compilation and analysis of the global retinal inherited disease 2 (GRID2) data set
Ayala	Katzir	Phenotypic-Genotypic Correlations in Ocular Cutaneous Albinism Type II
Tuvia	Horev	A Platform to Increase the accessibility of essential information that enables eradication of mutations causing autosoma...
Maayan	Avraham	Functional characterization of C19orf44, a novel gene associated with autosomal recessive retinal dystrophy
Melanie	Mysler	LCA in the Israeli population: clinical and molecular characteristics
Tamar	Ben-Yosef	Clinical and molecular characterization of ocular developmental disorders in the Israeli population
Sapir	Shalom	Correction of the achromatopsia-causingCNGB3-c.1663-1205G>A mutation using antisense oligonucleotides in patient-derive...
Sofia	Itskov	Pathogenic variants in YARS1 in individuals with a phenotype resembling Usher syndrome

● Glaucoma | Pediatric | Refraction

First Name	Last Name	Abstract Title
Alon	Zahavi	Cyclotorsion After Glaucoma Surgery: Quantitative Insights from Fundus Imaging
Ayellet	Segre	Genetic regulation discovery in the aqueous humor outflow pathways, macula and optic nerve head proposes causal mechanis...
Eddie	Barayev	Female Color vision deficiency is associated with increased prevalence of amblyopia, strabismus and ametropia
Itay	Shavit	Changes in Astigmatism in Children with Congenital Nasolacrimal Duct Obstruction Undergoing Probing and Irrigation
Liat	Gantz	Professionals' Perceptions of Vision Impairments of Children with Autism Spectrum Disorder
Lital	Smadar	Periocular Impetigo in Children: A Distinct Clinical Entity with Ocular Surface Involvement
Ravid	Doron	Myopia in Israeli children: Early educational exposure drives sex-specific patterns in ultra-orthodox children
Raz	Rubinshtein	Exploring the Shared Neurodegenerative Mechanisms Between Glaucoma and Alzheimer's Disease

Rivki	Bloom	Do yellow filters improve visual function in cases of simulated media opacity with and without glare
Yaara	Lisai-Goldstein	Association between topical beta-blockers use and Parkinson's disease: Evidence from a real-world multicenter cohort
Hadas	Mechoulam	Optimizing screening for type I retinopathy of prematurity using a machine learning-based risk prediction model
Diala	Abu Al-Halawa	Outcomes of cataract surgery in infants under one year compared to children aged one to five years: A propensity-score-m...
Jacob	Megreli	Glaucoma and pregnancy: Treatment patterns and medication adjustments
Mark	Krauthammer	Natural killer cells may promote corneal graft failure via direct corneal fibroblast killing in a murine model of pediat...
Lionel	Sebbag	Small-volume NanoDropper delivery maintains efficacy of tropicamide, latanoprost and brinzolamide-timolol: Insights from...

● Neuro-Ophthalmology | Oculoplastic | Oncology

First Name	Last Name	Abstract Title
Aviv	Fineberg	An Immunocompetent Young Adult with Acute Vision Loss
Tzur Shlomo	Feldestein	Nasal vs Temporal Melanopsin-Mediated Pupillary Light Reflex Reveals Retinal Circuit Alterations in Brain Lesions
Jonathan	Zontag	Chromatic Pupilloperimetry for Objective Diagnosis and Monitoring of Patients with Pseudotumor Cerebri
Maria	Gimmelshein-Vatkin	The role of CREB in uveal melanoma metabolism
Miriam	Ehrenberg	Predictive Value of Macular Ganglion Cell Thinning Artifact for Disease Severity in Pediatric Idiopathic Intracranial Hy...
May	Rian	Tumor-specific inhibition of retinoblastoma cells' ability to respond to hypoxia as a treatment for vitreal seeding in a...
Arieh S	Solomon	Mild carotid stenosis creates gradual, progresive,lifelong brain and eye damage:An experimental laboratoty rat model
Eilon	Shcolnik	Vascular-targeted photodynamic therapy eradicates conjunctival melanoma tumors
Tiran	Golani	Presumed Thyroid Eye Disease Without Systemic Thyroid Dysfunction or Detectable Autoantibodies: A Clinical Cohort Study
Maya	Eiger-Moscovich	Vitreoretinal lymphoma diagnosis by vitreous DNA methylation patterns

Talal	Salti	Optic nerve Crush Induce Acute Inflammation and Secondary Apoptosis
Vicktoria	Vishnevskia Dai	Epidemiology, Diagnosis, and Outcomes of Ocular (Choroidal and Orbital) Metastases: Retrospective Cohort Study from a ...

● Animal and Cell Models | Basic Science

First Name	Last Name	Abstract Title
Amanda	Qarawani	MSC-Derived Exosomes Convert Retinotoxic S100A9 Responses into Functional Enhancement in the Retina
Mohammed	Darawshe	Microbead-induced glaucoma model in mice: EndoCoat prolongs IOP elevation and increases retinal ganglion cell loss
Sami	Tuma	Glial and neuronal responses following optic nerve crush in diabetic and non-diabetic mice
Aviv	Mesika	NGLY1 Deficiency Disrupts Aqueous and Lipid Homeostasis in the Eye: Evidence from a Zebrafish Model
Basel	Obied	Assessing Coenzyme Q10 as a Neuroprotectant in Chronic Cobalt Intoxication: A TEM- Based Study
Elie	FRANK	Alström Syndrome modeling based on human pluripotent stem cells as a tool to understand the visual symptoms of the disea...
Lea	Zelianodjevo Engel	Assessment of Visual Functions and Pupil Light Reflex in Fragile X Carriers
Nairouz	Farah	Towards High-Acuity Vision Restoration: Hybrid Retinal Prosthesis Composed of a High-Density Multielectrode Array Integr...

● Retina | Retinal Degeneration | Uveitis

First Name	Last Name	Abstract Title
Itay	Nitzan	High-density lipoprotein cholesterol levels and risk of age-related macular degeneration
Nir	Zontag	Chronic Proton Pump Inhibitor Use Is Associated with Increased Risk of Diabetic Retinopathy: A Real-World Cohort Study
Or	Gil	Retinal Ischemic Events Following Cardiovascular Procedures: Temporal Patterns and Clinical Characteristics
Hadas	Pizem	Retinal Microvascular Changes After a 26-Hour On-Call Shift in Medical Residents

Raz	Tshuva Bitton	Retinal hemorrhage in AMD patients - Systemic comorbidities or antithrombotic therapy?
Shmuel	Kagasov	TARGETING TOLL-LIKE RECEPTOR 4 IN A MOUSE MODEL OF ADVANCED AMD
Lily	Masalha	Epidemiological Characterization of Intermediate uveitis: A Systematic review and Meta analysis
Avital	Eisenberg-Lerner	Mitochondria transplantation protects RGCs from diabetic retinopathy
Diana	Merezhko	Optimizing hiPSCs Sources for Retinal Organoids and Retinal Implant Integration
Maha	Othman Afifi	Early detection of retinal Beta-Amyloid accumulation in 5XFAD Alzheimer mice using Immunohistochemistry and Advanced Ima...
Michal	Kaminer Abargel	Sex-based differences in subretinal and intraretinal fluid Absorption dynamics in age-related macular degeneration: a lo...
Muhammad	Kridin	The risk of retinal vein occlusion among patients with neovascular age related macular degeneration: a large-scale cohor...
Shlomit	Jaskoll	From Risk to Progression: Genetic Insights into Atrophy Progression in AMD
Tzippora	Greenberg	Skin Carotenoid Levels in Israeli Patients with Age-Related Macular Degeneration

A Large Comprehensive Comparison of Large Language Models on Ophthalmology Board Exams

Alon Moore Galindo (1), Razan Saadi (1), David Schwartzman (2), Michael Kinori (3) (5),
Doron Pasternak (4), Anat Loewenstein (1) (5)

(1) Ophthalmology Division, Tel Aviv Sourasky Medical Center, Tel Aviv, Israel
(2) Computer Science Department, Saint Joseph's University, Philadelphia, Pennsylvania
(3) The Goldschleger Eye Institute, Sheba Medical Center, Tel-Aviv, Israel
(4) Clinical Research Center, Soroka Univers161617ity Medical Center, Beer-Sheva, Israel
(5) Grey Faculty of Medicine, Tel Aviv University, Tel Aviv, Israel

ABSTRACT

PURPOSE

Large Language Models (LLMs) are increasingly employed as medical search engines and clinical decision-support tools across various medical fields, including ophthalmology. Therefore, it is essential to comprehensively evaluate commonly used LLMs based on their performance characteristics and to analyze their reliability and safety in ophthalmology applications. The purpose of this study is to compare various LLMs using ophthalmology board exam datasets to resident performance.

METHODS

This study compares seven widely used LLMs: ChatGPT-5, ChatGPT-4, Gemini 2.5 Pro, Gemini 2.5 Flash, Claude 4.5 Sonnet, Grok-4 Fast Reasoning, and Perplexity Sonar Pro. Analysis was based on a dataset of 1,037 Israeli ophthalmology board questions (2020–2025), manually indexed by type (logical/informative), image modality, and 12 sub-specialties. Additionally, performance and model characteristics were assessed based on accuracy, response latency, question difficulty, and a self-appraised confidence score. Finally, AI performance was compared against residents' results.

RESULTS

Comparison Analysis of 1,037 questions revealed significant heterogeneity among models. Gemini 2.5 Pro achieved the highest accuracy (81.6%), outperforming all other LLMs and residents, followed by ChatGPT 5 with 77.15% ($p<0.001$). Model accuracy mirrored resident performance, declining systematically as difficulty increased. A significant performance gap emerged between modalities, with text-only accuracy (77.2%) outperforming image-based accuracy 57.5% ($p<0.001$). Among subspecialties, models struggled most with pediatrics and retina. confidence rate varied widely, with ChatGPT-5 showing superior calibration (AUC=0.827) compared to other LLMs.

CONCLUSIONS

LLMs' performance on ophthalmology board questions varied across models. The Gemini 2.5 Pro was observed to have the highest performance, surpassing the mean resident score. However, the majority of LLMs exhibit significant error rates and poor calibration of self-assessed confidence. To safely integrate LLMs into the clinical workflow, continuous evaluation is essential to guide ophthalmologists on LLMs' *characteristics* and clinical limitations.

Back to TOC

AI-Based Structure–Function Analysis for a Novel Visual Field Reliability Index

Nir Avisar [1], Roee Kattaby [2], Gal Cohen [1], Lior Wolf [2], Ari Leshno [1].

(1) Goldschleger Eye Institute, Sheba Medical Center, Tel Hashomer, Israel, affiliated to the Gray Faculty of Medicine, Tel Aviv University, Tel Aviv, Israel
(2) School of Computer Science, Tel Aviv University, Israel

ABSTRACT

PURPOSE

To develop a predictive model that aims to assist in estimating the reliability of abnormalities on Visual Field (HVF) tests using advanced machine learning model.

METHODS We retrospectively collected **842 24-2 SITA standard visual fields (VF) reports** with matching optical coherence tomography (OCT) disc scans obtained within 3 months of the VF. For the purpose of this study, we used the 24-2 pattern deviation grid. Each point on the grid was labeled based on the thickness percentile of the corresponding circumpapilary retinal nerve fiber layer (cpRNFL) Garway-Heath sector. Abnormal VF points (i.e., P< 5%) were considered reliable if they fell within a yellow/red cpRNFL sector (thickness percentile <5%) and non-reliable if they fell within a green sector. The dataset was split into training (80%) and test (20%) subsets using a holdout method. We compared three different approaches to identify discordant points (i.e., abnormal VF points that are not within an abnormal cpRNFL sector) based on VF data alone.

The first, compares each point to its neighbors to detect outliers (Nearest Neighbors), the second classifies zones based on the majority of their points (Region Majority Vote), and the third is a simple Convolutional Neural Network (CNN) that learns patterns in the data to automatically identify discordant points. Each test point receives a score between 0 and 1, representing the model's level of certainty regarding discordance.

We further assessed whether the model's predictions relate to established reliability indices. For this analysis, model outputs were thresholded at 0.5, such that locations with predicted probability >0.5 were counted as discordant. We then summed the number of discordant locations identified in each test and compared this total with the conventional false-negative (FN) percentage reported by the perimeter. After summation, we performed mathematical assessments to evaluate the distribution of the results and determine the most appropriate correlation metric for this analysis.

RESULTS The CNN-based model, utilizing advanced image analysis, achieved the highest performance in identifying cases with discordant visual field and OCT findings (F1 = 0.83, AUC = 0.99, PPV= 0.74, sensitivity=0.95) compared to Nearest Neighbors (F1 = 0.69, AUC = 0.81 PPV=0.74 , sensitivity=0.64) and Region Majority Vote (F1 = 0.67, AUC = 0.78 PPV=0.80 , sensitivity=0.57) models. A moderate positive Pearson correlation (r = 0.576) was observed, indicating that higher predicted discordance is associated with increased FN rates.

CONCLUSIONS The high AUC demonstrates the model's robust ability to detect functionally abnormal points unsupported by structural loss, highlighting its potential as a novel reliability metric. The moderate positive correlation with FN rates suggests that the model captures aspects of test unreliability reflected in conventional indices. Notably, the model identified a greater number of discordant locations than the FN metric, raising the possibility that it may be more sensitive. Further analyses will be required to determine whether the model provides a superior reliability measure compared with FN.

Back to TOC

The Use of Artificial Intelligence Based Chat Bots in Ophthalmology Triage

Daniel David, M.D.1,2,* Ofira Zloto, M.D.1,2,* Gabriel Katz, M.D.1,2, Ruth Huna-Baron, M.D.1,2, Vicktoria Vishnevskia-Dai, M.D.1,2 Sharon Armarnik, M.D.1,2, Noa Avni Zauberman, M.D.1,2, Elinor Megiddo Barnir, M.D.1,2, Reut Singer, M.D.1,2, Avner Hostovsky, M.D. 1,2 , ,Eyal Klang , M.D.2,3

(1) Faculty of Medicine, Tel Aviv University, Tel Aviv, Israel
(2) Goldschleger Eye Institute, Sheba Medical Center, Tel Hashomer, Israel
(3) Division of Data-Driven and Digital Medicine (D3M), Icahn School of Medicine at Mount Sinai, New York, NY, USA
*- Both authors contributed equally as first authors

ABSTRACT

PURPOSE

To evaluate AI-based chat bots ability to accurately answer common patient's questions in the field of ophthalmology.

Methods - An experienced ophthalmologist curated a set of 20 representative questions and responses were sought from two AI generative models: OpenAI's ChatGPT and Google's Bard (Gemini Pro). Eight expert ophthalmologists from different sub-specialties assessed each response, blinded to the source, and ranked them by three metrics – accuracy, comprehensiveness, and clarity, on a 1-5 scale.

RESULTS

For accuracy, ChatGPT scored a median of 4.0, whereas Bard scored a median of 3.0. In terms of comprehensiveness, ChatGPT achieved a median score of 4.5, compared to Bard which scored a median of 3.0. Regarding clarity, ChatGPT maintained a higher score with a median of 5.0, compared to Bard's median score of 4.0. All comparisons were statistically significant ($p<0.001$).

CONCLUSIONS

AI-based chat bots can provide relatively accurate and clear responses for addressing common ophthalmological inquiries. ChatGPT surpassed Bard in all measured metrics. While these AI models exhibit promise, further research is indicated to improve their performance and allow them to be used as a reliable medical tool.

Back to TOC

Systemic prostacyclin analogues in pulmonary hypertension are associated with reduced risk of age-related macular degeneration: a cohort study

Elad Eilon (1), Natan Lishinsky-Fischer (1), Jaime Levy (1,2)

(1) Faculty of Medicine, Hebrew University of Jerusalem, Jerusalem, Israel

(2) Department of Ophthalmology, Hadassah Medical Center, Faculty of Medicine, Hebrew University of Jerusalem, Jerusalem, Israel

ABSTRACT

PURPOSE

To assess whether systemic prostacyclin analogue (PCA) therapy in patients with pulmonary arterial hypertension (PAH) is associated with a reduced long-term risk of developing age-related macular degeneration (AMD).

METHODS

A retrospective cohort study was conducted using the TriNetX global health research network. Patients aged ≥50 with a diagnosis of PAH were included and stratified by PCA treatment. Propensity score matching (1:1) was applied to balance demographics and comorbidities. Incident diagnoses of non-neovascular AMD (non-nvAMD) and neovascular AMD (nvAMD) were compared across six follow-up intervals (3-15 years) using Kaplan-Meier analysis and Cox proportional hazards models.

RESULTS

Following matching, 9862 PCA-treated and 9862 untreated PAH patients were analysed. PCA-treated patients showed a consistently lower risk of non-nvAMD across all follow-up periods (hazard ratios [HRs] 0.30-0.37; all $p < 0.001$). A similar protective trend was observed for nvAMD, with significant associations emerging at longer follow-up (HR = 0.37-0.39 at 10-15 years; $p < 0.05$). The protective effect was robust and durable over time.

CONCLUSION

Systemic administration of prostacyclin analogues is associated with a significant and sustained reduction in AMD risk among patients with PAH. These findings suggest a potential preventive role for PCAs in AMD pathogenesis and merit further investigation in broader populations.

Back to TOC

Identification and localization of myopic macular neovascularization using deep learning

Hanna Moalem, MD, PhD [2], Einav Baharav Shlezinger, MD[1,2,3], Alon Tiosano, MD,[1,2,3], Bar Yacobi Bsc[2,4,5], Noam Fradkin Bsc[2], Irit Bahar,MHA,MD[1,2,3] ,Orly Gal-Or, MD [1,2,3]

(1) Department of Ophthalmology, Rabin Medical Center - Beilinson Hospital, Petach Tikva, Israel.
(2) Ophthalmology Artificial Intelligence Center, Rabin Medical Center (Beilinson Campus), Petah Tikva, Israel.
(3) Gray Faculty of Medicine, Tel Aviv University, Tel Aviv, Israel.
(4) Beilinson Medical Center Innovation, Artificial Intelligence Center, Rabin Medical Center, Petah Tikva, Israel.
(5) Faculty of Computer Science, Reichman University, Herzliya, Israel.

ABSTRACT

PURPOSE

Myopia is rapidly increasing worldwide, with macular neovascularization (MNV) representing a major cause of vision loss. Early diagnosis remains challenging.Our study aims to incorporate a Deep Learning (DL) model to identify and localize myopic MNV using OCT images.

METHODS

MNV images were manually tagged by bounding boxes and validated by a retina specialist. Data was split to train and validation sets in a ratio of 1:4 in a fivefold cross-validation setting. A YOLOv11 (You Only Look Once) detection model architecture was used for localizing MNV on OCT images. The performance of the trained models was evaluated using precision, recall, mAP50 (mean absolute precision at 50% Intersection over Union) and mean mAP50-95 scores to quantify performance.

RESULTS

A total of 6770 OCT images were collected from 54 patients of them 1590 images with MNV. The data set included additional myopia related pathologies to address additional factors for model robustness.

The YOLOv11 model achieved an average precision of 0.53 ± 0.14, recall of 0.59 ± 0.06, mAP50 of 0.54 ± 0.11 and mAP50-95 of 0.23 ± 0.07.

CONCLUSIONS

Myopic MNV can be identified and localized reliably using OCT images by AI model. Early detection and identification of MNV activity may facilitate timely and effective intervention with anti-VEGF treatment.

Back to TOC

Deep Learning-Based Localization and Classification of Retinal Anomalies on Fundus Images

Amit Lejtman (1,2,3), David Carmon (2,6), Alon Tiosano (1,2,3), Inbar Smila Perchik (2)
Bar Yacobi (2), Einav Baharav Shlezinger (1,2,3), Irit Bahar (1,2,3), Orly Gal-Or (1,2,3)

(1) Department of Ophthalmology, Rabin Medical Center - Beilinson Hospital, Petach Tikva
(2) Ophthalmology Artificial Intelligence Center, Rabin Medical Center (Beilinson Campus), Petach Tikva
(3) Sackler Faculty of Medicine, Tel Aviv University, Tel Aviv
(4) Beilinson Medical Center Innovation, Artificial Intelligence Center, Rabin Medical Center, Petah Tikva
(5) Faculty of Computer Science, Reichman University, Herzliya
(6) Department of Ophthalmology, Wolfson Medical Center,
Holon

ABSTRACT

PURPOSE

To develop and internally validate a robust **deep learning** model capable of both **detecting and localizing** a broad spectrum of anomalies within both central and peripheral fundus images. The goal is to construct a comprehensive diagnostic tool that transcends single-disease classification.

METHODS

A retrospective dataset of fundus images was acquired from the **Eidon fundus camera** at Rabin Medical Center. The dataset was validated, preprocessed, and annotated for the presence of various anomalies. Three distinct convolutional neural network (CNN) architectures—**ConvNeXt**, **ResNet-50**, and **ViT-Base**—were trained and benchmarked for the binary classification of anomalous versus normal images. Model performance was evaluated using standard metrics, including **Area Under the Receiver Operating Characteristic curve (AUROC)**, **Area Under the Precision-Recall curve (AUPR)**, Accuracy, Sensitivity, and Specificity. Anomaly localization was achieved through the generation of **heatmaps** and boundary **polygons**, augmenting model explainability.

RESULTS

The internal validation set comprised fundus images from **1,851 patients** (mean age: 49.2 years), with a pathology prevalence of 70%. The **ConvNeXt** architecture demonstrated superior discriminative performance, achieving a mean **AUROC of 0.935±0.020**, outperforming both ResNet-50 (0.901±0.012) and ViT-Base (0.823±0.122). ConvNeXt also attained the highest scores across all other metrics, including AUPR, Accuracy, Sensitivity, and Specificity.

CONCLUSIONS

Advanced **deep learning models**, particularly **ConvNeXt** architecture, can achieve high confidence in the automated detection and localization of diverse retinal anomalies in fundus images. Providing visual evidence via **heatmaps** enhances the **explainability** and clinical utility of AI models, establishing it as a valuable screening and diagnostic aid in pathology detection. Back to TOC

Prediction of axial length from macular OCT images using artificial intelligence

Ori Mekiten (1,2,3), Noam Fradkin (1,3), Bar Yacobi (1,3), Alon Tiosano (1,2,3), Einav Baharav (1,2,3), Irit Bahar (1,2,3), Orly Gal-Or (1,2,3)

(1) Department of Ophthalmology, Rabin Medical Center, Petah Tikva
(2) Ophthalmology Artificial Intelligence Center, Rabin Medical Center, Petah Tikva
(3) Gray Faculty of Medicine, Tel-Aviv University, Tel-Aviv

ABSTRACT

PURPOSE

To develop an artificial intelligence model capable of predicting axial length (AL) from macular OCT images, to approximate ocular dimensions traditionally measured by biometry devices.

METHODS

Models were trained on 3140 macular OCT B-scans paired with axial length measurements from Tomey OA2000 and IOLMaster-700 devices performed on 1850 patients. Data was split to train and validation sets in a ratio of 1:4 in a fivefold cross-validation setting. Each scan was preprocessed, then centrally cropped and resized to an Imagenet native size of 224×224-pixel image and normalized using ImageNet statistics. Class imbalance was addressed by down-sampling the amount of images of regular AL while up-sampling for myopic and hyperopic patients using augmentation. Pretrained computer vision model served as the backbone with its output layer replaced to a single linear output for AL regression. Performance was evaluated using MAE, MSE, and R^2 metrics. Final results were reported as mean ± SD scores from validation sets across folds. Model explainability was achieved using Grad-CAM analysis to highlight OCT regions contributing to model decisions.

RESULTS

The regression model achieved an average mean absolute error score of 0.87 ± 0.04 and a mean R^2 of 0.44 ± 0.09. Grad-CAM analyses highlighted OCT regions corresponding to clinically relevant retinal and choroidal features. Conclusions
Axial length can be estimated using AI models trained on macular OCT images.

CONCLUSIONS

This ability may help identify myopic and hyperopic patients from OCT images, assess their retinal pathology, and manage them accordingly. These findings support the concept that macular OCT features contain biometric information that may enrich future OCT-based assessment tools.

Back to TOC

Evaluating ChatGPT's Accuracy in Recommending Surgical Intervention for Epiretinal Membrane: A Comparison with Expert Ophthalmologists

Razan Saadi[1], Aya Wattad[1], Michaella Goldstein[1,2], Anat Loewenstein[1,2]

(1) Ophthalmology Division, Tel Aviv Sourasky Medical Center, Tel Aviv, Israel
(2) Grey Faculty of Medicine, Tel Aviv University, Tel Aviv, Israel

ABSTRACT

PURPOSE

To evaluate the diagnostic accuracy of ChatGPT in interpreting OCT test results of patients with epiretinal membrane (ERM) for the need for surgical intervention, and to compare its performance to that of retina specialists.

METHODS

Sixty anonymized retinal cases were independently assessed by four raters: two retinal experts and two AI models (ChatGPT-4 and ChatGPT-5). All were asked to classify the ERM in the case, detection of intraretinal fluid (IRF), subretinal fluid (SRF), lamellar holes and surgical recommendations. Agreement was evaluated using percent agreement, unweighted kappa, and linear mixed models.

RESULTS

ChatGPT-5 detected ERM in 55.2% of cases, compared with 32.8% for ChatGPT-4o. ChatGPT-4o achieved moderate concordance with experts for ERM classification (κ = 0.25) and IRF detection (κ = 0.39), while ChatGPT-5 achieved κ = 0.18 and κ = 0.36, respectively. Both models demonstrated near-perfect SRF agreement (96.7%) and high nominal agreement for lamellar holes (> 90%), although κ values were non-significant due to class imbalance. For surgical recommendation, ChatGPT-5 achieved the strongest alignment with the expert consensus (κ = 0.45, 74.5% agreement), followed by ChatGPT-4o (κ = 0.37, 70.6% agreement). Inter-model agreement was excellent (κ = 0.74).

CONCLUSIONS

Both ChatGPT-4o and ChatGPT-5 demonstrated moderate concordance with retina specialists in ERM evaluation and surgical decision-making, with ChatGPT-5 exhibiting greater consistency and clinical alignment. These findings highlight the progressive improvement of newer LLMs, which, despite their advances, should currently be regarded as complementary decision-support tools rather than replacements for clinical expertise.

Back to TOC

Words Have Meaning: How Commercial LLMs are Fooled by Report Labels

Shai Dushnitzky (1,2,3), Donald Hood (4), Ari Leshno (1,2,3)

(1) Goldschlager Eye Institute, Sheba Medical Center, Ramat Gan
(2) Gray Faculty of Medical & Health Sciences, Tel Aviv University, Tel Aviv
(3) Arrow Program for Medical Research Education, Sheba Medical Center, Ramat Gan
(4) Department of Ophthalmology, Columbia University Irving Medical Center, New York

ABSTRACT

PURPOSE

To expose the flaws and dangers of using commercial LLMs to diagnose glaucoma based on imaging data alone.

METHODS

Commercially available OCT reports (Triton, Topcon, Inc.) were selected from a large dataset to represent both healthy (N=31) and glaucoma cases of varying degree of severity (N=8). Each single-eye report included thickness and deviation maps for the RNFL and GCL as well as a derived circumpapillary RNFL scan with cpRNFL thickness plot. A glaucoma expert independently classified all OCT reports based solely on structural data, these expert assessments served as the reference standard for comparison. The reports were processed uniformly into four different presets of labels and text included in the report. Each version of the report was uploaded as an image to *ChatGPT-5*, using the same prompt that asked it to identify whether the eye in the image has glaucoma. The LLM's confidence scores in its diagnosis and corresponding explanations were documented.

RESULTS

When the original reports were used, including all the textual elements of the report, ChatGPT classified all glaucomatous eyes correctly (score >50), but assessed 25 of 31 healthy cases as glaucomatous, achieving specificity of only 19.3%. In report presets in which all text other than image labels was removed, the model improved specificity to 61.3%, while not harming any sensitivity ($p<0.01$).When we removed all text instances including the labels, we saw better specificity (70.9%) than the original reports ($p<0.01$), but this also led to a reduced sensitivity of only 75%. After the prompt was adjusted and an explanation of the report content was added, we saw a small improvement in both sensitivity (74.2%) and specificity (87.5%). Reproducibility analysis across repeated runs showed good reliability ($p < 0.001$), confirming that *ChatGPT-5* produced consistent, non-random classifications.

CONCLUSIONS

ChatGPT's diagnostic decisions were strongly influenced by textual elements embedded within the OCT reports, leading to a high false-positive rate when such "rogue" text was present. Removing these elements markedly improved specificity, whereas a complete lack of contextual labeling impaired interpretation. Although *ChatGPT*-5 demonstrated reproducible and moderately accurate performance, further review of the confounding factors that bias the models' classifications and examination of the tool's limitations are needed to use it as a reliable diagnostic tool.

Back to TOC

Drusen Subtypes as Biomarkers in Neovascular AMD: Insights from Volumetric AI-OCT Analysis

Ben Mizrahi (1,2), Yara Otor (3), Tunde Peto (4), Gidi Benyamini (5), Moshe Havilio (5), Anat Loewenstein (1,6), Marganit Shachar (1), Dinah Zur (1,6)

(1) Department of Ophthalmology, Tel Aviv Sourasky Medical Center, Tel Aviv, Israel
(2) Faculty of Medicine, Hebrew University of Jerusalem, Jerusalem, Israel
(3) Rambam Health Care Campus, Haifa, Israel
(4) Centre for Public Health, Queen's University Belfast, Belfast, UK
(5) Notal Vision, Tel Aviv, Israel
(6) Gray Faculty of Medical & Health Sciences, Tel Aviv University, Tel Aviv, Israel

ABSTRACT

PURPOSE

Distinct drusen phenotypes have been linked to differential risk in non-neovascular AMD, yet their significance in eyes already manifesting neovascular AMD (nAMD) remains unclear. In clinical practice, treatment response and macular atrophy (MA) occurrence remain largely unpredictable. We therefore aimed to investigate a large dataset with fully automated OCT analysis to test whether drusen type could serve as a biomarker of nAMD phenotype, treatment response, and co-existing MA.

METHODS

We retrospectively analyzed 450 treatment-naïve nAMD eyes treated with intravitreal anti-VEGF therapy at Tel Aviv Medical Center, Israel. Drusen were classified as soft, cuticular, or subretinal drusenoid deposits (SDD), allowing pure and mixed phenotypes. AI-based OCT analysis (NOA™, Notal) quantified intraretinal fluid (IRF), subretinal fluid (SRF), pigment epithelial detachment (PED), and total retinal fluid (TRF) volumes at baseline and after ≥3 injections. Treatment response rates were assessed in eyes with baseline TRF≥1nL and defined as complete, partial, or non-responsive (≥30%, <30% TRF reduction, respectively). Associations of drusen subtype with fluid phenotype, 6-month response, and presence of MA were tested using chi-square, ANOVA/Welch tests, and logistic regression.

RESULTS

Soft drusen were most frequent (47.6%), followed by cuticular (26.4%) and SDD (26.0%). Mixed phenotypes predominated (58.0%). Fluid distribution differed significantly by drusen subtype ($p = 0.011$). SDDs were strongly associated with higher IRF volume ($p = 0.036$) and soft drusen with greater PED volume ($p = 0.001$), while SRF and TRF volumes showed no differences across subtypes. Response did not significantly vary by drusen phenotype ($p = 0.502$). MA was present in 37.8% of eyes at baseline, with a strong association with cuticular drusen (51.3% vs. 30.4% in soft; OR = 3.73, 95% CI 1.52–3.83, $p < 0.001$. 51.3% vs. 37.6% in SDD; OR = 2.71, 95% CI 1.07-6.86, $p = 0.036$).

CONCLUSIONS

Drusen subtypes represent clinically meaningful biomarkers in nAMD, with distinct associations to fluid compartments and GA development, though not to anti-VEGF treatment response. By applying AI-enhanced OCT analysis to a large real-world cohort, this study provides the first comprehensive characterization of drusen subtypes in Namd, reinforcing their role in prognosis and underscoring the importance of drusen phenotyping in personalized disease management and clinical trial design.

Back to TOC

Early Detection of Keratoconus Using Corneal Tomography Image Analysis by GPT-4o

Eitan Livny (1,2), Daniela Kamar (1,2), Jacob Megreli (1,2), Olga Reitblat (1,2), Ruti Sella (3), Irit Bahar (1,2), Yoav Nahum (1,2), Noa Kapelushnik (1,2)

(1) Department of Ophthalmology, Rabin Medical Center, Petach Tikva, Israel
(2) Gray Faculty of Medical and Health Sciences, Tel Aviv University, Tel Aviv, Israel
(3) Department of Ophthalmology, Mayo Clinic, Rochester, MN, USA

ABSTRACT

PURPOSE

To evaluate the diagnosRc performance of GPT-4o (OpenAI), a mulRmodal large language model (LLM), in detecRng forme-fruste keratoconus (ffKC) from corneal tomography images.

METHODS

This retrospecRve study included 70 eyes examined with Scheimpflug tomography (OCULUS Pentacam) at Rabin Medical Center (2019–2025). The ffKC group comprised 30 eyes from paRents with keratoconus in the fellow eye that required corneal cross-linking, and 40 normal eyes served as controls. For each eye, one four-map composite image (anterior axial curvature, anterior and posterior elevaRon, and pachymetry) was extracted. Images were analyzed using GPT-4o through a standardized prompt instrucRng the model to classify each case as "*normal*", "*forme-fruste keratoconus*", "*keratoconus*", or "*other corneal disease*". DiagnosRc performance was evaluated using sensiRvity, specificity, predicRve values, overall accuracy, and receiver operaRng characterisRc (ROC) analysis.

RESULTS

GPT-4o correctly idenRfied 21 ffKC eyes and 17 normal eyes, yielding a sensiRvity of 70.0% and specificity of 42.5%. The posiRve predicRve value was 47.7%, and the negaRve predicRve value was 65.4%. Overall diagnosRc accuracy was 54.3%, with an area under the ROC curve (AUC) of 0.56, inducing limited discriminaRve performance.

CONCLUSIONS

GPT-4o demonstrated moderate sensiRvity but limited specificity in detecRng ffKC from corneal tomography images.

Back to TOC

Machine learning to predict outcomes of anti-VEGF treatment for neovascular age-related macular degeneration

Ilanit Trifonov (1), David Wright (2), Marganit Shahar-Gonen (1), Anat Loewenstein (1), Tunde Peto (2), Dinah Zur (1)

(1) Ophthalmology Division, Tel Aviv Medical Center, Tel Aviv, Israel.
(2) Centre for Public Health, Queen's University Belfast, Belfast, UK.

ABSTRACT

PURPOSE

The aim of this study was to develop machine learning (ML) models using optical coherence tomography (OCT) derived fluid metrics to predict long-term anti-vascular endothelial growth factor (anti-VEGF) treatment intensity and visual acuity outcomes in two large real-world datasets of patients with neovascular age-related macular degeneration (nAMD).

METHODS

This retrospective study analyzed data from 2922 eyes of 2475 patients treated in two centers in the UK and Israel (Belfast and TLVMC). Longitudinal clinical data together with baseline and 6-month OCT scans were automatically analyzed using a deep learning algorithm (NOA™, Notal Ltd.) to extract volumetric fluid measurements and retinal parameters. ML models were first fully trained and applied to the Belfast dataset to predict total anti-VEGF injections and absolute VA at years 1–3 since treatment initiation. To evaluate generalisability, the final Belfast-trained models were applied to the independent TLVMC cohort for external validation.

RESULTS

The total number of anti-VEGF injections was predicted with high accuracy in the Belfast-EMR dataset with 99.6%, 95.5%, and 97.1% of eyes predicted within two injections in years 1–3. For the VA outcomes, predictions were within ≤0.2 logMAR units (≤2 ETDRS lines) for 92.5%, 73.5% and 76.5% of eyes in years 1-3, respectively. In the TLVMC cohort, model performance was reduced with 45.0–53.8% of injection predictions and 26.3–41.1% of VA predictions meeting the accuracy thresholds.
Injection burden prediction was mainly driven by 6-month subretinal fluid volumes, while intraretinal fluid was most influential for VA outcomes.

CONCLUSIONS

ML models based on automated OCT-derived fluid metrics can accurately predict long-term treatment burden and visual acuity outcomes within the clinical environment in which they are developed. Although external performance was reduced, likely due to differences in healthcare systems and treatment policies between countries, locally trained models remain highly valuable. Early identification of high and low-burden treatment trajectories can support individualized decision-making and enhance patient counselling. Importantly, these predictive tools can help ophthalmology services, often operating under significant resource constraints, to plan capacity, streamline follow-up, and allocate limited staff and imaging resources more efficiently, addressing a growing need as demand for nAMD care continues to rise.

Back to TOC

Towards Non-Invasive Blood Count Using a Deep Learning Pipeline from Bulbar Conjunctiva Videos

Ygal Rotenstreich (1,2,3), Tamir Denis (4), Emily Prasiman (1), Marian Haiadry (1,2), Amir Zag (1,4,5,6), Ohad Benjamini (2,7), Abraham Avigdor (2,7), Keren Asraf (8), Ram Doolman (8), Lior Wolf (4), Haim Suchowski (9), Ifat Sher (1,2).

(1) Goldschleger Eye Institute, Sheba Medical Center, Tel-Hashomer, Israel (2)
(2) Gray School of Medicine, Gray Faculty of Medical and Health Sciences, Tel Aviv University, Tel Aviv, Israel
(3) School of Computer Science, Faculty of Exact Sciences, Tel Aviv University, Tel Aviv, Israel
(4) Department of Bioinformatics, School of Public Health, Faculty of Medical and Health Sciences, Tel Aviv University, Tel Aviv, Israel
(5) The Andrew and Erna Viterbi Faculty of Electrical and Computer Engineering, Technion - Israel Institute of Technology, Haifa, Israel
(6) Arrow Program for Young Researchers, Sheba Medical Center, Tel-Hashomer, Israel
(7) Division of Hematology and Bone Marrow Transplantation, Sheba Medical Center, Hashomer, Israel
(8) The Dworman Automated-Mega Laboratory, Sheba Medical Center, Tel-Hashomer, Israel
(9) School of Physics and Astronomy, Faculty of Exact Sciences, Tel Aviv University, Tel Aviv, Israel
(10) Sagol School of Neuroscience, Tel Aviv University, Tel Aviv, Israel

ABSTRACT

PURPOSE

Invasive venous blood draws remain the clinical standard for hematology, yet they are invasive, time-consuming, and costly. We aimed to develop a non-invasive blood test based on imaging of the bulbar conjunctiva capillaries.

METHODS

We developed Video-to-Vessels, a computer-vision pipeline that converts high-magnification videos of bulbar conjunctiva capillaries into low-dimensional spatiotemporal vessel representations, reducing video dimensionality by ~200-fold while preserving hemodynamic information. These representations feed VesselNet, a multi-instance regression network that encodes each vessel with a modified ConvNeXt backbone, fuses vessel-specific thickness via cross-attention, and predicts blood biomarkers from concatenated embeddings. In this study, 224 adults were enrolled in the Sheba Hemato-Oncology Department. Each subject underwent a standard blood test and imaging of the bulbar conjunctiva within four hours of venipuncture.

RESULTS

VesselNet achieved a hemoglobin-based anemia ROC-AUC of 82.8% and a Spearman's ρ of 0.47, while attaining a ρ of 0.46 for red-blood-cell (RBC) count regression. Removing local stabilization and segmentation-denoising lowers ρ by 38 % for hemoglobin and 19% for RBC, underscoring their contributions.

CONCLUSIONS

This proof-of-concept study presents, to the best of our knowledge, for the first time, the feasibility of assessing RBC count and hemoglobin concentration using bulbar conjunctival high-magnification videos and deep learning analysis. Our results mark a step toward a fully non-invasive complete blood count, coupling representation learning with ocular imaging.

Back to TOC

Corneal power estimation from anterior corneal surface images using artificial intelligence

Alon Tiosano (1,2,3), Einav Baharav-Shlezinger (1,2,3), Inbar Smila Perchik (2), Dolev Dollberg (1,3), Bar Yacobi (4,5), Orly Gal-Or (1,2,3), Irit Bahar (1,2,3), Uri Elbaz (1,2,3)

(1) Department of Ophthalmology, Rabin Medical Center, Petah Tikva, Israel
(2) Ophthalmology Artificial Intelligence Center, Rabin Medical Center, Petah Tikva, Israel
(3) Gray Faculty of Medicine, Tel Aviv University, Tel Aviv, Israel
(4) Beilinson Innovation Center, Artificial Intelligence Center, Rabin Medical Center, Petah Tikva, Israel
(5) Faculty of Computer Science, Reichman University, Herzliya, Israel

ABSTRACT

PURPOSE

This study aims to develop an automated artificial intelligence (AI) model, to predict K1 and K2 values from anterior corneal surface images, both with and without placido ring.

METHODS

Anterior corneal surface placido ring images from the TOMEY-OA2000 device were collected and preprocessed. Images were cropped to focus on the central corneal region. A masking process was applied to isolate the mire rings. A preprocessing step involved extracting the third mire ring from the original image and overlaying it onto the corresponding ringless image to enhance feature clarity. A ConvNeXt model, modified with a multi-output regression head, was trained to simultaneously estimate the K1 and K2 values. The model was trained using a 5-fold cross-validation. Model performance was assessed using mean squared error (MSE), mean absolute error (MAE), and the coefficient of determination (R^2).

RESULTS

10,126 placido ring images were obtained. The K1 values ranged from 32.4 to 53.7 diopters, while K2 values spanned from 34.4 to 58.9 diopters. The model trained without the placido ring achieved an MAE of 0.64 (±0.02), an MSE of 1.60 (±0.72), and a R^2 score of 0.64 (±0.10). In comparison, the model trained with the placido ring achieved a MAE of 0.46 (±0.01), a MSE of 0.53 (±0.07), and a R^2 score of 0.85 (±0.01).

CONCLUSIONS

The proposed AI model provides a novel approach for K1 and K2 values estimation from anterior corneal surface images without placido rings. Its predictive accuracy suggests a future clinical potential in intra-operative and in-office assessment of corneal power. Back to TOC

Automated detection of the Annular Dark Shadow for early identification of keratoconus using image-processing

Arige Gideon Abou Said (1), Joan Gispets (2) Manel Larrosa Exposito (2), Eva Jimenez Vargas (3) and Einat Shneor (1)

(1) Department of Optometry and Vision Science, Jerusalem Multidisciplinary College, Jerusalem, Israel
(2) Department of Optics and Optometry, Universitat Politècnica de Catalunya, Violinista Vellsolà, 37, E08222, Terrassa, Spain.
(3) Facultat d'Informàtica de Barcelona, Universitat Politècnic a de Catalunya, Violinista Vellsolà, 37, E08222, Terrassa, Spain.

ABSTRACT

PURPOSE

Detecting early or early-suspect keratoconus remains difficult. This study evaluated the Annular Dark Shadow (ADS) as a diagnostic tool for keratoconus using computerized image-processing techniques. We developed an automated workflow for analyzing smartphone-acquired ADS images and assessed its performance against clinical assessments in distinguishing levels of disease severity.

METHODS

This multicenter study included 69 subjects who underwent best-corrected visual-acuity, slit-lamp-biomicroscopy, retinoscopy, corneal-tomography, and smartphone-ophthalmoscope ADS imaging. Based on clinical diagnosis, 107 eyes were classified as keratoconus (N=51), keratoconus-mild/suspect (N=20) and healthy controls (N=36). The initial dataset contained 458 images. The automated pipeline identified the pupil using a YOLO-based segmentation model and detected the ADS as a keratoconus biomarker using a convolutional neural network (CNN).

RESULTS

A total of 381 images met quality criteria. The YOLO segmentation model detected and isolated the pupil with 99.4% precision. The CNN model demonstrated strong binary performance in distinguishing healthy from diseased eyes, achieving 94% accuracy per image and 92% accuracy per patient after aggregating images. In the multiclass classification setting (healthy, mild, and keratoconus (accuracy reached 78% per image and 85% per patient.

CONCLUSIONS

Automated ADS image analysis appears to be a promising method for detecting keratoconus and estimating its severity. Integrating this approach into screening programs may enable earlier diagnosis, reduce reliance on examiner experience, and support cost-effective, large-scale screening using smartphone-based imaging and AI-driven analysis.
Back to TOC

Phacoemulsification in patients with ocular cicatricial pemphigoid (OCP/MMP)

Timna Leshchinski (1), Yoav Nahum (1), Eitan Livny (1), Irit Bahar (1)

(1) Department of Ophthalmology, Rabin Medical Center, Petach Tikva

ABSTRACT

PURPOSE

To assess the outcomes of Phacoemulsification in patients with Ocular Cicatricial Pemphigoid (OCP/MMP). Design: Retrospective case series.

METHODS

SETTING: Multicenter retrospective case series. PATIENTS\INTERVENTION: Phacoemulsification in patients with Ocular Cicatricial Pemphigoid between 2013-2025 in Rabin Medical Center. Main outcome measures: Pre/postoperative corrected distance visual acuity (CDVA), preoperative and postoperative complications.

RESULTS

The study included 12 phacoemulsification procedures performed in 12 eyes of 3 males and 4 females aged 52-78 years. All patients were in remission prior to surgery following immunosuppression with azathioprine (1 patient) cyclophosphamide (2 patients) Rituximab (3 patients) or IVIG (1 patient). All patients received 20mg-40mg prednisone 2 weeks following the surgery. Of all eyes none developed flare-up of OCP. One eye developed severe candida keratitis, and two eyes of one patient developed persistent Cystoid macular edema. No other serious complications were noted. The CDVA postoperatively improved in most eyes (8), 2 patients achieved 6/6, 2 achieved 6/7.5, 3 reached between 6/10 to 6/15, 4 had 6/60 or worse and 1 had visual acuity of HM.

CONCLUSIONS

Phacoemulsification can be done safely in quiet eyes with ocular cicatricial pemphigoid.

Back to TOC

Reproducibility and Within-Subject Variability of the Dry Eye Analyzer in Young Adults With and Without Dry Eye Symptoms: Preliminary Results

Efrat Netanya (1), Liat Gantz (1), Reut Ifrah (1)

(1) Department of Optometry and Vision Science, Jerusalem Multidisciplinary College, Jerusalem, Israel

ABSTRACT

PURPOSE

Reliable assessment is essential for diagnosing and managing dry eye disease and meibomian gland dysfunction. The Dry Eye Analyzer (DEA, Moptim) is a multifunctional device that integrates key ocular surface tests, including the Dry Eye Questionnaire (DEQ-5), non-invasive TBUT, tear meniscus height (TMH), bulbar and limbal redness grading, and meibography. This prospective study examined its reliability by evaluating inter-examiner reproducibility (IER) and within-subject variability (WSV).

METHODS

Symptomic vs. asymptomatic subgroups were determined based on DEQ-5 scores (≥6 being considered symptomatic), and outcomes were compared using Mann–Whitney and Fisher Exact tests. Outcomes were measured three consecutive times by two examiners (E1, E2) that were masked to each other's results, in a counter-balanced design. IER and WSV were calculated using 95% confidence intervals (CIs), within-subject standard deviations (Sw) and intra-class correlation coefficients (ICC).

RESULTS

The non-invasive TBUT (E1: 6.7±3.2 sec, E2: 8.9±3.6 sec, p=0.09, ICC=0.73, 95%CI:0.25-0.90), TMH (E1: 0.2±0.0 mm, E2: 0.2±0.1 sec, p=0.80, ICC=0.62, 95%CI:-0.05-0.86), bulbar (E1:Grade 1: 19%, Grade 2: 81%, Grade 3: 0%; E2: Grade 1: 19%, Grade 2: 56%, Grade 3: 25%; χ^2=4.73, p=0.09, ICC=0.64, 95%CI:-0.04-0.87) and limbal redness (E1:Grade 1: 31%, Grade 2: 63%, Grade 3: 6%; E2: Grade 1: 38%, Grade 2: 50%, Grade 3: 12%; χ^2=0.65, p=0.72, ICC=0.50, 95%CI:-0.43-0.83), and meibomian gland loss of the upper lids (E1: 27.3±13.0%, E2: 21.6±6.3%, p=0.3, ICC=0.15, 95%CI:-1.35-0.69) were not significantly different between examiners for all 17 participants (mean age: 22±2 years, 19–28, 7 symptomatic), and between subgroups. Meibomian gland loss of the lower eyelids differed significantly between examiners (E1: 26.9±8.7%, E2: 39.4±14.8%, p=0.01, ICC=0.71, 95%CI:0.21-0.90), for all but the asymptomatic subgroup. IER ICC values ranged between 0.15-0.73 for all measurements, and all WSV Sw values were <8.25%.

CONCLUSIONS

The DEA device demonstrates good reproducibility and low WSV, and is a reliable clinical instrument for all outcomes except meibomian gland loss of the lower eyelids. Back to TOC

A Novel Method of Video Recording Ophthalmic Surgical Procedures Using the Smartphone

Josh Kruger (1), Karen Hendler (1)

(1) Department of Ophthalmology, Hadassah–Hebrew University Medical Center, Jerusalem

ABSTRACT

PURPOSE

To develop and evaluate a simple method for obtaining high-quality smartphone surgical recordings in ophthalmic operating rooms for surgeons who operate with loupes rather than a surgical microscope.

METHODS

A smartphone-based recording technique was developed in which the phone was secured to the housing of the operating microscope, using the microscope only as a stable suspension platform, positioned at a height greater that the surgeon's head, and directed to the surgical field. Video was captured using the native camera application at 4K 60fps with autofocus lock. The microscope pedal facilitated focus control, and horizontal XY adjustments. Smartphones were connected to the operating room monitor for real-time viewing, and remote control was enabled using a draped laptop linked to the phone. The technique was used in 20 surgeries, including strabismus and eyelid procedures performed by multiple surgeons. Feasibility, quality, and workflow compatibility were assessed qualitatively.

RESULTS

Twenty surgeries were successfully recorded with no compromise of the surgeon’s view, and no interference with workflow. All videos were qualitatively judged to be adequate or superior for surgical documentation and educational use. Real-time displays on the operating room monitor were appreciated by nurses and trainees.

CONCLUSIONS

This method provides a practical, accessible, and cost-effective solution for recording ophthalmic surgeries performed without a surgical microscope. It uses readily available equipment, integrates easily into the operating room environment, and produces high-quality video suitable for clinical documentation and education. The technique offers a viable option for widespread clinical adoption in settings where traditional microscope-based recording systems cannot be used. Back to TOC

Comparison of Patient-Reported Outcome Measures (PROMs) Following Cataract Surgery at Hadassah Medical Center

Zipora Boim (1), Itay Chowers (1), Itay Lavy (1), Hadas Ben-Eli (1,2)

(1) Eye Department, Hadassah Medical Center**,** Jerusalem
(2) Optometry Department, Jerusalem Multidisciplinary College

ABSTRACT

PURPOSE

Cataract surgery is one of the most common surgeries in ophthalmology and is the primary treatment for clouding of the lens of the eye that impairs visual acuity and quality of life. In recent years there has been increasing recognition of the importance of assessing the success of surgery from the patient's perspective, using subjective measures of visual function and satisfaction. Measures PROMs (Patient-Reported Outcome Measures) are designed to provide direct information from the patient about the impact of medical intervention on their functioning and quality of life and serve as a significant tool for clinical and service evaluation. The aim of this study was to assess the change in PROMs scores after cataract surgery, and to compare the scores at three time points : before surgery, one month after surgery, and three months after surgery , as well as to examine differences between groups according to gender, age, religion/ethnicity, type of implanted lens, and the operated eye.

METHODS

The study included patients who underwent cataract surgery at Hadassah Medical Center (January-October 2025) and completed the CATPROM-5 questionnaire, plus three questions from the validatedVFQ (Visual Function Questionnaire), at at least two time points: before surgery and once after. Each participant completed the electronic questionnaire that was sent to them by text message before arriving at the clinic, as well as one month and three months after surgery. The results of the questionnaires were automatically entered into the patient's medical record and presented to the attending physician at the time of the visit, to integrate the patient's opinion into the clinical assessment. Comparisons between times were performed using paired t-test and comparisons between groups according to demographic and clinical characteristics were performed usingt-test. . and ANOVA-

RESULTS

Between 1.1.25–22.10.25, 820 pre-surgery questionnaires were sent, with a response rate of 42 %. The response rate to the questionnaire sent about a month after the surgery was 49 % and the questionnaire sent three months after the surgery 50 %. Of the 347 patients who completed at least one of the questionnaires, 114 patients completed questionnaires at all three time points and were included in the statistical analysis,the mean preoperative score was 15.9 ± 7.8, after a month 9.8 ±5.6. And after three months 7.2 ± 4.6, with a lower score indicating higher satisfaction. The average decrease in score Between pre-surgery and the first questionnaire was 7.0 points, and between the first and third questionnaires 2.5 Additional points. 78% of patients reported improvement between the first and second questionnaires, and 72% reported further improvement between the second and third questionnaires. There was a significant decrease in scores between pre-surgery and one month after surgery ($p < 0.001$) between pre-surgery and three months, ($p < 0.001$), and between one month and three months ($p = 0.002$) It was also found that men reported higher satisfaction than women ($p = 0.004$), while no significant differences were found by age ($p = 0.73$), religion/ethnicity($p = 0.60$), type of lens implanted ($p = 0.12$), or operated eye ($p = 0.32$) .

CONCLUSIONS

It was found that there was a significant improvement in the PROMs indices after cataract surgery. , with a continuing improvement trend up to three months after surgery. The combination of PROMs questionnaires allows for a more comprehensive assessment of the results of surgery from the patient's perspective, contributes to understanding the impact of surgery on quality of life, and serves as an important clinical tool for improving the quality of care and satisfaction with the healthcare system.

Association Between Contact Lens Type and Dry Eye Outcomes in Keratoconus

Reut Ifrah[1], Rivki Bloom[1], Liat Gantz[1]

(1) Department of Optometry and Vision Science, Jerusalem Multidisciplinary College, Jerusalem, Israel

ABSTRACT

PURPOSE

Keratoconus (KC) patients wearing contact lenses (CLs) often exhibit increased corneal weakening, a hallmark of dry eye disease (DED). This study aimed to assess associations between CL modalities and clinical signs and symptoms of DED and meibomian gland dysfunction (MGD) in KC patients.

METHODS

In this prospective cross-sectional study, KC patients were grouped by CL modality: soft, SoftK, RGP mini-scleral/scleral, and non-CL wearers. Visual acuity, aberrometry, invasive and non-invasive tear break-up time (TBUT), tear meniscus height, Schirmer test, meibography, meibomian gland (MG) expressibility (MES) and quality, corneal and conjunctival staining, and the lid margin were evaluated. DE was defined as Ocular Surface Disease Index (OSDI) Questionnaire score ≥13 with TBUT/NITBUT <10 seconds ;MGD as DE with > 25% MG loss. Statistical analyses included Chi-Square, Kruskal-Wallis, and linear regressions.

RESULTS

Among 46 KC patients (91 eyes, mean age: 45±13, range: 20–69 years) ,48 eyes had no CLs, 20 wore soft, 13 wore RGPs, and 10 wore SoftK CLs. DE (44%) and MGD (32%) prevalence did not differ across groups (DE: $p = 0.60$; MGD: $p = 0.79$). RGP wearers had significantly worse visual acuity, ocular aberrations, and loss of upper eyelid MGs than non-CL wearers (0.30±0.30 vs. 0.71±0.27, 4.89±3.00 vs. 2.79±2.16, 38.60±31.69 vs. 24.52±11.07, $p<0.02$ for all comparisons, respectively). TBUT was significantly longer in soft CL wearers (b=1.87, CI: 0.24-1.27, $p=0.004$). Soft CL wearers had significantly less lid margin telangiectasia and notching ($p=0.049$ and $p=0.03$, respectively) with more MES grade 1 compared with other sub-groups ($p<0.001$). Corneal and conjunctival staining grade 5 were significantly more prevalent among RGP wearers ($p=0.049$). Symptoms did not differ across sub-groups.

CONCLUSIONS

While prevalence of DE and MGD was similar across CL modalities, RGP wearers demonstrated more severe ocular surface signs, highlighting the importance of regular ocular surface monitoring in KC patients, particularly RGP wearers. Back to TOC

Immune Regulation of the Limbal Stem Cell Niche by Dendritic and γδ T Cells

Shira Hadad-Porat[1], Aya Amitai-Lange[1], Shalini Dimri[1], Anna Altshuler[1], Noam Tarazi[1] and Ruby Shalom-Feuerstein[1]

(1) Department of Genetics & Developmental Biology, The Rappaport Faculty of Medicine & Research Institute, Technion Integrated Cancer Center, Technion – Israel Institute of Technology, Haifa, Israel

ABSTRACT

PURPOSE

The limbal epithelial stem cell (LSC) microenvironment, or "niche", plays a critical role in regulating LSC function and maintaining corneal homeostasis. A deeper understanding of this niche is essential for deciphering corneal pathologies developing novel therapeutic approaches. However, current studies offer only limited insight into the insight of the complex mechanisms governing interactions between LSCs and their surrounding niche components. This study aims to characterize immune cell subpopulations within the limbal niche and evaluate their potential regulatory roles in LSC maintenance and dynamics.

METHODS

We characterized immune cell populations using immunostaining, light sheet microscopy and flow cytometry. To assess the functional role of immune regulation as LSC niche, we examined the effect of broad-immune suppression as well as the genetic depletion of dendritic immune cells, γδ T cells, or both.

RESULTS

We identified numerous $CD45^+$ immune cells preferentially residing within the LSC niche, including the epithelium and upper stroma. These populations comprise substantial numbers of $CD11c^+$ dendritic cells and γδ T cells, which are particularly enriched in the outer limbus in close proximity to quiescent LSCs. Interestingly, immunodeficient mice lacking T cells, or mice treated with pan immunosuppressor, Dexamethasone, displayed loss of quiescence, reduced expression of quiescent LSCs markers, and delayed wound healing. In addition, genetic depletion of dendritic cells using diphtheria toxin, resulted in a marked enhancement in proliferation rates, while combined depletion of dendritic cells and γδ T cells led also to corneal opacification. Functional study in vivo and in-vitro reveals that IL-1β and TNF-α, that are expressed in limbal dendritic cells, mediate the regulation of LSC quiescence and LSC differentiation markers.

CONCLUSION

This study suggests that dendritic and γδ T cells reside within the limbal niche, and function as active niche cells that control LSC function. We propose that clinical use of immunosuppressors treatment may affect LSC function and explain the adverse effect of prolong immunosuppression of epithelial healing. Future work should investigate the translational potential of immune niche cells derived cytokines on LSC growth ex vivo and rescue in LSC-related pathology in situ.

Back to TOC

Predicting keratoconus progression using machine learning analysis of tomographic images

Yamit Cohen-Tayar (1, 2, 3), Hadar Cohen (4), Dor Key (1, 2, 3), Roy Azaria (3), Irit Bahar (1, 2, 3), Yoav Nahum (1, 2, 3)

(1) Department of Ophthalmology, Rabin Medical Center, Petach Tikva

(2) Laboratory of Eye Research, Felsenstein Medical Research Center, Petach Tikva

(3) Faculty of Medicine, Tel Aviv University, Tel Aviv

(4) Faculty of Physics, Tel Aviv University, Tel Aviv

ABSTRACT

PURPOSE

To enhance early prediction of keratoconus progression by integrating deep learning analysis of Pentacam tomographic images with our previously identified raw data parameters.

METHODS

Building upon our prior work that achieved ROC-AUC of 0.75 using tabular data from serial examinations, we now apply neural networks to Pentacam four-map displays (anterior elevation, posterior elevation, axial curvature, and pachymetry maps). We retrieved 11,760 tomography tests performed in patients with keratoconus. Eyes were labelled as unstable if referred for corneal cross-linking, while those not requiring intervention were labelled stable. Deep learning architecture extracts spatial features from individual tomographic maps, identifying subtle morphological signatures predictive of future progression.

RESULTS

Our previous study showed that single tomography tabular data examination yielded poor prediction (ROC-AUC 0.59), yet clinicians require tools for early intervention before deterioration manifests. The current multimodal approach combining image-based spatial analysis with our previously identified key parameters (age, CKI, Rs B, and D10mm pachymetry) addressed this need and improved the single-examination prediction accuracy. Image analysis revealed spatial patterns and morphological features, that numerical parameters did not capture.

CONCLUSIONS

This study demonstrates that integrating visual biomarkers from tomographic maps with raw data parameters provides significant additive predictive value. This approach offers a more comprehensive assessment of corneal structural integrity and progression risk. The current results may enhance early detection of eyes with keratoconus that are prone to progress, potentially supporting more timely clinical decision-making regarding cross-linking intervention before visual deterioration occurs.

Back to TOC

The miR-184/ATF3 Axis Controls Active Limbal Stem Cell Identity and Corneal Epithelial Renewal

Gharam Yassen[1], Swarnabh Bhattacharya[1], Sara Nagosa[1], Aya Lange-Amitai[1], Eran Bercovic[2], Ramez Barbara[2], Beatrice Tiosano[2], Ami Aronheim[1], Ruby Shalom-Feuerstein[1]

(1) Department of Genetics & Developmental Biology, The Rappaport Faculty of Medicine & Research Institute, Technion Integrated Cancer Center, Technion – Israel Institute of Technology, Haifa, Israel
(2) Department of Ophthalmology, Rambam Health Care Campus, Haif, Israel

ABSTRACT

PURPOSE

Recently we discovered two discrete limbal epithelial stem cell (LSC) populations in the murine cornea: a quiescent LSC (qLSC) pool that acts as a reservoir for wound repair, and an active LSC (aLSC) population that is highly proliferative and essential for normal corneal cell turnover. However, very little is known about the genetic regulation of these cells. This study aims to investigate how microRNA-184 (miR-184), a gene whose point mutations cause congenital corneal disease and blindness, regulates the active LSC population and its role in controlling stem and progenitor cell output.

METHODS

We stained for miR-184 and ATF3 and characterized their expression in limbal and corneal stem/progenitor cells. We employed miR-184 knockout (KO) mice and ATF3-KO mice, together with the aLSC reporter line K15-GFP, to study the influence of miR-184 and ATF3 on tissue renewal. We investigated, both in silico and in vitro, the regulation of miR-184 and the transcription factor ATF3 on the promoter of the limbal stem cell marker K15. Intravital imaging and lineage tracing were used to assess how loss of miR-184 or ATF3 affects stem/progenitor behavior and tissue integrity under stress. Finally, primary human LSCs were analyzed to determine whether the miR-184/ATF3 regulatory axis is conserved in humans.

RESULTS

In situ hybridization and immunostaining revealed that miR-184, ATF3, and K15 are co-expressed in active limbal stem cells (LSCs), whereas miR-184 is additionally expressed in corneal basal progenitors but absent from post-mitotic differentiated cells. miR-184 knockout (KO) mice exhibited reduced expression of aLSC markers, including ATF3 and K15-GFP, along with changes in stem and progenitor gene profiles. Loss of miR-184 accelerated LSC proliferation, enhanced corneal epithelial stratification, increased limbal–corneal tissue turnover, and delayed wound healing. Promoter assays confirmed that miR-184 positively regulates ATF3, which in turn activates the K15 promoter. ATF3-KO mice similarly showed reduced aLSC marker expression, supporting a miR-184/ATF3/K15 regulatory axis of stemness. Studies in primary human LSCs demonstrated that the miR-184/ATF3 pathway is conserved in humans.

CONCLUSIONS

The miR-184/ATF3 axis is essential for maintaining active limbal stem cell identity, regulating stem and progenitor cell output, and fine-tuning the pace of corneal epithelial renewal. Elucidating how miR-184 controls downstream targets provide new insights into corneal disease mechanisms and stem cell fate regulation.

Back to TOC

Triack, A Novel Irreversible High Potency Thrombin Pathway Modulator in Eye Drops Penetrates to Murine and Pig Retina

Shany Gofrit[1], Efrat Shavit-Stein[1, 2], Joab Chapman[1, 2], Ifat Sher[3, 4]
Ygal Rotenstreich[3, 4], Valery Golderman[1], Zehavit Goldberg[1, 2]

(1) Neurology, Sheba Medical Center, Israel
(2) Neurology and Neurosurgery, Gray Faculty of Medical and Health Sciences, Tel Aviv University, Israel
(3) Goldschleger Eye Institute, Sheba Medical Center, Israel
(4) Ophthalmology, School of Medicine, Gray Faculty of Medical and Health Sciences, Tel Aviv University, Israel

ABSTRACT

PURPOSE

We developed two thrombin–Protease activated receptor 1(PAR1) modulators, PARIN5 and TRIACK (five and three amino acid sequences, respectively), with potential applications in retinal neuroinflammation. Their high potency and irreversible inhibition profile support evaluation as candidates for topical administration.

METHODS

Penetration of the compounds into intact pig eyes was assessed both ex-vivo and in-vivo following topical administration. Retinal penetration was evaluated by measuring inhibition of intrinsic thrombin activity in the neuroretina, while aqueous humour penetration was assessed by inhibition of either intrinsic or exogenously added thrombin.

RESULTS

Ex-vivo exposure of intact eyes to both compounds reduced thrombin activity in the neuroretina and the aqueous humour compared with controls (Neuroretina: PARIN5: 0.10 ± 0.02 vs. 0.20 ± 0.02 mU/ml, respectively, $p<0.01$; TRIACK: 0.015 ± 0.009 vs. 0.27 ± 0.03 mU/ml, respectively, $p<0.0001$, aqueous humour: PARIN5 2mM 0.003±0.002 mU/ml vs. TRIACK:0.002±0.002 mU/ml vs. 6.9±0.03mU/ml). In-vivo topical TRIACK administration conducted in healthy, intact eyes affected neuroretinal thrombin activity compared with the control eye (0.38 ± 0.04 vs. 0.26 ± 0.03 mU/ml, respectively, $p<0.05$), with the largest effect observed in the central retina.

CONCLUSIONS

The modulators of the thrombin–PAR1 pathway demonstrated significant penetration into pig eyes and exerted measurable biological effects on the retina. These findings support their potential development as topical eye-drop therapies for retinal diseases associated with neuroinflammation and diabetes. Back to TOC

Family Planning in Genetic Optic Atrophies in Israel, a Case Series and a Discussion of Ethical Considerations

Eliane Rozanes, MD, MSc [1]; Yftach Yassur MD [1,2]; Irit Bahar MD [1,2]; Eitan Livny MD [1,2]

(1) Department of Ophthalmology, Rabin Medical Center, Petach-Tikva, Israel
(2) Sackler Faculty of Medicine, Tel Aviv University, Tel Aviv, Israel

ABSTRACT

PURPOSE

This study aims to share the valuable lessons learned from our initial experience with osteo-keratoprosthesis (OKP) surgery in patients with ocular cicatricial pemphigoid (OCP). We address the challenges encountered during this complex procedure to provide insights for surgeons beginning their journey in performing OKP in this patient demographic.

METHODS

We conducted a retrospective case series involving five OCP patients who underwent OKP as a last-resort intervention for visual salvage at Rabin Medical Center between 2010 and 2024. All procedures were performed by the same, experienced team of ophthalmologic and orthopedic surgeons. Patient demographics, surgical details, and postoperative complications were meticulously recorded.

RESULTS

All five patients successfully underwent OKP; however, we encountered the following significant complications.

- Three patients experienced poor mucosal graft integration and required multiple grafting procedures, including skin grafts.
- One patient developed corneal keratitis, necessitating a hot graft corneal transplant, along with additional treatment for an epiretinal membrane (ERM) and cystoid macular edema (CME) through steroid injections and pars plana vitrectomy (PPV). This patient later faced device extrusion attributed to osteopenia.
- Another patient with a pre-existing thin cornea experienced a psychotic episode following vision restoration.
- Additionally, one patient demonstrated recurrent mucosal overgrowth over the optic device and developed scratches on the optic lens for months post-surgery.

CONCLUSIONS

OKP represents a transformative surgical option for restoring sight in patients with OCP, though it is a technically demanding procedure with a steep learning curve. Our findings indicate that complications predominantly arise from mucosal graft failure, corneal and retinal issues, and challenges related to the optical device. These experiences underscore the necessity for highly skilled surgical teams in managing such intricate cases and highlight the importance of thorough preoperative evaluation and postoperative care.

Back to TOC

Genetic Diagnosis of Inherited Retinal Diseases Improved by Whole Genome Sequencing

Johanna Valensi (1), Kareem Husseini (1), Sapir Shalom (1), Eyal Banin (1), Dror Sharon (1)

(1) Division of Ophthalmology, Hadassah Medical Center, Faculty of Medicine, The Hebrew University of Jerusalem, Israel

ABSTRACT

PURPOSE

Inherited retinal diseases (IRDs) are a clinically heterogeneous and complex group of disorders caused by pathogenic variants in at least 277 nuclear and mitochondrial genes, leading to vision loss worldwide. Their marked clinical and genetic heterogeneity makes identification of the underlying genetic cause particularly challenging. Here, we performed whole-genome sequencing (WGS) on 70 previously unsolved cases from our cohort of Israeli and Palestinian families with IRDs, enabling the detection of both copy-number variants (CNVs) and single-nucleotide variants (SNVs).

METHODS

All participants underwent comprehensive clinical examinations. WGS was performed on DNA samples by CNAG (Spain). Initial analyses were conducted by CNAG, followed by detailed SNV and CNV interpretation using the Franklin (Genoox) platform. Co-segregatation was performed on available blood samples. The RPGR-ORF15 region was manually examined using the IGV platform.

RESULTS

We analyzed by WGS 70 index cases with IRDs, most of whom underwent prior genetic testing, including whole exome sequencing (WES) or targeted IRD panels, but remained unsolved. WGS identified the genetic cause in 12 (17%) of the cases. This analysis revealed a previously unreported inheritance pattern for *IMPG2* in patients with retinitis pigmentosa (RP) and suggested seven potential novel IRD-associated genes that are still under analysis. In a patient with blue cone monochromacy (BCM), we detected a deletion of exon 2 of the OPN1LW gene. In another patient with a combination of RP and color vision deficiency, we identified two elusive mutations on the X-chromosome: a nonsense mutation in the difficult for sequencing RPGR-ORF15 region (c.2557G>T, p.Glu853*) and a CNV (deletion of exon 5) in the genes coding for the red opsin gene. In addition, we identified a deep intronic variant in TRPM1 that is predicted to create a pseudoexon leading to congenital stationary night blindness (CSNB) and a homozygous large deletion encompassing MYO7A exons 47-49 leading to Usher syndrome type I.

CONCLUSIONS

This is the first report of a comprehensive WGS analysis of IRD patients in the Israeli population. The analysis allowed us to identify elusive causative variant including a new inheritance pattern, potential novel genes, deep intronic variants, and CNVs. We are planning to improve the analysis pipeline to better identify deep intronic and regulatory pathogenic variants.

Back to TOC

A Knock-In Mouse Model for the Human *TRPM1*- p.Lys294* Mutation as the Cause of Congenital Stationary Night Blindness

Manar Salameh (1), Alex Oblenskey (1), Rotem Mizrachi (1), Chen Matsevich (1), Eyal Banin (1), Dror Sharon (1)

(1) Division of Ophthalmology, Hadassah Medical Center, Faculty of Medicine, The Hebrew University of Jerusalem, Israel

PURPOSE

Congenital stationary night blindness (CSNB) has been studied in several animal models, including dogs, zebrafish, horses, rats, and mice. Among these, a *Trpm1* knockout mouse with a deletion of exons 4–6 has been previously described.
However, no knock in (KI) model to date has carried a human disease-causing *TRPM1* mutation. Here, we present the first *Trpm1* KI mouse model engineered to harbor the human CSNB-associated mutation **p.Lys294*** that is relatively prevalent in East Jerusalem.

METHODS

The KI model was generated using CRISPR/Cas9-mediated genome editing. Heterozygous carriers were backcrossed with wild-type C57BL/6 mice for five generations to establish a congenic line, followed by intercrossing to obtain homozygous mutants. Genotyping from ear punches was performed by Sanger sequencing. Retinal RNA was analyzed by RT-PCR. Ophthalmic characterization included optical coherence tomography (OCT) and electroretinography (ERG).

RESULTS

A donor sequence of 86 bp containing the human *TRPM1* mutation was successfully integrated into the mouse genome via homology-directed repair. Sanger sequencing confirmed the correct genomic modification. RT-PCR demonstrated complete skipping of exon 7 that harbored the nonsense mutation due to its effect on an exonic sequence enhancer, without evidence of nonsense-mediated mRNA decay. ERG recordings revealed a characteristic negative waveform consistent with human CSNB, while OCT imaging showed preserved retinal structure.

CONCLUSIONS

We have generated the first mouse model carrying the most prevalent *TRPM1* mutation found in Israeli and Palestinian CSNB patients. This KI model faithfully recapitulates key molecular and functional aspects of the disease and provides a valuable platform for developing and evaluating genomic and RNA-based therapeutic strategies.

Back to TOC

TRPM1 p.K294*: A Dual-Effect Mutation and Implications for Developing Targeted Therapies

Nina Schneider (1), Jonathan Eintracht (1), Samer Khateb (1), Manar Salameh (1), Eyal Banin (1), Dror Sharon (1)

(1) Department of Ophthalmology, Hadassah Medical Center, Faculty of Medicine, The Hebrew University of Jerusalem, Israel

ABSTRACT

PURPOSE

A founder *TRPM1* variant (c.880A>T; p.K294*) unique to the East Jerusalem population is the most common cause of CSNB in Israel. Previously classified solely as a nonsense variant and considered suitable for ADAR-mediated site-directed RNA editing (SDRE), we now show—using multiple models—that this variant also induces exon skipping. We further evaluate the implications of this dual pathogenic mechanism for SDRE-based therapy.

METHODS

The *TRPM1* exonic sequence harboring the c.880A>T variant was analyzed for exonic splice-enhancing (ESE) motifs using ESEfinder3.0. For splicing characterization, minigene splice plasmids carrying either the mutant or WT variant were transfected into HeLa cells, and splice patterns were measured through capillary gel electrophoresis and Sanger sequencing. Homozygous patient-derived retinal organoids were harvested for RNA extraction at days 120 and 210, and splicing patterns were visualized on agarose gels and Sanger sequenced. SDRE simulation was performed in HeLa cells using a minigene plasmid harboring both the variant and an altered ESE motif.

RESULTS

ESEfinder3.0 analysis indicated that the variant lies within a proposed SRSF1 binding motif and abolishes this motif. Capillary electrophoresis of the splice assay showed that the mutant plasmid produced 16% full-length transcripts and 84% exon-7–skipped transcripts, compared with 86% full-length transcripts for the WT plasmid. Gel electrophoresis of pooled homozygous patient organoids showed only exon-skipped bands, while pooled WT organoids showed strong full-length bands and faint exon-7–skipped bands. To model SDRE A>G changes mediated by ADAR, we performed a splice assay using a plasmid carrying both the variant and a 5′ neighboring A>G change designed to introduce a new SRSF1 motif. Capillary electrophoresis showed 89% full-length transcripts, theoretically rescuing the splicing error and converting the nonsense variant into a missense variant.

CONCLUSIONS

This study demonstrates that a common CSNB-causing *TRPM1* variant, previously thought to be solely a nonsense variant, also causes exon skipping. This dual effect indicates that SDRE therapy must act prior to splicing, reinstate an ESE motif, and eliminate the stop codon. Preliminary editing simulations suggest that achieving both outcomes with a single SDRE strategy may be feasible, though further study is needed.

Back to TOC

A p63 point mutation impairs limbal stem cell and niche function that is rescued by the small molecule PRIMA-1Met (APR-246)

Rabea Misherki[1], Waseem Nasser[1,2], Shalini Dimri[1], Swarnabh Bhattachariya[3], Aya Amitai-Lange[1], Ramez Barbara[4], Caterina Missero[5], Daniel Aberdam[6] and Shalom-Feuerstein Ruby[1]

(1) Department of Genetics and Developmental Biology, Technion, Haifa, Israel; (2) Rambam Medical Center, Haifa, Israel; (3) Dana-Farber Cancer Institute and Harvard Medical School, Boston, MA, US; (4) Hilel Yafe Medical Center; (5) CEINGE Biotecnologie Avanzate, Napoli, Italy; (6) INSERM U976, Paris, France

ABSTRACT

PURPOSE

Previously, we reported that the small molecular weight compound, PRIMA-1Met (APR-246), reinstates the activity of mutated p63 protein in ectodermal dysplasia (ED)-derived patient cells in vitro and improves healing of 3 ED patient skin erosions in compassionate care treatments. In the present study, we examined the effect of PRIMA-1Met in genetically engineered limbal stem cell deficiency (LSCD) mouse model. Furthermore, we aimed to elucidate the mechanism by which PRIMA-1Met acts on mutated limbal stem cells (LSCs) and their niche.

METHODS

We developed an advance transgenic allele enabling an eye specific inducible mutagenesis in Pax6+ cells, that stimulates the switch from a transcription of a wild type to a L514F p63-mutated transcript. PRIMA-1Met was intraperitoneally twice weekly injected for up to 4-months. To test the therapeutic effect of the compound, we monitored the transparency and vascularization of the cornea, performed immunostaining for LSC and corneal epithelial markers, and we conducted single-cell RNA sequencing to identify changes in signaling pathways. To explore the function and the dynamics of wild-type and mutant stem and progenitor cells, with or without PRIMA-1Met treatment, we established an advanced multi-color lineage tracing system and tested the proliferative capacity, and clonal growth patterns over time.

RESULTS

PRIMA-1Met significantly attenuated the development of neovascularization and opacification of the mutants in aging or following injury. Immunofluorescence staining revealed that treatment with PRIMA-1Met partly improved marker expression of mutated corneas. Single-cell transcriptomics reveal disrupted expression of p63 target genes and niche cell dysregulation in p63-mutant mice. Treatment with PRIMA-1Met rebalances the expression of putative p63 target genes and restores limbal stromal niche cell transcriptomic profiles. Lineage tracing analysis showed that PRIMA-1Met partially restored the renewal patterns of the cornea.

CONCLUSIONS

This study demonstrates that PRIMA-1Met effectively prevents the onset of LSCD in mutated corneas both under homeostatic and injury-induced conditions. The compound inhibits neovascularization and preserves corneal transparency. Remarkably, PRIMA-1Met significantly restores the transcriptome of both LSCs and their supporting limbal stromal niche cells, as well as restoring key p63 target gene expression. These findings highlight the potential of PRIMA-1Met for rapid translation into clinical applications for patients with LSCD.

Back to TOC

Title: Probing the Molecular Mechanisms Underlying the Protective Role of Systemic Immunity in the *Fam161a* Knock-out Mouse Model of Retinitis Pigmentosa

Rotem Mizrahi, Ayala Ejzenberg, Alexey Obolensky, Chen Matsevich, Dror Sharon and Eyal Banin

Center for Retinal and Macular Degenerations, Department of Ophthalmology, Hadassah-Hebrew University Medical Center, Jerusalem, Israel

ABSTRACT

PURPOSE

Inherited retinal diseases (IRDs) are primarily driven by monogenic mutations; however, systemic and local immune responses can significantly modulate disease onset and progression. To determine the contribution of innate immunity to retinal degeneration, we compared disease course in the *Fam161a* knock-out (KO) mouse model of retinitis pigmentosa (RP) under immunocompetent versus severely immunodeficient conditions. Longitudinal functional and structural assessments, together with unbiased retinal proteomics, were performed.

METHODS

Visual acuity, full-field ERG, fundus autofluorescence, OCT and histology were performed in C57BL/6J, NSG, *Fam161a* KO and NSG-*Fam161a* KO mice at predefined ages. For proteomics, retinas were collected at 6 and 18 weeks (w) of age (n=9/group). Three replicates per group were generated by pooling 3 retinas each.
Proteins were extracted and analyzed by label-free data-independent acquisition mass spectrometry. Differentially abundant proteins were subjected to pathway and upstream regulator analysis using Ingenuity Pathway Analysis software.

RESULTS

NSG-*Fam161a* KO mice showed markedly accelerated retinal degeneration compared with *Fam161a* KO mice, with faster deterioration of visual function and rapid loss of the outer nuclear layer. Retinal proteomic analysis of both *Fam161a* KO and NSG-*Fam161a* KO mice revealed enrichment of pathways associated with photoreceptor maintenance and visual phototransduction, consistent with progressive retinal degeneration in both models. In NSG-*Fam161a* KO retinas, early (6w) proteomic changes were additionally enriched for pathways related to immune and inflammatory signaling, including activation of innate inflammatory and interferon-associated responses accompanied by reduced activity of immune-regulatory pathways. By 18w, the predominant proteomic signature in NSG-*Fam161a* KO mice shifted toward pathways that reflect a transition to an advanced degenerative stage.

CONCLUSIONS

The data suggests that in the presence of impaired systemic immunity, early dysregulation of immune-related pathways is associated with accelerated degeneration and retinal functional decline, thus supporting a model in which an intact immune system beneficially modulates the retinal response to a primary genetic insult. The findings highlight the critical role of immune-genetic interactions in the pathogenesis of RP and suggest the possibility that therapeutic modulation of immune balance may potentially serve to attenuate disease progression in IRDs.

Back to TOC

A UGA stop codon suppressor tRNA therapy for gene-agnostic treatment of inherited retinal diseases

Asodu Sandeep Sarma (1), Jonathan Eintracht (1), Alaa Saleh (1), Hala Kamal (1), Samer Khateb (1), Eyal Banin (1), Dror Sharon (1).

(1) Department of Ophthalmology, Hadassah-Hebrew University Medical Centre, Jerusalem, Israel

ABSTRACT

PURPOSE

Currently, there is no effective cure for the vast majority of inherited retinal diseases **(**IRDs). The lack of available therapy is due to several reasons such as, high genetic and clinical heterogeneity, diagnostic challenges, complex gene expression, and open-reading-frame size. While recent advances have yielded innovative genetic therapies most have not yet reached the clinic, remaining in development or clinical trials. A critical limitation is that these approaches are largely gene or variant specific, each requiring its own costly and time-consuming development and regulatory pipeline, creating a massive bottleneck for treating IRDs. This study focuses on engineering a single, optimized tRNA to suppress the most common arginine (Arg>Ter) nonsense variants, thereby creating a broad-spectrum treatment for a genetically diverse patient population.
S

METHODS

We engineered an ACE-tRNA^{Arg}UGA optimized for the efficient suppression of the UGA nonsense codon. Its efficacy was evaluated using an mCherry-eGFP dual-fluorescence reporter system, where successful PTC suppression restores translation of downstream eGFP. The 12 most prevalent IRD-causing Arg>Ter variants were cloned into this reporter. Qualitative assessment of suppression was performed via fluorescent microscopy. For quantitative analysis, transfected HeLa cells were analyzed by flow cytometry, and Western blot. Skin biopsies were collected from two patients with nonsense variants (FAM161A:p.R523* and KIZ:p.R76*), reprogrammed to hiPSCs, and later differentiated into retinal pigment epithelial cells.

RESULTS

To establish a clinically relevant target panel, we first curated nonsense variants data from over 35,000 IRD patients reported in the literature, which identified the 12 most frequent Arg>Ter variants. Our optimized ACE-tRNA^{Arg}UGA demonstrated robust and variable suppression across the panel of 12 different Arg>Ter variants. The observed suppression efficiencies ranged from 10% to over 90%, indicating that the tRNA is capable of restoring full-length protein synthesis for a wide spectrum of nonsense variants. Further we tested ACE-tRNA^{Arg}UGA efficiency using patient derived RPE cells.

CONCLUSIONS

We have successfully developed a potent and broad-spectrum ACE-tRNA^{Arg}UGA capable of suppressing a wide range of the most common Arg>Ter nonsense variants that cause IRDs. This proof-of-concept study demonstrates that a single therapeutic tRNA can potentially treat numerous patients with different genetic variants, bypassing the need for developing individual gene-specific therapies. This mutation-agnostic approach represents a promising and scalable strategy to significantly accelerate the development of treatments for the genetically heterogeneous landscape of IRDs.

Back to TOC

Compilation and analysis of the global retinal inherited disease 2 (GRID2) data set

Alaa Saleh (1), Nina Schneider (1), Dror Sharon (1)

(1) Division of Ophthalmology, Hadassah Medical Center, Faculty of Medicine, The Hebrew University of Jerusalem, Israel

ABSTRACT

PURPOSE

Retinal inherited diseases (IRDs) are a heterogeneous group of disorders caused by mutations across a wide spectrum of genes. To facilitate therapeutic research and precision medicine, we developed the Global Retinal Inherited Disease database (GRID2), a comprehensive resource integrating mutational, clinical, and therapeutic feasibility data.

The three primary objectives of GRID2 are: (1) to establish a centralized database with detailed mutation-level annotations; (2) to guide therapeutic decision-making by flagging mutations amenable to existing gene therapy approaches, such as AAV-based gene augmentation; and (3) to assess the feasibility of emerging RNA-based editing strategies, particularly for mutations not suitable for conventional therapies. Each entry includes a therapy candidacy score, with special consideration for the correction potential of RNA editing (e.g., G>A transitions) and readthrough-based approaches for treating nonsense mutations.

METHODS

We systematically analyzed 27 peer-reviewed studies including case-level genetic information. For each mutation, GRID2 compiles detailed annotations including gene identity, genomic location, codon and protein change, inheritance pattern, transcript type, patient frequency, and potential therapeutic relevance.

Data processing and analysis were conducted using Python, R, and online genomic repositories, including OMIM, UCSC, TransVar, and Franklin.

RESULTS

GRID2 includes 10,049 unique IRD-causing mutations across 267 genes, identified in 36,691 patients. The most frequently mutated genes are ABCA4, USH2A, and EYS. The three most common pathogenic variants identified were ABCA4:c.5882G>A, EYS:c.4957dup, and USH2A:c.2276G>T. The distribution of mutation types was: missense (39.19%), frameshift (23.26%), stop-gain (18.32%), and splice-site variants (12.54%), highlighting a high proportion of variants potentially amenable to RNA editing or readthrough strategies.

CONCLUSIONS

GRID2 offers several benefits: it provides mutation and patient frequency data to support genetic counseling, facilitates identification of gene therapy targets, and improves understanding of genotype–phenotype correlations. Ultimately, GRID2 serves as a strategic framework for personalized treatment development and a guideline for future therapeutic research in IRDs.

Back to TOC

Phenotypic-Genotypic Correlations in Ocular Cutaneous Albinism Type II

Ayala Katzir (1), Shoham Kubovsky (1), Natan Lishinsky (1) Anat Blumenfeld (1),

Claudia Yahalom (1)

(1) Department of Ophthalmology, Hadassah Medical Center, Jerusalem

ABSTRACT

PURPOSE

Oculocutaneous Albinism (OCA) is a rare genetic disorder characterized by impaired melanin production, resulting in widespread hypopigmentation and severe visual impairment, which constitutes the primary clinical handicap. OCA2, the most prevalent worldwide form of Oculocutaneous Albinism, is an autosomal recessive disorder where carriers may exhibit subtle, previously unrecognized phenotypic manifestations. Our purpose is to rigorously establish a comprehensive genotype-phenotype correlation in OCA2 patients.

METHODS

A retrospective study was conducted at The Michaelson Institute for Rehabilitation of Vision within the Department of Ophthalmology, Hadassah University Medical Center, Jerusalem, Israel, and included 136 patients with genetically confirmed Oculocutaneous Albinism Type II (OCA-II).
Visual acuity (VA) and key ocular pathologies (including nystagmus, strabismus, foveal hypoplasia, albinotic fundus and iris transillumination) were measured and documented to evaluate differences among subjects carrying various OCA2 mutation genotypes.

RESULTS

Included were 136 patients with OCA2 mutations (67 girls, 49.26\%). The cohort was predominantly of Ashkenazi Jewish descent (109 patients, 80.15\%). The most frequent genotype was homozygous c.79G>A (p.G27R) {G27R + L440F} found in 61 individuals. The remaining patients were classified into seven additional mutation groups, with a final group combining rare mutations (<5 members per mutation).
VA showed significant variability across genotypes. The worst Binocular Best Corrected Visual Acuity (BCVA) was observed in the heterozygous c.79G>A / c.1441G>A {A481T} group (Mean ± SD LogMAR VA 0.58 ± 0.284), followed by the mutation c.79G>A / c.1320G>C+c.1327G>A {V443I} (Mean ± SD LogMAR VA 0.43± 0.197). The best VA was recorded in the hetereozygous c.1320G>C / c.2373_2375\delCGT {V791del} group (Mean ± SD LogMAR VA 0.2 ± 0.054). Nystagmus was a near-universal finding across the cohort, but its incidence was significantly lower in the A481T heterozygous group (60%) compared to the homozygous group G27R + L440F (98.4\%; p=0.003). The rate of strabismus surgery was also significantly higher in the V791del group (28.6%) compared to the homozygous group G27R + L440F (3.3%; p=0.024). No statistically significant differences were found between groups regarding strabismus (overall incidence), foveal hypoplasia, albinotic fundus, or iris transillumination.

CONCLUSIONS

Our cohort demonstrates distinct genotype–phenotype clustering within OCA2. Specifically, the A481T and V443I combinations were associated with significantly poorer visual acuity, whereas the V791del combination showed a milder phenotype. The common Ashkenazi G27R + L440F haplotype exhibited a moderate and relatively stable phenotype. These findings are highly consistent with prior functional studies of P-protein activity, and provide one of the largest genotype-segregated clinical datasets

Back to TOC

A Platform to Increase the accessibility of essential information that enables eradication of mutations causing autosomal dominant retinitis pigmentosa and allied diseases

Tuvia Horev (1), Yossi Saidov (2), Nadine Hollander (3), Michal Macarov (4), Sapir Shalom (5), Shiri Soudry (6), Dror Sharon (7)

(1) SFaculty of Health Sciences. Ben-Gurion University of the Negev. Beer-Sheva (retired)
(2) Founder of the community 'Seeing Far', community of Israeli who live with Retinitis Pigmentosa. Jerusalem
(3) CEO of Lirot – the Israeli Research Association for Eye Health and Blindness Prevention
(4) Michaelson Institute, the genetic counseling clinic, Hadassah Medical Center. Jerusalem
(5) Division of Ophthalmology, Hadassah Medical Center, Faculty of Medicine, The Hebrew University, Jerusalem
(6) Faculty of Medicine, School of Continuing Medical Education. Tel Aviv University
(7) Division of Ophthalmology, Hadassah Medical Center, Faculty of Medicine, The Hebrew University, Jerusalem

ABSTRACT

PURPOSE

Using Preimplantation Genetic Diagnosis (PGD) among target groups who carry a mutant copy of an autosomal dominant (AD) disease gene, such as those causing retinitis pigmentosa (RP), may eradicate the disease from the family within one or two generations. The current challenge is that the information is accessible to those who come for counseling and there is no certainty that the information is distributed in the family. Even when it is transmitted by a family member, there is no control over the quality of the information. The purpose of the current study is to raise awareness and knowledge among a target population: young people aged 17-35 from families diagnosed as carriers of the autosomal-dominant mutation causing inherited retinal diseases (IRDs).

METHODS

We collected information regarding AD-IRD genes and mutations identified in the Israeli population. A video that will include the required information will be distributed to target populations using relevant platforms and might be used also by professionals.

RESULTS

We identified 297 families including 597 patients affected with AD-IRDs, the most common ones are RHO causing ADRP in 88 Israeli patients and BEST1 causing AD-Best disease in 86 cases. A short (4.5 minutes long) video was prepared, including professional messages and explanations presented by a genetic counselor, a senior ophthalmologist, a retina specialist; and a senior researcher in the field of eye genetics. In addition, we interviewed a couple, one of whom is a blind person carrying an ADRP mutation, who underwent PGD; and an ultra-Orthodox rabbi who is a genetic counselor by training. The video was presented in a pilot meeting to 8 members of an extended family carrying a PRP3 mutation. The professionals who participated in the meeting included experts in relevant fields.
The main insights that emerged during the meeting were barriers to making a positive decision to perform PGD, including late discovery, errors in information and guidance etc. Behavioral characteristics that were mentioned included denial, ignoring and avoiding discussion on the subject.

CONCLUSIONS

An important platform has been developed that may serve as a tool for increasing awareness and changing behavior among carriers of a dominant gene that leads to blindness. The video can serve also as a central tool around which professionals can conduct an effective dialogue with carriers of the relevant age, to reduce the chance of blindness in future generations. The program will reach out to the appropriate communities to deliver the message.

The project was sponsored by the Lirot Association, Israel

Back to TOC

Functional characterization of *C19orf44*, a novel gene associated with autosomal recessive retinal dystrophy

Maayan Mizrahi-Avraham and Tamar Ben-Yosef

The Ruth & Bruce Rappaport Faculty of Medicine, Technion-Israel Institute of Technology, Haifa, Israel

ABSTRACT

PURPOSE

Biallelic pathogenic variants of *C19orf44* are associated with autosomal recessive late-onset retinal dystrophy. The current work aims to investigate the role of *C19orf44* in the retina, and specifically its putative role in retinal ageing.

METHODS

Intracellular localization of the encoded protein was examined by immunostaining of cultured cells (HeLa and hTERT RPE-1). To induce DNA damage, cells were exposed to UVC radiation. Generation of *C19orf44*-knockdown cells was performed by CRISPR/Cas9-mediated gene editing.

RESULTS

To study the involvement of C19orf44 in ageing, immunofluorescence was performed on young and old human primary fibroblasts. In old fibroblasts, C19orf44 was detected both in the nucleus and cytosol, whereas in young fibroblasts it was primarily nuclear. Additionally, C19orf44 localization was altered following UVC-induced DNA damage. *C19orf44*-knockdown cells were generated by CRISPR/Cas9-mediated gene editing. These cells are currently being used to assess the effect of reduced C19orf44 levels on cellular response to different stress conditions.

CONCLUSIONS

C19orf44 is a novel gene, which is crucial for normal human retinal function. Based on our preliminary data, C19orf44 may be involved in protecting cells against stress, including UV radiation.

Back to TOC

LCA in the Israeli population: clinical and molecular characteristics

Melanie Mysler, Michal Macarov, Rotem Azmon, Ben Ezra Kathan, Karen Hendler, Claudia Yahalom

Michelson Institiute,s Hadassah Ein Kerem Medical Center, Jerusalem, Israel

ABSTRACT

PURPOSE

Leber congenital amaurosis (LCA) is a group of early-onset severe retinal degenerative disorders, resulting in blindness in childhood. This study aimed to describe the clinical and genetic characteristics of a cohort of patients with LCA in the Israeli population.

METHODS

Children with LCA followed at a national referral center for low vision were included in the study. Data obtained from medical files included clinical characteristics, optical coherence tomography (OCT) in cooperative patients and molecular findings when available.

RESULTS

We identified 47 children with LCA (mean age at presentation 4.0 years). Genetic data were obtained using panel-based next-generation sequencing. Main genes identified included *CRB1* in 11 patients followed by *GUCY2D, RDH12,*
RPE65, CFAP410 and *RPGRIP* genes in decreasing order. Fundus appearance ranged from normal to severe retinopathy. OCT was done in 35 cases, showing mainly discontinuity/thinning in photoreceptor layer and abnormal foveal pit. Cystoid macular edema was seen exclusively in children with *CRB1* gene mutation. Nystagmus was present in 38 patients, strabismus in 20 patients (mostly exotropia).

CONCLUSIONS

Most common genes associated with LCA in the Israeli population were *CRB1, GUCY2D, RDH12, RPE65, CFAP410* and *RPGRIP*, differing from genes identified in other populations with LCA, like *CEP290* gene, known to cause around15-20% of worldwide LCA cases. Early diagnosis is crucial for appropriate management including visual and emotional support, family planning and potential therapeutic interventions, particularly with the advent of gene-specific treatments.

Back to TOC

Clinical and molecular characterization of ocular developmental disorders in the Israeli population

Yakov Rabinovich (1), Yoav Vardizer (1), Shirley Pincovich (2), Marva Wolowelsky (3), Sofia Kulyamzin (3), Miriam Ehrenberg (4,5), Inbal Man Peles (1), Rina Leibu (6), Tamar Ben-Yosef (3), Nitza Goldenberg-Cohen (1,3)

(1) Department of Ophthalmology, Bnai Zion Medical Center, Haifa, Israel (2) Department of Ophthalmology, Galilee Medical Center, Nahariya, Israel (3) Rappaport Faculty of Medicine, Technion-Israel Institute of Technology, Haifa, Israel (4) Department of Ophthalmology, Schneider Children's Medical Center of Israel, Petach Tikva, Israel (5) Gray Faculty of Medical and Health Sciences, Tel Aviv University, Tel Aviv, Israel (6) Department of Ophthalmology, Rambam Health Care Campus, Haifa, Israel

ABSTRACT

PURPOSE

Microphthalmia, anophthalmia, and ocular coloboma (MAC) are rare developmental eye disorders and major contributors to childhood visual impairment. Although over 100 causative genes and chromosomal anomalies have been identified, the molecular spectrum and genotype–phenotype correlations remain incompletely understood, particularly in genetically diverse populations. We set to molecularly characterize MAC in the Israeli population and investigate genotype–phenotype correlations and recurrent or founder variants.

METHODS

We conducted an observational cohort study of MAC patients. After institutional review board approval and informed consent, detailed ophthalmic and systemic examinations, demographic data, and family histories were obtained. DNA was obtained from patients and family members and subjected to whole exome sequencing (WES). Variants were filtered for rarity, predicted deleteriousness, and location in known MAC genes. Sanger sequencing was used to confirm candidate variants and for segregation analysis in available family members. For selected variants, functional studies such as minigene assays were performed.

RESULTS

Forty seven MAC affected individuals from 43 unrelated families were enrolled. The most common phenotype was microphthalmia (64% of patients) followed by a combination of microphthalmia and coloboma (17%). WES was completed in 30 probands. Pathogenic or possibly pathogenic variants were identified in 11 different MAC-causative genes. Definite or likely molecular diagnoses were achieved in 13/30 genetically analyzed probands (43%). One proband carried a monoallelic variant in an autosomal recessive MAC-associated gene, while 16 genetically analyzed probands remained unsolved.

CONCLUSIONS

In this Israeli cohort with MAC, exome-based evaluation provided a definite or likely molecular diagnosis in 43% of the cases, which is within the reported range of genetic diagnosis in other studies (19-47%). The large number of genes involved demonstrates the marked genetic heterogeneity of MAC. These results underscore the value of broad genomic testing combined with targeted functional assays in the routine work-up of MAC and for optimizing genetic counseling in this population. The proportion of unsolved families highlights the need for further genomic and functional studies to identify additional MAC-associated genes and mechanisms. Back to TOC

Correction of the achromatopsia-causing *CNGB3*-c.1663-1205G>A mutation using antisense oligonucleotides in patient-derived retinal organoids

Sapir Shalom (1), Jonathan Eintracht (1), Nina Schneider (1), Samer Khateb (1), Eyal Banin (1), Dror Sharon (1)

1 - Division of Ophthalmology, Hadassah Medical Center, Faculty of Medicine, The Hebrew University of Jerusalem, Israel

ABSTRACT

PURPOSE

Achromatopsia (ACHM) is an autosomal recessive disease characterized by lack of cone function leading to low visual acuity, absence of color vision, photophobia and nystagmus. We previously reported a deep intronic *CNGB3* mutation that creates a pseudoexon, leading to a premature stop codon. Antisense oligonucleotide (ASO) therapy is an emerging therapeutic modality that has successfully restored aberrant splicing in disease models. Here, we aimed to identify an efficient ASO for correcting the splicing defect of the *CNGB3*-c.1663-1205G>A mutation and test the ASO in retinal organoids.

METHODS

ASOs for the mutation were designed based on various parameters, including temperature, secondary RNA structure, and GC ratio. The efficacy of the ASOs was assessed in HeLa and 661W cells transfected with a plasmid expressing the mutant sequence. A skin biopsy was taken from a patient homozygous for the pathogenic mutation and fibroblasts were further reprogrammed to induce pluripotent stem cells and differentiate to retinal organoids. On day 120, protein and RNA levels of *CNGB3* were evaluated by western blot and reverse transcription (RT)-PCR in wildtype (WT) and patient retinal organoids.

RESULTS

Five possible ASO sequences were identified by applying the determined parameters. Splicing analysis of the *CNGB3*-c.1663-1205G>A mutation in HeLa and 661W cells revealed the generation of a pseudoexon in 52% of transcripts in both cell lines. Following the application of the most efficacious three ASOs, more than 85% of normal transcripts were detected in HeLa and 661W cells. On day 120, patient retinal organoids exhibited incorporation of a pseudoexon in *CNGB3* transcripts compared to WT, and western blotting revealed a 55% reduction of *CNGB3* expression in patient retinal organoids.

CONCLUSIONS

We have developed three possible ASOs for the *CNGB3*-c.1663-1205G>A mutation that can efficiently restore correct splicing in the studied cell lines. Retinal organoids will be differentiated to later timepoints where *CNGB3* expression localize to outer segments. This will enable testing of ASOs in a more physiologically relevant model of ACHM. Back to TOC

Pathogenic variants in *YARS1* in individuals with a phenotype resembling Usher syndrome

Sofia Kulyamzin (1), Lidia Fernández-Caballero (2), Mathieu Quinodoz (3), Olfat Aboleile Zoubi (4), Elana Chervinsky (4), Stavit A Shalev (1,4), Frans P. M. Cremers (5), Carlo Rivolta (3), Susanne Roosing (5), Carmen Ayuso (2), Tamar Ben-Yosef (1)

(1) The Ruth & Bruce Rappaport Faculty of Medicine, Technion-Israel Institute of Technology, Haifa, Israel (2) Department of Genetics & Genomics, Instituto de Investigación Sanitaria-Fundación Jiménez Díaz University Hospital, Universidad Autónoma de Madrid, Spain (3) Institute of Molecular and Clinical Ophthalmology Basel, Switzerland (4) Genetics Institute, Emek Medical Center, Afula, Israel (5) Department of Human Genetics, Radboud University Medical Center, Nijmegen, the Netherlands

ABSTRACT

PURPOSE

Usher syndrome (USH) is an autosomal recessive condition, characterized by a combination of sensorineural hearing loss (SNHL) and retinitis pigmentosa (RP). USH is classified into three major types, USH1-3, and a rarer type, USH4. To date, at least 12 USH-causative genes have been identified, with additional genes implicated in rare USH-like phenotypes. The aminoacyl-tRNA synthetase (ARS) family comprises proteins responsible for attaching the appropriate amino acid to its corresponding tRNA molecule. Pathogenic bi-allelic variants in histidyl-tRNA synthetase (*HARS1)*, are associated with USH3B. Biallelic pathogenic variants in tyrosyl-tRNA synthetase 1 (*YARS1)*, are associated with infantile-onset multisystem neurologic, endocrine, and pancreatic disease 2 (IMNEPD2). SNHL and retinal symptoms have been described in some affected individuals. The purpose of the current work was to characterize the phenotype of individuals from three families, harboring rare missense variants in *YARS1*, and to functionally characterize these variants.

METHODS

Genetic analysis of affected individuals was performed by whole genome sequencing. Affected individuals underwent complete ophthalmic evaluation, hearing tests and a physical examination. Functional evaluation of the missense variants in mammalian cultured cells and in a yeast model is underway.

RESULTS

Two variants in the *YARS1* gene were identified in four individuals from three families. Three individuals from two Muslim Arab families which reside in the same village in Northern Israel were affected with SNHL and RP, and were diagnosed with USH1. Genetic analysis revealed an ultra rare homozygous variant in *YARS1*, c.790A>T; p.(Ile264Phe), which segregated with the phenotype in these families. Affected individuals demonstrated no additional features of IMNEPD2. In the third family, both parents originated from the same samll village in Spain. The proband presented with SNHL and RP, leading to a diagnosis of USH1. He also had hepatomegaly, myopathy, hypoglycemia, and mild intellectual disability, and was diagnosed with Hemochromatosis. Genetic analysis revealed compund heterozugous variants in the *HFE* gene (c.187C>G ;p.(His63Asp) and c.845G>A; p.(Cys282Tyr)), underlying Hemochromatosis type 1, as well as a rare homozygous variant in *YARS1*, c.176T>C; p.(Ile59Thr).

CONCLUSIONS

Our findings support the conclusion that SNHL and RP in the families described here are caused by the identified variants in the *YARS1* gene, and that some variants in this gene may lead to an USH-like phenotype, with or without additional, relatively mild, phenotypic features. Back to TOC

Cyclotorsion After Glaucoma Surgery: Quantitative Insights from Fundus Imaging

Alon Zahavi (1,2), David Carmon (3), Amir Msheal (1), Itay Gabbay (1,2), Basel Obied (4,5), Noa Cohen Sinai (4), Nitza Goldenberg Cohen (4,5), Noa Geffen (1,2)

(1) Ophthalmology Department and Eye Research Laboratory, Felsenstein Medical Research Center, Rabin Medical Center, Petach Tikva, Israel
(2) Gray Faculty of Medical and Health Sciences, Tel Aviv University, Tel Aviv, Israel
(3) Ophthalmology Department, Edith Wolfson Medical Center, Holon, Israel
(4) Ophthalmology Department, Bnai-Zion Medical Center, Haifa, Israel
(5) The Krieger Eye Research Laboratory, Bruce and Ruth Faculty of Medicine, Technion-Institute of Technology, Haifa, Israel

ABSTRACT

PURPOSE

To evaluate the development of cyclotorsional deviations following glaucoma surgery using quantitative fundus-based disc-fovea angle analysis.

METHODS

A retrospective study was conducted at Rabin Medical Center including 73 eyes that underwent glaucoma surgery (trabeculectomy, PreserFlo MicroShunt, Xen, or Ahmed valve implantation) and 72 non-surgical glaucoma control eyes. In each fundus image, a line was manually drawn between the optic disc center and the fovea, and the image was processed with an AI-based algorithm calculating the angle between this line and the horizontal axis. Postoperative measurements were compared both to the control group and to each eye's preoperative baseline at four postoperative timepoints: 1 week, 1 month, 3 months, and ≥6 months. Statistical analysis included Mann-Whitney and Fisher's exact tests with Bonferroni correction for multiple comparisons, and rank-biserial correlation (*r*) for effect size. Eyes with advanced AMD, extreme myopia, or poor-quality images where the fovea could not be identified were excluded.

RESULTS

A progressive postoperative torsional deviation was observed. PreserFlo eyes demonstrated a significant excyclotorsional shift one month after surgery ($p<0.05$, $r\approx0.45$), which diminished over time. Ahmed valve implantation was associated with a significant late and persistent excyclotorsional deviation at ≥6 months ($p<0.05$, $r\approx0.52$). Trabeculectomy produced a mild, non-significant incyclotorsional trend ($p\approx0.09$), while Xen showed no measurable effect. The location of the implant or bleb did not correlate with the degree of torsion.

CONCLUSIONS

Glaucoma surgeries produce small but quantifiable cyclotorsional changes that have not been systematically characterized before. Using AI fundus-based analysis, this study identifies distinct torsional patterns for different procedures and shows that these deviations are common yet remain clinically silent. The findings establish an objective framework for detecting subtle postoperative alignment changes and demonstrate the value of AI-assisted torsion measurement as a new outcome metric in glaucoSSma surgery research.

Back to TOC

Genetic regulation discovery in the aqueous humor outflow pathways, macula and optic nerve head proposes causal mechanisms for glaucoma

Puja A. Mehta[1,2], Rinaldo F. Catta-Preta[1,2], Abbi Engel[3,4], Jason P. Turner-Maier[1,2], Sudeep Mehrotra[1,2], Iris Cheng[1,2], Timothy Cherry[3,4], Janey L. Wiggs[1,2], Kinga Bujakowska[1,2], Ayellet V. Segrè[1,2]

[1]Department of Ophthalmology, Massachusetts Eye and Ear, Harvard Medical School, Boston, MA

[2]Broad Institute of Harvard and MIT, Cambridge, MA, USA

[3]Center for Developmental Biology and Regenerative Medicine, Seattle Children's Research Institute, Seattle, WA

[4]University of Washington, Department of Pediatrics, Seattle, WA

ABSTRACT

PURPOSE

Primary open-angle glaucoma (POAG), characterized by retinal ganglion cell death, is a leading cause of irreversible blindness worldwide, yet it has no cure. While elevated intraocular pressure (IOP), caused by reduced aqueous humor outflow in the trabecular meshwork (TM)/Schlemm's canal (SC) and ciliary body (CB), is a major risk factor, >30% of POAG patients have IOP in the normal range, suggesting IOP-independent processes may also affect optic nerve degeneration. >300 noncoding common variants have been associated with POAG risk, which may point to new causal mechanisms. However, genetic regulatory effects have not been measured in glaucoma-relevant eye tissues, aside for retina.

METHODS

We collected TM/SC, CB, macula (MR), and optic nerve head (ONH) samples from 100 postmortem non-diseased donor eyes, performed RNA-sequencing on all samples, whole genome sequencing (WGS) on the donors' DNA, and ATAC-seq on the 4 tissues from 6 donors. Quality control (QC) was performed on the omic datasets, gene expression was quantified using RNA-SeQC, splicing events were detected using LeafCutter, and open chromatin regions were detected with MACS2. Expression and splicing quantitative trait loci (eQTLs, sQTLs) mapping was applied to common variants (MAF>0.05) in *cis* (±1Mb) to all expressed genes, adjusting for sex, age, batch effects, top genotype principal components, and inferred expression covariates, using FastQTL. Colocalization analysis was applied to >300 POAG and >100 IOP GWAS loci and co-occurring e/sQTLs in any of the eye tissues using eCAVIAR.

RESULTS

QC yielded 86 TM/SC, 89 CB, 92 MR and 87 ONH high-quality RNA-seq and WGS samples. Tissue-specific and tissue-shared gene expression and splicing events, and >100k open chromatin regions across these tissues were detected. We identified 1,435 to 3,579 genes with significant eQTLs (eGenes) at false discovery rate (FDR)<0.05 and 763 to 2,207 genes with significant sQTLs (sGenes) per tissue, 7-16% of which were

not significant in any of the 49 GTEx v10 tissues. The eye tissue eGenes were enriched in metabolic and immune-related biological processes, and sGenes in mitochondrial processes (FDR<0.05). Significant colocalization was found for 50 POAG and/or IOP loci, e.g. *ANGPTL2* eQTL in TM, *IL34* eQTL in CB, *TXNRD2* eQTL in ONH, and *GCAT* Sqtl in MR. ATAC-seq peaks were used to fine-map the loci.

CONCLUSIONS

The ocular e/sQTLs proposed causal genes and tissues for POAG that may serve as new targets for IOP lowering or neuroprotective therapies.

NIH/NEI R01 EY031424, NIH/NEI P30 EY014104, Lions VisionGift Investigator-Concept Study Grant Back to TOC

Female Color vision deficiency is associated with increased prevalence of amblyopia, strabismus and ametropia

Edward Barayev MD, MHA[1,2]; Michael Shapiro MD, MSc[2,3]; Eran Greenbaum MD [2,4]; Yuval Ran MD, MHA, MPA[2,3], Assaf Gershoni MD[1,2], Gad Dotan MD[2,5]

(1) Department of Ophthalmology, Rabin Medical Center, Petach Tikva, Israel
(2) Gray Faculty of Medical & Health Sciences, Tel Aviv University, Tel Aviv, Israel
(3) Israel Defense Forces, Medical Corps, Ramat Gan, Israel
(4) DepartmenSSt of Ophthalmology, Meir Medical Center, Kfar Saba, Israel
(5) Ophthalmology Unit, Schneider Children's Medical center of Israel, Petach Tikva, Israel

ABSTRACT

PURPOSE

To examine the association between female color vision deficiency (CVD) and other ophthalmic disorders including amblyopia and strabismus.

METHODS

A retrospective, cross-sectional analysis of female adolescents undergoing military medical assessments between the years 2000 and 2020 was conducted.
The prevalence of ophthalmic conditions, such as amblyopia, strabismus, and ametropia, was examined in both females with CVD and those with normal color vision. Demographic and socioeconomic data were also collected and analyzed.

RESULTS

Included were 912 females with CVD (mean age 17.1 ± 0.2 years), found within a cohort of 621,471 Israeli army female recruits. Female adolescents with CVD had higher prevalence of amblyopia (4.61% vs 0.66%, p<0.001), strabismus (2.96% vs 0.81%, p<0.001), and ametropia (moderate – less than 6.00 diopters, 40.46% vs 37.48%, p<0.001, and high – higher than 6.00 diopters, 4.50% vs 1.95% p<0.001) compared to females with normal color vision. Specific refractive data was available for a subgroup of 256 CVD females, demonstrating higher prevalence of both mild to moderate hyperopia (up to +6.00 diopters, 7.36% vs 2.72%, p<0.001) and high hyperopia (≥+6.00 diopters, 1.16% vs 0.13%, p<0.001), but not for myopia or astigmatism.

CONCLUSIONS

CVD in females is strongly associated with strabismus, hyperopia and amblyopia, suggesting that early population screening for CVD at a young age could identify girls at a higher risk for preventable vision loss.

Back to TOC

Changes in Astigmatism in Children with Congenital Nasolacrimal Duct Obstruction Undergoing Probing and Irrigation

Itay Shavit MD [1,3], Omer Lev Ari MD[2], Hillah Levy Berkowitc MD [1], Oded Rock MD [1,2], Ofira Zloto MD[1,2,3]

[1]School of Medicine, Faculty of Medical and Health Sciences, Tel Aviv University, Tel Aviv, Israel.

[2]Goldschleger Eye Institute, Sheba Medical Center, Tel-Hashomer, Israel.

[3]Arrow Program for Medical Research Education, Sheba Medical Center, Ramat-Gan, Israel.

ABSTRACT

PURPOSE

Congenital nasolacrimal duct obstruction (CNLDO) is a frequent condition during infancy. While it is often self-limited, persistent cases may require probing and irrigation (P&I). Because this disorder affects the critical period of visual development, concerns have been raised about its potential role in amblyopia through induced refractive changes, particularly astigmatism.

METHODS

A Retrospective, single-center cohort study. Medical records of children with CNLDO treated at Sheba Medical Center (2009-2024) were reviewed. Inclusion required P&I and paired cycloplegic refractions before surgery and 6-36 months postoperatively. Pre- and postoperative spherical equivalent (SE) and cylinder were compared using paired t-tests, stratified by age at last procedure (<24 vs ≥24 months). Proportions with any measurable cylinder were tested with McNemar's test.

RESULTS

Of the 401 children screened, 25 met the inclusion criteria. Fourteen were treated before 24 months of age, and 11 at or after 24 months. SE showed a nonsignificant myopic shift (Δ = - 0.43D, p = 0.065). In contrast, cylinder values increased from -0.39 ± 0.70D to -0.87 ± 0.98D (p = 0.040). The proportion of measurable cylinder rose from 32% to 68% (p = 0.012). Later treated children had a greater mean increase (to -1.20 ± 1.14D), and among those with baseline cylinder, the mean reached -1.47D, which is a borderline amblyogenic value.

CONCLUSION

CNLDO is associated with increased cylinder and astigmatism, with children treated later in life showing an even higher risk of progression toward amblyogenic levels. These findings support structured postoperative refractive follow-up and early surgical intervention whenever possible. Back to TOC

Professionals' Perceptions of Vision Impairments of Children with Autism Spectrum Disorder

Liat Gantz[1], Ayelet Baisa[2] Lior Naamati Schneider[2]

(1) Department of Optometry and Vision Science, Jerusalem Multidisciplinary College (JMC), Israel
(2) Department of Communication Disorders, Jerusalem Multidisciplinary College (JMC), Israel
(3) Department of Health Systems Management, Jerusalem Multidisciplinary College (JMC), Israel

ABSTRACT

PURPOSE

Autism spectrum disorder (ASD) diagnosis relies on visual behaviors such as reduced eye contact, eye tracking, joint attention, delayed response to visual stimuli, and prolonged visual exploration of objects. However, these visual behaviors may also result from undiagnosed and untreated visual impairments, leading to diagnostic overshadowing and less effective treatment. This study explored how physicians who diagnose ASD and therapists who treat individuals with ASD perceive and address visual impairments, and how clinical reasoning and health system factors influence their integration into diagnostic and therapeutic processes.

METHODS

This qualitative study included in-depth interviews of 23 healthcare professionals (developmental pediatricians, psychologists, occupational and speech-language therapists) that were analyzed thematically to identify theoretical and emergent insights.

RESULTS

Four themes emerged. (1) Although practitioners are aware that vision should be assessed, vision assessments are an unstructured component in the diagnosis and treatment with practitioners not necessarily requiring examination results and/or recommending them and/or following up to ensure vision was assessed. (2) Practitioners did not consider visual impairment in the differential diagnosis, did not consider visual needs in therapeutic aids, and often prioritized hearing over vision, mainly due to limited professional awareness of the association between visual function and ASD. (3) Practitioners depended on parental responses, were limited in comprehension of the necessity in ongoing monitoring of visual capabilities or interpreting results of vision test summaries, and were limited in application of clinical tools and guidelines. (4) Interviewees underwent a reflective process triggered during the interview fostering an awareness and desire to explore further learning and adapt their practice accordingly.

CONCLUSIONS

A persistent gap exists between professionals' awareness of vision-related deficits and their systematic integration into ASD care. Structural barriers, such as limited follow-up mechanisms and dependence on parental initiative, often impede the translation of this awareness into action. Strengthening professional education, promoting interdisciplinary collaboration and holistic care protocols may enhance diagnostic accuracy and the overall intervention effectiveness. Back to TOC

Periocular Impetigo in Children: A Distinct Clinical Entity with Ocular Surface Involvement

Lital Smadar, Or Gil, Guy Ben Simo, Sharon Bloom Meirovich, Daphna Landau

(1) Goldschleger Eye Institute, Sheba Medical Center, Tel-Hashomer, Israel

ABSTRACT

PURPOSE

Periocular impetigo is underrecognized and often misdiagnosed as herpes simplex or molluscum contagiosum, leading to missed ocular-surface assessment. To characterize the clinical and microbiological profile of periocular impetigo with emphasis on anterior-segment findings, and to distinguish it from mimicking dermatologic/ocular conditions.

METHODS

Retrospective review (2009–2025) of patients with periocular rashes/lesions suspicious for impetigo. Comparative analyses included demographics, microbiology, and ocular-surface signs (conjunctival injection/discharge/irritation).

RESULTS

Sixty-eight patients were included (56% female; mean age 22.8 ± 14.6 years). Sixteen (23%) had a final diagnosis of periocular impetigo by a pediatrician/dermatologist, supported by swab testing when available. Impetigo patients were younger (median 7 vs. 12 years, p=0.047). *Staphylococcus aureus* (including MRSA) was isolated in 56% of tested cases. Conjunctival involvement occurred in 43.8% of impetigo cases vs. 11.5% of non-impetigo presentations (p=0.009).

CONCLUSIONS

Periocular impetigo may present with concurrent ocular-surface inflammation and should be included in the differential diagnosis of periocular rash and “conjunctivitis-like” presentations in children. Routine eyelid examination with slit-lamp evaluation of the conjunctiva and swab-based confirmation can improve diagnostic accuracy. Most cases respond to topical and/or oral antibiotics; heightened awareness of anterior-segment findings may facilitate earlier, targeted management.

Back to TOC

Myopia in Israeli children: Early educational exposure drives sex-specific patterns in ultra-orthodox children

Ravid Doron (1), Jonathan Levine (1), Ayelet Goldstein (2), Ariela Gordon-Shaag (1), Lisa A. Ostrin (3), Kevin Davidson (4) and Einat Shneor (1)

(1) Department of Optometry, Jerusalem multidisciplinary college, Jerusalem, Israel
(2) Department of Computer Science, Jerusalem multidisciplinary college, Jerusalem, Israel
(3) College of Optometry, University of Houston, Houston, TX, USA
(4) Texas Institute for Measurement, Evaluation, and Statistics, Houston, TX, USA

ABSTRACT

PURPOSE

To examine sex differences in refractive status within three educational systems: Religious (R), Secular (S), and Ultra-Orthodox (UO), and to determine whether these differences are explained by behaviors.

METHODS

Data were derived from the iRead Study. Participants were 6–12 years old and included 272 children (F 43%:M 57%) with best-corrected visual acuity of 6/9 or better. Cycloplegic autorefraction was performed, and Actiwatch devices recorded light exposure, activity, and sleep for 10–14 days. Parents completed questionnaires on demographics, parental myopia, near work, screen use, and educational environment. Myopia was defined as spherical equivalent refraction (SER) ≤−0.50D. Children were classified into R, S, or UO groups. Age was matched between boys and girls in each group. Statistical analyses included ANOVA for SE and axial length (AL), chi-square tests for myopia prevalence, and t-tests for behavioral and familial factors.

RESULTS

The findings for boys showed significant SER differences across groups ($p<0.001$). UO boys were more myopic (SE= −0.79±1.72D) than R boys (0.07±1.16D, $p<0.002$) and S boys (0.26±1.10D, $p<0.005$). Myopia prevalence in boys also differed (UO: 45.6%; R: 25.4%; S: 20.0%; $p<0.02$). Axial length did not differ among boys ($p=0.15$). In girls, SER ($p=0.17$), AL ($p=0.36$), and myopia prevalence ($p=0.45$) showed no group differences. Myopia prevalence showed no sex difference ($p>0.1$). Prevalence was 45.6% in UO boys vs. 30.0% in UO girls ($p=0.07$). In R, boys were more myopic than girls (0.07±1.16 vs. −0.04±1.20D; $p<0.04$) and had longer AL (23.27±0.99 vs. 22.87±0.82mm; $p<0.02$). In S, SE did not differ ($p=0.13$), but boys had longer AL (23.26±0.85 vs. 22.61±0.88mm; $p<0.001$). In UO, boys were more myopic (−0.79±1.72 vs. −0.36±1.75D; $p<0.03$) and had longer AL (23.60±1.07 vs. 22.93±1.07mm; $p<0.001$). Across all groups, there was no difference in age, parental myopia, near work or screen use (all $p>0.12$). However, boys spent more time outdoors than girls (all $p<0.05$), and UO boys also spent more school hours in school ($p<0.001$).

CONCLUSIONS

Boys showed more myopic refractions than girls in R and UO groups and had longer AL across all groups. Compared to girls, boys spent more time outdoors than girls in all groups and had longer school hours in the UO system. These findings suggest that the refractive differences may originate early in childhood, as UO boys begin intensive schooling at younger ages.

Back to TOC

Exploring the Shared Neurodegenerative Mechanisms Between Glaucoma and Alzheimer's Disease

Raz Rubinshtein (1), Basel Obied (1,2), Alon Zahavi (3,4), Talal Salti (1), Nitza Goldenberg-Cohen (1,2)

(1) The Krieger Eye Research Laboratory, Bruce and Ruth Faculty of Medicine, Technion- Institute of Technology, Haifa, Israel
(2) Department of Ophthalmology, Bnai-Zion Medical Center, Haifa, Israel
(3) Department of Ophthalmology & Laboratory of Eye Research, FMRC, Rabin Medical Center, Petach Tikva, Israel
(4) Gray School of Medicine, Faculty of Medical and Health Sciences, Tel Aviv University, Tel Aviv, Israel

ABSTRACT

PURPOSE

Glaucoma and Alzheimer's disease (AD) are major neurodegenerative disorders with increasing evidence of shared pathogenic pathways. Glaucoma involves progressive optic nerve degeneration and irreversible vision loss, often associated with elevated intraocular pressure (IOP) but also occurring independently of it. AD, the leading cause of dementia, results in progressive cognitive and functional decline. Epidemiological studies report higher co-prevalence of glaucoma and AD in older adults. This study assessed IOP in a transgenic AD mouse model to explore whether AD pathology is associated with altered ocular pressure as a potential shared neurodegenerative mechanism.

METHODS

Ten young (25 weeks old; 9 males and 1 female) and fifteen aged 5xFAD (57 to 60 weeks old; 5 males and 10 females) transgenic mice, a well established amyloidogenic model of AD, were examined. Aged matched control groups included ten young wild type (WT) mice (9 males and 1 female) and fourteen aged WT mice (7 males and 7 females). IOP was measured repeatedly without anesthesia using a rebound tonometer (Icare Tonolab) calibrated for mice. Four IOP measurement sessions were performed at approximately age of 25, 30, 32, and 36 weeks in young mice, and age of 58, 63, 66, and 69 weeks in aged mice, with all measurements conducted during midday hours (11:00–14:00) to minimize circadian variability.

RESULTS

IOP remained stable across most groups and time points. Aged 5xFAD mice exhibited transient, statistically significant fluctuations that showed an initial rise followed by a decrease. Age matched WT mice showed no significant longitudinal change. Aged 5xFAD mice demonstrated higher IOP than aged WT controls in only one of the four measurement sessions, occurring at approximately 63 weeks of age.

CONCLUSIONS

5xFAD mice did not exhibit sustained IOP elevation compared with WT controls. The transient fluctuations observed in aged animals likely reflect physiological variability rather than glaucoma-related pressure changes. Given that retinal ganglion cell loss and visual dysfunction have been reported in AD mouse models, our findings support the possibility that Aβ-driven neurodegeneration produces glaucoma-like features independently of ocular hypertension, indicating distinct mechanisms underlying visual field impairment in AD versus glaucomatous optic neuropathy. Back to TOC

Do yellow filters improve visual function in cases of simulated media opacity with and without glare

Rivki Bloom 1, Deborah Kassabi 1, Frantisek Pluhacek 2, Klara Kocianova 2, Kristyna Zidkova 2, Eliska Najmanova 2, Liat Gantz 1

(1) Department of Optometry and Vision Science, Jerusalem Multidisciplinary College, Jerusalem
(2) Department of Optics, Faculty of Science, Palacký University, Olomouc

Purpose This study examined the effect of simulated ocular media opacity on photopic and mesopic visual acuity (VA) and contrast sensitivity (CS), with and without glare. It further examined if a yellow filter could improve vision under these conditions.

METHODS

This prospective cross-over study included 30 adults (aged: 29 ± 9 years) with normal or corrected-to-normal vision who were tested monocularly, in pseudo-randomised order, under baseline and simulated opacity conditions (induced using Tiffen Black Pro Mist (BPM) filters 1 and 2). Each condition was examined with and without a Rodenstock L480 yellow filter. Photopic and adapted mesopic VA and CS were measured, and CS was assessed using the CSV-1000 at four spatial frequencies (3, 6, 12, and 18 cpd). The effect of mesopic glare on CS was measured using the Mesotest II.

RESULTS

Both BPM filters significantly reduced photopic and mesopic VA, with no improvement from the yellow filter. Photopic and mesopic CS decreased with both BPM filters for most spatial frequencies, except for photopic CS at 3 cpd. The yellow filter generally did not significantly effect on CS, except for a reduction at 6 cpd under baseline and mesopic conditions. Mesopic glare significantly reduced CS to near zero for both opacity levels, and the yellow filter did not mitigate this decline.

CONCLUSIONS

Simulated ocular opacity significantly impaired VA and CS, particularly under mesopic glare where CS was almost abolished. The yellow filter did not improve visual performance under any tested condition.

Back to TOC

Association between topical beta-blockers use and Parkinson's disease: Evidence from a real-world multicenter cohort

Yaara Lisai-Goldstein (1), Natan Lishinsky-Fischer (1), Nir Zontag (1), Jaime Levy (2)

(1) Faculty of Medicine, Hebrew University of Jerusalem, Jerusalem.
(2) Department of Ophthalmology, Hadassah Medical Organization and Faculty of Medicine, Hebrew University of Jerusalem, Jerusalem.

ABSTRACT

PURPOSE

To evaluate whether topical beta-blockers therapy in patients with glaucoma is associated with an increased risk of Parkinson's disease (PD) diagnosis compared with matched non-beta-blockers users.

METHODS

We performed a retrospective cohort study using the TriNetX network, which contains de-identified electronic health records from multiple healthcare organizations. Adults (≥18 years) with a diagnosis of glaucoma were identified and categorized as topical beta-blocker users or non-users. Propensity score matching (1:1) was applied based on demographic and clinical characteristics, including comorbidities and medications known to influence PD risk. Patients were followed for up to 10 years for incident PD. Hazard ratios (HRs) and 95% confidence intervals (CIs) were estimated using Cox proportional hazards models, and PD-free survival was evaluated with Kaplan–Meier analysis. Positive (bradycardia, syncope, dizziness) and negative (acute appendicitis) control outcomes were used for internal validation.

RESULTS

After matching, 41,950 patients remained in each cohort. During follow-up, 493 patients (0.587%) developed PD, 284 beta-blocker users and 209 non-users. The risk of

PD did not significantly differ between the groups (HR 1.075; 95% CI 0.899-1.286; p=0.703). Kaplan-Meier curvSes similarly showed no significant difference in PD-free survival (p=0.425). The positive and negative controls performed as expected, supporting the rigor and reliability of the study design.

CONCLUSIONS

In this large real-world cohort of glaucoma patients, topical beta-blocker use was not significantly associated with the risk of developing Parkinson's disease. Prospective studies are needed to further confirm these findings.

Back to TOC

Optimizing screening for type I retinopathy of prematurity using a machine learning-based risk prediction model

Hadas Mechoulam (1), Ayelet Goldstein (2), Milka Matanis-Suidan (1), Edna Granit (1,3), Hadas Ben-Eli (1,3)

(1) Department of Ophthalmology, Hadassah-Hebrew University Medical Center, Jerusalem
(2) Department of Computer Science, Jerusalem Multidisciplinary College, Jerusalem
(3) Department of Optometry and Vision Science, Jerusalem Multidisciplinary College, Jerusalem

ABSTRACT

PURPOSE

Retinopathy of prematurity (ROP) is a blinding disease that is preventable with appropriate screening and treatment. We aim to reduce the load of screening examinations using population specific machine learning (ML) tools.

METHODS

Several machine learning models were trained using gestational age, birth weight, and early weight gain on a retrospective cohort of premature infants admitted to Hadassah Neonatal Units between 2023-2025. SHapley Additive exPlanations (SHAP) were used to interpret ML predictions. Sensitivity, specificity, precision, and reduction in screening load for type I ROP detection in ML model, current practice, the North American screening criteria and the G-ROP screening criteria (gestational age > 29 weeks, birth weight < 1051 grams, and weight gain during days 10-39) were compared.

RESULTS

Out of 2,159 infants with available records, 193 infants met the inclusion criteria for G-ROP and ML evaluation and had complete data. Six infants developed type I ROP. The ML logistic regression model achieved 100% sensitivity, 82.9% specificity, and reduced screening by 77% relative to current practice, while G-ROP criteria reduced screening by only 15%. SHAP analysis showed that thresholds for gestational age, birth weight, and weight gain aligned with G-ROP cutoffs but integrated more features for improved discrimination.

CONCLUSIONS

A locally developed machine learning model preserved full sensitivity while substantially reducing unnecessary examinations compared to current practice, G-ROP and North American screening criteria. These findings highlight the importance of local validation and the potential of interpretable ML approaches to optimize ROP screening protocols.

Back to TOC

Outcomes of cataract surgery in infants under one year compared to children aged one to five years: A propensity-score-matched cohort study

Diala Abu Al-Halawa (1), Natan Lishinsky-Fischer (2), Hadas Mechoulam (1), Irene Anteby (1)

(1) Ophthalmology Department, Hadassah Medical Center, Jerusalem, Israel
(2) Faculty of Medicine, The Hebrew University of Jerusalem, Jerusalem, Israel

ABSTRACT

PURPOSE

To compare the incidence of postoperative complications in children undergoing cataract surgery before the age of one year with those aged one to five years, with and without IOL implantation.

METHODS

Retrospective cohort study of children under the age of five who underwent cataract surgery, identified from the TriNetX Global Collaborative Network. Two cohorts were constructed based on age at the time of first cataract-related surgery: infants (≤1 year) and young children (1-5 years). Propensity score matching was performed to control for demographic and clinical differences. The prevalence of glaucoma, strabismus, secondary cataract, secondary intraocular lens (IOL) implantation, and retinal detachment was compared over a 7-year follow-up period using survival analyses and Cox proportional hazards models.

RESULTS

After 1:1 matching, 1,293 children were included in each group. Over a 7-year follow-up period, infants who underwent surgery at or before one year of age had significantly higher risks of glaucoma (14.35% vs. 6.7%, HR 1.79, 95% CI: [1.37, 2.33], p<0.0001), glaucoma surgery (7.6% vs. 2.76%, HR 2.38, 95% CI: [1.6, 3.53], p<0.0001), secondary IOL insertion (9.94% vs. 1.97%, HR 4.1, 95% CI: [2.63, 6.41], p<0.0001) and strabismus (42.12% vs. 18.36%, HR 2.25, 95% CI: [1.87, 2.71], p<0.0001) compared to those aged one to five. In subgroup analysis per IOL status, aphakic infants had higher risk of glaucoma (24.76% vs. 4.27%, HR = 6.02, 95% CI [3.06, 11.87]; p<0.0001), glaucoma surgery (9.63% vs. 4.33%, HR = 4.19, 95% CI [1.58, 11.11]; p=0.0018), and glaucoma treatment (20.56% vs. 4.57%, HR = 11.85, 95% CI [4.26, 33.01]; p<0.0001), when compared to pseudophakia infants. However, differences in secondary cataract, retinal detachment and endophthalmitis rates were not statistically significant. Among aphakic infants, surgery before one year was also linked to higher risks of glaucoma procedures, secondary cataract, strabismus and need for secondary IOL as compared with aphakic children undergoing later cataract surgery. Among pseudophakic groups, early surgery before one year was mainly associated with strabismus without increased glaucoma risk.

CONCLUSIONS

Cataract surgery performed in infancy is associated with an increased risk of glaucoma, need for glaucoma intervention, and strabismus compared to surgery performed between ages one and five. The risk for glaucoma is higher in infants left aphakic when compared to pseudophakia in this age group.

Back to TOC

Glaucoma and pregnancy: Treatment patterns and medication adjustments

Jacob Megreli (1,2), Yogev Giladi (2,3), Alon Tiosano (1,2), Yael Sharon (1,2), Noa Geffen (1,2), Alon Zahavi (1,2,4)

(1) Department of Ophthalmology, Rabin Medical Center, Petach Tikva
(2) Gray Faculty of Medical and Health Sciences, Tel Aviv University, Tel Aviv
(3) Department of Ophthalmology, Shamir Medical Center, Zerifin
(4) Laboratory of Eye Research, Felsenstein Medical Research Center, Rabin Medical Center, Petach Tikva

ABSTRACT

PURPOSE

Managing glaucoma during pregnancy is challenging, requiring a balance between effective intraocular pressure control and medication safety for both mother and fetus. Many anti-glaucoma drugs pose potential risks, often leading to treatment modifications or discontinuation. However, data on pregnant women with glaucoma and their medication patterns remain scarce. This study aims to assess the characteristics of this population and analyze changes in their anti-glaucoma treatment during pregnancy.

METHODS

This population-based, cross-sectional study analyzed pregnant patients with a glaucoma diagnosis within Clalit Health Services between 2010 and 2022. Demographic data, medical and ocular history, and anti-glaucoma medication use were collected.
Medication usage was documented from one year prior to pregnancy through the duration of pregnancy. Changes in treatment regimens were assessed.

RESULTS

A total of 161 women with glaucoma became pregnant, representing 0.037% of all pregnant women in the Clalit Health Services database during the study period. The average number of anti-glaucoma medications per patient decreased by 44% during pregnancy (pre-pregnancy: 1.42±0.58 vs. during pregnancy: 0.80±0.67, $p<0.001$). Beta-blockers were the most frequently used medication before and during pregnancy. SProstaglandin analogs, beta-blockers, alpha agonists, and topical carbonic anhydrase inhibitors usage decreased during pregnancy by 57.1%, 35%, 33.3%, and 32.4%, respectively (all, $p<0.001$). Only three patients required an increase in treatment, while 69 (43%) discontinued all glaucoma medications during pregnancy. Among those who discontinued treatment, 81% had previously been on a single anti-glaucoma agent.

CONCLUSIONSS

This study highlights a significant reduction in anti-glaucoma medication use among pregnant women with glaucoma, with a substantial proportion discontinuing treatment entirely. Beta-blockers were the most commonly used medication. These findings emphasize the need for individualized risk-benefit assessments when managing glaucoma in pregnant patients. Further research is essential to develop safe and effective treatment strategies that optimize both maternal ocular health and fetal safety. Back to TOC

Natural killer cells may promote corneal graft failure via direct corneal fibroblast killing in a murine model of pediatric penetrating keratoplasty

Krauthammer, Mark[1]; Esquivel Herrera, Antonio[1]; Bednar, Michael[1]; Chauhan, Sunil[1]; Dana, Reza[1]; Dohlman, Thomas H.[1]

(1) Schepens Eye Research Institute, Harvard Medical School, Boston, MA, United States

ABSTRACT

PURPOSE

Penetrating keratoplasty survival is significantly decreased in the pediatric population, and heightened innate immunity has been implicated as a factor in decreased graft survival. Here, we evaluate the specific mechanisms by which Natural Killer (NK) cells contribute to graft failure in a murine model of pediatric penetrating keratoplasty.

METHODS

Donor corneal grafts from 10-week-old C57BL/6 male mice were transplanted into young (3.5-week-old) or adult (10-week-old) BALB/c male mice. Graft survival was followed for 8 weeks post transplantation. A subset of transplant recipients was euthanized at day 14 and the population of graft-infiltrating NK cells was evaluated by flow cytometry. Quantities of all NK cells (CD45+CD3-CD49+) and activated NK cells (CD45+CD3-CD49+IFNγ+) were assessed. In vitro co-cultures consisting of NK cells and corneal fibroblasts were performed and fibroblast cell viability was assessed after 24 hours using the CellTiter 96™ Aqueous (MTS) assay. A subset of NK cells was activated with IL-12 (10ng/ml).

RESULTS

Eight-week graft survival was 20% in young mice and 45% in adult mice. On flow cytometric analysis, there were significantly higher frequences of graft-infiltrating NK cells in young compared to adult recipients (12.95±4.8 vs 4.55±1.5 percent out of corneal WBC, for young and adult mice, respectively, p<0.01), with similar frequencies of activated NK cells (1.83±0.9 vs 2.09±1.1 percent out of corneal WBC, for young and adult mice, respectively, p=0.35). Significantly lower viability of corneal fibroblasts was seen upon co-culture with activated NK cells versus non-activated NK cells (81.5±0.1 vs 94.36±6.4, p=0.03).

CONCLUSIONS

In a murine model of penetrating keratoplasty, young recipients had lower corneal graft survival and greater NK cell graft infiltration. The increased presence of NK cells, along with decreased corneal fibroblast viability upon co-culture with NK cells in vitro, suggest that NK cell-mediated killing of corneal fibroblasts may contribute to the decreased graft survival seen in young mice.

Grants: Research to Prevent Blindness Career Development Award Alcon Research Institute. Back to TOC

Small-volume NanoDropper delivery maintains efficacy of tropicamide, latanoproSst and brinzolamide-timolol: Insights from canine eyes

Lionel Sebbag (1), Bar Fruchter (1), Sara Afar (1), Oren Pe'er (1), Ron Ofri (1)

(1) Koret School of Veterinary Medicine, The Hebrew University of Jerusalem, Rehovot, Israel

ABSTRACT

PURPOSE

To compare the pharmacodynamic effects of small-volume drop delivery using the NanoDropper adapter versus conventional delivery on pupil diameter (PD) and intraocular pressure (IOP) following topical administration of tropicamide, latanoprost, and brinzolamide-timolol in dogs.

METHODS

In a prospective randomized study, eight healthy adult dogs underwent three treatment sessions separated by ≥1-week washout. In each session, one eye received a single small-volume drop eluted through a NanoDropper adapter and the fellow eye received a standard-volume drop (using a commercial bottle) of 0.5% tropicamide, 0.005% latanoprost or 1% brinzolamide / 0.5% timolol. PD and IOP were measured at baseline and up to 8 h. Volume of drops delivered by both methods was measured. Data were analyzed using repeated-measures ANOVA, paired t-tests, and area under the curve (AUC) comparisons.

RESULTS

The mean dispensed volume per 100 drops was 38.6 ± 5.0 µL (conventional) and 11.3 ± 1.6 µL (NanoDropper), representing a ~70% reduction ($P < 0.001$). For tropicamide, both delivery methods induced significant ($P \leq 0.019$) mydriasis from 1-3 h (NanoDropper) and 1-4 h (control); PD AUC was slightly lower in NanoDropper eyes ($P = 0.009$) but IOP was unaffected by method ($P = 0.814$). For latanoprost, both delivery methods induced significant miosis from 20 min onwards ($P < 0.001$) and significant IOP reduction from 2 h onwards ($P \leq 0.037$). PD was larger in NanoDropper vs. control eyes from 5-8 hours ($P \leq 0.041$), yielding a slightly larger PD AUC ($P = 0.016$). IOP decreased similarly (−3.3 to −3.9 mmHg) in both groups ($P = 0.278$). For brinzolamide-timolol, both delivery methods induced significant miosis from 15 min onwards ($P < 0.001$) and significant IOP reduction from 40 min onwards ($P \leq 0.046$). IOP decreased similarly (−4.5 to −4.6 mmHg) in both groups ($P = 0.969$).

CONCLUSIONS

Across three pharmacologic classes, small-volume delivery via NanoDropper preserved the overall ocular effects of tropicamide, latanoprost, and brinzolamide-timolol on PD and IOP. These findings support the NanoDropper as a practical strategy to reduce drop volume, waste, and potential side-effects and toxicity while maintaining clinical efficacy in treated eyes. Back to TOC

An Immunocompetent Young Adult with Acute Vision Loss

Aviv Fineberg[1,3], Axel Petzold[4,5], Iliya Simantov[1,3], Yamit Cohen-Tayar[1,2,3], Omer Bialer[1,3], Hadas Stiebel-Kalish[1,2,3]

(1) Department of Ophthalmology, Rabin Medical Center, Petah Tikva, Israel
(2) Laboratory of Eye Research, Felsenstein Medical Research Center, Tel Aviv University
(3) Gray Faculty of Medical and Health Sciences, Tel Aviv University, Tel Aviv, Israel
(4) Moorfields Eye Hospital NHS Foundation Trust & National Hospital for Neurology and Neurosurgery, University College London, Hospitals NHS foundation Trust, London, UK
(5) Queen Square Institute of Neurology, UCL, London, UK

ABSTRACT

PURPOSE

To describe the diagnostic and management challenges in differentiating infectious from para infectious optic neuritis (ON) in the setting of an acute viral infection, demonstrated by a rare case of cytomegalovirus (CMV) associated ON in an immunocompetent young adult.

METHODS

Evaluation included ophthalmic examination, visual field testing, magnetic resonance imaging of the brain and orbits, cerebrospinal fluid analysis and comprehensive infectious and autoimmune laboratory testing. A focused literature review was conducted to aid in differentiating infectious ON from para infectious ON, a difference which dictates management.

RESULTS

The clinical and paraclinical evaluation were consistent with bilateral ON with severely impaired visual fields, bilateral retrobulbar pain, and asymmetric disc edema. The patient presented with bilateral headaches, malaise, elevated liver enzymes, splenomegaly and positive CMV IgM serology as well as detectable CMV particles on polymerase chain reaction (PCR). Fundoscopy was monitored closely to ensure continuous lack of CMV retinitis. The patient experienced rapid improvement in pain and visual fields following intravenous methylprednisolone (IVMP), without antiviral therapy. The lack of CMV retinitis, the excellent response to IVMP, and the fact that the patient was immunocompetent support a para infectious, immune mediated etiology rather than direct viral optic nerve involvement.

CONCLUSIONS

In immunocompetent adults with acute CMV infection, bilateral ON without retinitis is more likely to represent a para infectious rather than infectious ON. Recognizing the distinguishing features of each etiology is essential for selecting appropriate management and avoiding unnecessary antiviral therapy. This case underscores the importance of familiarity with the updated-ON diagnostic and classification criteria, the clinical distinctions between infectious and para infectious ON and the value of early treatment.

Back to TOC

Nasal vs Temporal Melanopsin-Mediated Pupillary Light Reflex Reveals Retinal Circuit Alterations in Brain Lesions

Tzur Feldstein (1,2,3), Amit Hamburg (1,2), Shlomit Zorani (1,2), Daniel Moverman (1,2), Estela Derazne (2), Marian Haiadry (1,2), Sagi Harnof (4), Jacob Zauberman (2,5), Anton Wohl (2,5), Zvi R. Cohen (2,5), Ruth Huna-Baron (1,2), Ygal Rotenstreich (1,2), Ifat Sher (1,2)

(1) Goldschleger Eye Institute, Sheba Medical Center, Tel-Hashomer, Israel
(2) Gray Faculty of Medical and Health Sciences, Tel-Aviv University, Tel Aviv, Israel
(3) Arrow Program for Young Researchers, Sheba Medical Center, Tel-Hashomer, Israel
(4) Department of Neurosurgery, Rabin Medical Center, Petach Tikva, Israel
(5) Department of Neurosurgery, Sheba Medical Center, Tel-Hashomer, Israel

ABSTRACT

PURPOSE

To assess the effect of anterior and posterior intracranial lesions on the visual pathways mediating the pupil light response (PLR) at the central and peripheral retina.

METHODS

Seventeen patients with intracranial lesions and seventy-four age-similar controls were enrolled. Patients were divided into three groups based on the lesion location: group I included patients with brain tumors involving the anterior visual pathway. Group II included patients with brain tumors involving the optic radiation with no apparent contact with the optic nerve or optic tract. Group III included patients with lesions with no apparent contact with the optic nerve, optic tract, or optic radiation neurons. The PLR for small (0.43□) blue and red light stimuli presented at the central and peripheral visual field (VF) locations were measured using Chromatic Pupilloperimetry**.**

RESULTS

Cone- and rod-mediated PLR did not significantly differ from the controls. In contrast, the melanopsin-mediated PLR was attenuated in all patient groups at the central and nasal targets, while at the temporal target, significant impairment was observed only in groups I and group II compared to the controls. Group I showed the highest discrimination at the temporal location (ROC AUC=88.06%, $p<0.0001$). Group II showed the highest discrimination at the temporal location (ROC AUC=84.52%, $p<0.0001$). Group III showed the highest discrimination at the central location (ROC AUC=80.31%, $p<0.0001$).

CONCLUSIONS

Melanopsin-mediated PLR is selectively impaired by intracranial lesions, with distinct spatial patterns reflecting lesion location. Chromatic pupilloperimetry provides objective discrimination between anterior and posterior pathway involvement, supporting its potential as a non-invasive biomarker for brain lesion localization and monitoring in clinical practice. Back to TOC

Chromatic Pupilloperimetry for Objective Diagnosis and Monitoring of Patients with Pseudotumor Cerebri

Jonathan Zontag (1,2,3), Yossi Eshel (1), Ifat Sher (1,4), Ruth Huna-Baron (1,4), Ygal Rotenstreich (1,4)

(1) The Goldschleger Eye Institute, Sheba Medical Center, Tel Hashomer, Israel
(2) Arrow Program for Young Researchers, Sheba Medical Center, Tel Hashomer
(3) Faculty of Medicine, Hebrew University of Jerusalem, Jerusalem, Israel
(4) Ophthalmology Department, Gray Faculty of Medical and Health Sciences, Tel-Aviv University, Tel Aviv, Israel

ABSTRACT

PURPOSE

To characterize rod, cone and melanopsin mediated pupil responses (PLR) for small focal chromatic light stimuli presented at peripheral and central retinal locations in patients with Pseudotumor Cerebri (PTC) before and after initiation of intracranial pressure (ICP) reduction treatment**.**

METHODS

9 PTC patients (all females, Age: 29.1±8.5 YO) and 15 age-similar healthy controls (all females, Age: 27.2±9.8 YO) were enrolled. The pupil light responses (PLR) for small (0.43degrees) and short (1 second) red (624 ± 5 nm, 1000 cd/m2) and dim blue light stimuli (485 ± 5 nm, 170 cd/m2) presented at 54 locations of a 24-2 visual field were recorded and the PPC (percentage of pupil constriction) was calculated. In addition, the PLR for prolonged (8 seconds) bright blue light stimuli (485 ± 5 nm, 6000cd/m^2) presented at four central and four peripheral VF locations was recorded, and the PPR (percentage of pupil recovery) was calculated. Patients underwent follow-up chromatic pupilloperimetry tests 7 days and 3 months after initiation of ICP-lowering treatment. All subjects underwent a complete ophthalmic exam, standard Humphrey automated perimetry (24-2), color vision test, best-corrected visual acuity test, and Optical Coherence Tomography (OCT) imaging**.**

RESULTS

In the first visit, slower maximal contraction velocity in response for blue and red light stimuli were recorded in the patients compared to controls in the right eye (10.5 ± 22.4 pixel/sec vs. 19.53 ± 7.89 pixel/sec, $p < 0.0001$; 3.68 ± 20.34 pixel/sec vs. 10.14 ± 6.7 pixel/sec, $p < 0.0001$, respectively) and the left eye (17.7 ±9.5 pixel/sec vs. 22.8 ± 7.3 pixel/sec, $p < 0.0001$; 10.25 ± 7.4 pixel/sec vs. 12.6 ± 7.3 pixel/sec, $p < 0.0001$, respectively). No statistically significant differences were observed in the melanopsin-related pupil recovery. However, there was a trend towards faster pupil recovery in patients' eyes compared with controls in the nasal targets**.**

CONCLUSIONS

Patients with PTC exhibit impaired extrinsic activation of melanopsin-expressing retinal ganglion cells, most evident in reduced pupil response velocity, accompanied by a measurable but less pronounced deficit in intrinsic activation. Back to TOC

The role of CREB in uveal melanoma metabolism

Maria Gimmelshein-Vatkin (1,2), Ori Shalev (3), Alik Honigman (2), Shahar Frenkel (1,4)

(1) The Ocular Oncology Laboratory, Faculty of Medicine, Hebrew University of Jerusalem, Jerusalem, Israel; (2) Department of Biochemistry and Molecular Biology, IMRIC, The Hebrew University-Hadassah Medical School, Jerusalem, Israel; (3) The Metabolic Profiling Unit, The Research Core Facility, The Faculty of Medicine, The Hebrew University of Jerusalem, Israel; (4) Ocular Oncology Unit, Division of Ophthalmology, Hadassah Medical Center, Jerusalem, Israel

ABSTRACT

PURPOSE

In a previous work, we found that uveal melanoma (UM) mouse xenografts with CREB knockdown have a markedly inhibited growth and do not express the major tumor glucose transporter (Glut-1). The purpose of this work is to uncover the mechanism leading to this finding and the changes in the tumor metabolism.

METHODS

We infected UM cells with Lenti-vectors expressing mCherry (LmCh) and both mCherry and shRNA targeting CREB (LmCh-CREB). 48hrs post-infection, the cells were cultured in normoxic or hypoxic conditions for an additional 30hrs before they were tested for viability and infection rate by FACS. RNA was extracted for Real-Time qPCR to assess the knockdown efficiency. Infection efficacy was 96% for LmCh and LmCh-CREB. Knockdown efficacy was 62%. Over 209 metabolites were identified using LCMS-based metabolomics study.

RESULTS

Metabolomic analysis of UM cells in normoxia and hypoxia demonstrates that CREB knockdown decreases energy production (e.g., 34% reduction of Glucose-6-phosphate and a 50% reduction of Fructose-6-phosphatase in normoxia), mostly in normoxic vs. hypoxic conditions. Additionally, there increases in the levels of metabolites in the ferroptosis pathway in hypoxia were markedly attenuated by CREB knockdown (L-Cystine –44%, Glutamine –33%), indicating that this pathway is active in UM cells.

CONCLUSIONS

These findings provide a molecular and metabolic explanation for how CREB knockdown attenuated UM xenograft growth.

Back to TOC

Predictive Value of Macular Ganglion Cell Thinning Artifact for Disease Severity in Pediatric Idiopathic Intracranial Hypertension

Miriam Ehrenberg, MD [1, 2]; Amir Sternfeld, MD [1,2], Raz Tshuva, MD [3]; Nili Golan, MD [2, 3]; Gad Dotan, MD [1, 2]

(1) Ophthalmology Unit, Schneider Children's Medical Center, Petah Tikva, Israel
(2) Gray Faculty of Medical & Health Sciences, Tel Aviv university, Tel Aviv, Israel
(3) Ophthalmology department, Rabin Medical Center, Petah Tikva, Israel

ABSTRACT

PURPOSE

In children and adolescents, idiopathic intracranial hypertension (IIH) manifests with clinical features that differ from those observed in adults. Optical coherence tomography (OCT) provides a non-invasive method to evaluate optic nerve structure, including the peripapillary retinal nerve fiber layer (RNFL) and ganglion cell layer (GCL), which may serve as objective indicators of disease severity and progression. Our aim was to identify OCT-based risk factors predictive of greater GCL loss in pediatric patients with IIH, thereby enabling early stratification of patients at higher risk for irreversible damage.

METHODS

We conducted a retrospective analysis of clinical and OCT imaging data, focusing on RNFL and GCL dynamics over time, in a cohort of pediatric patients diagnosed with IIH. The study aimed to evaluate structural changes and identify prognostic imaging markers associated with poorer outcomes.

RESULTS

Thirty-four children were included. OCT analysis categorized patients into two distinct subgroups based on their baseline average GCL thickness: Group 1, with a GCL thickness < 60 µm, and Group 2, with GCL thickness ≥ 60 µm. Children from group 1 had higher RNFL measurements at presentation and lower final GCL levels, as compared to Group 2.

CONCLUSIONS

OCT-based parameters, particularly peripapillary RNFL thickness >300 µm and GCL thickness <60 µm at presentation, are associated with increased risk of final GCL loss in pediatric patients with IIH. These findings suggest that early OCT evaluation can support risk stratification and guide follow-up intensity in this population.
Back to TOC

Tumor-specific inhibition of retinoblastoma cells' ability to respond to hypoxia as a treatment for vitreal seeding in a mouse xenograft model

May Rian (1), Maria Gimmelshein-Vatkin (1,2), Sondus Aref (1,2), Alik Honigman (2), Shahar Frenkel (1,2,3)

(1) The Ocular Oncology Laboratory, Faculty of Medicine, Hebrew University of Jerusalem, Jerusalem, Israel; (2) Department of Biochemistry and Molecular Biology, IMRIC, The Hebrew University-Hadassah Medical School, Jerusalem, Israel; (3) Ocular Oncology Unit, Division of Ophthalmology, Hadassah-Hebrew University Medical Center, Jerusalem, Israel

ABSTRACT

PURPOSE

We found that CREB knockdown (KD) increases the sensitivity of hepatocellular carcinoma (HCC) to hypoxia and increases the sensitivity of HCC and uveal melanoma to chemotherapy, especially in hypoxia. Retinoblastoma (Rb) is the model of hypoxia sensitivity, but aggressive Rb, especially vitreal seeds, survives in hypoxic conditions. The purpose is to test whether CREB-KD inhibits Rb growth and increases its sensitivity to chemotherapy in a mouse xenograft model.

METHODS

We used lenti vectors expressing mCherry (LmCh) to monitor the infection rate and shRNA targeting mCh-CREB (Lmch-CREB) to infect Y79 cells, which already express *luc*. 48Hr post-infection, the cells were injected into the vitreal cavity of the left eye of SCID mice. Seven days post-inoculation, the eyes were injected with either saline or a suboptimal dose of topotecan (0.0075□g/□l) to allow us to detect the combined effect of CREB-KD and topotecan. Tumor growth was monitored *in vivo* with the IVIS camera. Then, in a similar experiment, we inoculated mouse eyes with luc-expressing Rb cells and a week later infected the eyes with the lenti vectors to monitor the therapeutic feasibility of *in vivo* infection.

RESULTS

Infection efficacy was 96% for LmCh and LCREB. Knockdown efficacy was 20%. CREB-KD reduced the intraocular growth rate by 30%. The growth of tumors with CREB-KD treated with topotecan was reduced by 30.7% vs. tumors with normal levels of CREB treated with topotecan, indicating a synergistic effect. In vivo infection resulted in a growth inhibition of 25%. The growth of tumors with CREB-KD treated with topotecan was reduced by 50.0% vs. tumors with normal levels of CREB treated with topotecan, indicating a synergistic effect.

CONCLUSIONS

CREB-KD reduces Rb tumor growth in a mouse xenograft model. Moreover, it increases the sensitivity of the tumor cells to chemotherapy. Additionally, we have proven the feasibility of this vector as a therapeutic tool. Further work is required to improve the knockdown efficiency and the dosing before moving towards a clinical trial.

Back to TOC

A life course effect of mild carotid stenosis on brain morphology, eye morphology and behavior: A rat model

Arieh S Solomon, MD, PhD[1,2], Rudoler N .VMD, PhD, [1]Piontkewitz Y.[3] PhD, Tzameret A., [1]PhD Burzel M., MSc, Ziv H. PhD, Pri - Chen S., PhD, Nitzan A., PhD

(1) Goldschleger Eye Research Institute, Faculty of Medicine, Tel Aviv University
(2) Sagol School of Brain Sciences, Faculty of Life Sciences
(3) Straus Center for Computational Neuroimaging

ABSTRACT

PURPOSE

Medical society considers that, in human, carotid stenosis of 80% and more might be the cause of clinical symptoms such as transient ischemic attack. When carotid stenosis exists, but no symptoms are expressed, the condition is called Asymptomatic Carotid Stenosis. Our hypothesis is that carotid stenosis of lesser degree such as 20% - 40% may damage gradually the brain along the time course and be a high-risk factor of brain function and brain diseases such as AD.

METHODS

Male laboratory rats, 12 weeks old underwent, carotid stenosis on the right side and an equal number underwent a bilateral carotid stenosis. The animals were kept alive 11months to 13 months. At the end of the term Evaluation of the brain morphology by MRI, histological evaluation of retina,
and behavioral test were done.

RESULTS

MRI revealed brain damage in the thalamus and hypocampus area. Bilateral carotid occlusion crated much more damage than unilateral. Behavioral tests, Morris water maze and Open Field presented slow regress in cognitive function which was expressed by growing latency in response to the exposure to the two cognitive tests. Histology of the retina presented death of retinal ganglion cells in both eyes.

CONCLUSIONS

The research presents clear data that strength our hypothesis that mild carotid stenosis is not an asymptomatic pathology. We must change our protocol of treating the pathology and evaluate the brain function as soon as mild carotid stenosis develops and start anticholesterol treatment to stop and might dissolve the plaque creating the stenosis?!
Back to TOC

Vascular-targeted photodynamic therapy eradicates conjunctival melanoma tumors

Eilon Shcolnik [1], Keren Ben-Yaakov [1], Ortal Zaks [1], Ziv Rotfogel [1,2], Arie L. Marcovich [1,2], Avital Eisenberg-Lerner [1]

(1) Ophthalmology Research Laboratory, Department of Ophthalmology, Kaplan Medical Center, Rehovot, Israel
(2) Faculty of Medicine, Hadassah Medical School, The Hebrew University of Jerusalem, Israel

ABSTRACT

PURPOSE

Conjunctival melanoma is an aggressive ocular malignancy associated with significant morbidity and mortality. Management typically involves margin-controlled excision, which must carefully balance complete tumor removal with preservation of conjunctival and eyelid structure and function. Narrow margins risk local recurrence, whereas overly extensive resection can cause significant anatomical and functional compromise. Novel therapeutic approaches are needed to either reduce tumor burden prior to surgery or serve as standalone treatments, improving outcomes while minimizing morbidity. We propose vascular Targeted Photodynamic Therapy (VTP) through activation of the photosensitizer WST11 as a minimally invasive approach to addresses the unmet need in the treatment of conjunctival melanoma, by selectively induce tumor cell death. Specifically, WST11-VTP is activated by near infrared light, is confined to tumor vasculature and triggers localized vascular collapse and tumor necrosis.

METHODS

We employed an orthotopic mouse model of conjunctival melanoma to examine the efficacy of WST11-VT treatment of conjunctival tumors. Luciferase-expressing B16 cells were implanted subconjunctivally. Tumor bearing mice were treated with WST11-VTP and near infra red illumination, or illumination only as control. Tumor growth was monitored by bioluminescence imaging and survival was recorded. Representative tumors were analyzed by histology to identify tumor necrosis.

RESULTS

Mice treated with WST11 showed a marked and sustained reduction in tumor burden, associated with rapid and extensive tumor necrosis within 48 hours of treatment. Further, WST11-treated mice demonstrated significantly prolonged survival compared to controls.

CONCLUSIONS

These results suggest that WST11-VTP can effectively eradicate local conjunctival melanoma and significantly improve survival in mice. Back to TOC

Presumed Thyroid Eye Disease Without Systemic Thyroid Dysfunction or Detectable Autoantibodies: A Clinical Cohort Study

Tiran Golani (1,2) David Carmon (1,2,3) Bar Klain (1,2) Elad Alexander (1,2) Havi Murad (4) Nancy Agmon-Levin (2,5) Tali Cukierman-Yaffe (2,6) Ayelet Priel (1,2) Ofira Zloto (1,2) Daphna Landau (1,2) Guy J. Ben Simon (1,2)

(1) Goldschleger Eye Institute, Sheba Medical Center, Ramat Gan.
(2) Faculty of Medical & Health Sciences, Tel-Aviv University, Tel-Aviv.
(3) Department of Ophthalmology, Wolfson Medical Center, Holon.
(4) The Gertner Institute for Epidemiology and Health Policy Research, Sheba Medical Center, Ramat-Gan.
(5) Clinical Immunology, Angioedema and Allergy institute, The Zabludowicz Center for Autoimmune Diseases, Sheba Medical Center, Ramat Gan.
(6) Division of Endocrinology & Metabolism, Sheba Medical Center, Ramat Gan.

ABSTRACT

PURPOSE

To investigate patients with clinical and radiologic evidence of thyroid eye disease (TED) who lacked thyroid dysfunction and autoantibodies at presentation, representing a rare subset of euthyroid TED.

METHODS

This retrospective cohort study included all patients evaluated at the multidisciplinary TED Clinic of a tertiary ophthalmology center between 2008 and 2024. Presumed TED was defined by characteristic clinical and radiologic findings of TED with normal thyroid function and negative autoantibodies at baseline. Demographic, clinical, and treatment characteristics were compared between presumed and confirmed TED groups.

RESULTS

A total of 362 patients were included in the analysis, of whom 18 (5%) met criteria for presumed TED. Male sex was more common in presumed TED (61.1% vs. 27.6%, P = 0.0021), and family history of thyroid disease was less frequent (6.3% vs. 29.8%, P = 0.0424). Disease duration at presentation was shorter in presumed TED (8.0 vs. 25.0 weeks, P = 0.0026). Visual acuity, proptosis, diplopia, and clinical activity score were comparable between groups during follow-up. Systemic corticosteroids were used more often in presumed TED (27.8% vs. 10.5%, P = 0.0239), and orbital steroid injections were administered only in this group (5.6% vs. 0%, P < 0.0001). Four presumed TED patients developed TSI antibodies during follow-up.

CONCLUSIONS

SPresumed TED accounted for 5% of patients and exhibited male predominance and higher corticosteroid use. A subset developed TSI antibodies during follow-up, while others remained seronegative. Given the rarity of antibody-negative TED, this cohort represents one of the largest systematically characterized series to date.

Back to TOC

Vitreoretinal lymphoma diagnosis by vitreous DNA methylation patterns

Maya Eiger-Moscovich (1,2), Amit Horn (2), Ruth Shemer (2), Shahar Frenkel (1,2), Jacob Pe'er (1,2), Yuval Dor (2)

(1) Division of Ophthalmology, Hadassah Medical Center, Jerusalem
(2) Faculty of Medicine, the Hebrew University, Jerusalem

ABSTRACT

PURPOSE

Vitreoretinal lymphoma (VRL) is a rare type of primary central nervous system lymphoma (PCNSL). The diagnosis of VRL is a challenge for clinicians as the symptoms of VRL can mimic those of posterior uveitis. The gold standard for VRL diagnosis is cytology of vitreous fluid (VF), used to identify a monoclonal neoplastic B lymphocyte population. However, cytomorphological evaluation often fails to detect lymphoma cells because of limited sample volume, low cellularity, and cell lysis during vitrectomy. Ancillary tests such as flow cytometry, interleukin-10 to interleukin-6 cytokine ratio, and the detection of MYD88 mutations or immunoglubin gene rearengement in tumor cells can aid the diagnosis in some patients. Recently, several studies reported the genetic profiles of VRL using VF circulating tumor DNA sequencing. We aim to diagnose VRL by assessing cell type-specific DNA methylation patterns in the vitreous fluid.

METHODS

Vitreous fluid samples from five patients who underwent diagnostic pars plana vitrectomy for suspected VRL were examined for immune cells composite by DNA methylation patterns.

RESULTS

There were three patients diagnosed with VRL by cytology, cytokine ratio or MYD88 mutation. All three patients had high precentage of B cell DNA (26-55%) and low levels of monocytes DNA (6-11%). Two patients were diagnosed with uveitis by cytology and cytokine ratio. Both had high levels of monocytes DNA (50-67%) and low levels of B cell DNA (0.3-3%). Interestingly, lymphoma patients had also high concentration of DNA from neutrophils, potentially reflecting secondary inflammation.

CONCLUSIONS

This preliminary study suggests that cell type-specific methylation patterns of DNA extracted from the vitreous fluid can potentially contribute to the diagnosis of vitreoretinal lymphoma. Back to TOC

Optic nerve Crush Induce Acute Inflammation and Secondary Apoptosis

Talal Salti (1), Basel Obied (1, 2), Irit Mann (1, 2), Alon Zahavi (3, 4), Nitza Goldenberg-Cohen (1, 2)

(1) The Krieger Eye Research Laboratory, Bruce and Ruth Faculty of Medicine, Technion- Institute of Technology, Haifa, Israel
(2) Department of Ophthalmology, Bnai-Zion Medical Center, Haifa, Israel
(3) Department of Ophthalmology & Laboratory of Eye Research, FMRC, Rabin Medical Center,
(4) Petach Tikva, Israel
(5) Gray School of Medicine, Faculty of Medical and Health Sciences, Tel Aviv University, Tel Aviv, Israel

ABSTRACT

SPURPOSE

Optic nerve crush (ONC) is the most widely used mouse model for studying optic neuropathies. Therapeutic agents are traditionally delivered via intravitreal injection. Recently, biomimetic nanoparticle (BNP)–based platforms have demonstrated the ability to deliver proteins to the eye using topical administration. In this study, we evaluated the feasibility of delivering antibodies directly to the vitreous, both by intravitreal injection and by topical drops, to detect inflammatory and apoptotic responses following ONC.

METHODS

ONC was induced in the right eye of 20 mice. Twenty-four hours later, antibodies against CD45, IBA1, caspase-3, and annexin V were delivered either by intravitreal injection or by BNP-based topical administration. Three days after ONC, retinal flat mounts were prepared and imaged using confocal microscopy, with and without secondary antibody staining.

RESULTS

Retinal flat mounts revealed marked infiltration of white blood cells through the optic nerve head into the injured retina, while control eyes showed no such response. Apoptotic cells were clearly detected. Delivery efficiency of antibodies via BNP topical administration was comparable to intravitreal injection.

CONCLUSIONS

BNP-based delivery represents a promising, minimally invasive alternative to intravitreal injection for delivering biologics to the eye. If validated in further studies, this approach may reduce the need for intraocular intervention and provide a safer, more accessible method for diagnosing and treating optic neuropathies.

Back to TOC

Epidemiology, diagnosis, and outcomes of ocular (choroidal and orbital) metastasis: retrospective cohort study from a tertiary center

Vicktoria Vishenevskia Dai, Arad Dotan, Rodin Merom, Niv Goldberg, Ofira Zloto

The Goldschleger Eye Institute, Sheba Medical Center, Faculty of Medicine

Tel-Aviv University, Israel

ABSTRACT

PURPOSE

Ocular metastases are the most common ocular tumors. It is most frequently associated with breast cancer in females and lung cancer across both sexes, highlighting the connection between systemic malignancies and ocular health.

METHODS

This is retrospective 19-year cohort study from a single tertiary referral center in Israel. Data was collected on demographics, clinical features, imaging, treatment modalities, and ocular and systemic outcomes.

RESULTS

The cohort included 71 patients: 59 with choroidal mets and 10 with orbital involvement. The mean age at ocular mets was 59 years old (SD 15), with 62% female. Ocular or visual symptoms were present in 90.1% of patients, including blurred or decreased vision, diplopia, and eye pain, among others, while 9.9% were asymptomatic. Bilateral eye involvement occurred in 24% of cases, with multifocal lesions in 28%. Ocular mets were the first cancer manifestation in 19% of cases. Breast cancer was the most common primary cancer (44%), followed by lung cancer (35%). Treatment modalities included systemic and local therapys. Concomitant brain mets were present in 35%, while bone mets were the most common systemic spread (62%). Complete regression was achieved in 8.3% of cases, while 58% experienced sufficient mets shrinkage, 19% showed no change, and 15% had disease progression. The mean follow-up from systemic malignancy diagnosis was 6.3 years (SD 5.0) and 2.74 years (SD 2.35) from ocular mets diagnosis. Survival analysis from ocular mets diagnosis included Kaplan-Meier (Figure 1), the log-rank test, and Cox regression (Table 1). The log-rank test ($p = 0.35$) showed no significant survival difference between choroidal and orbital mets in univariate analysis. However, Cox regression identified orbital mets as a significant predictor of higher mortality (HR = 3.093, 95% CI: 1.112–8.606, $p = 0.031$). Primary cancer type, gender, multifocal involvement, and age at ocular or systemic mets diagnosis were not significant predictors of mortality.

CONCLUSION

This study highlights the clinical characteristics, diagnostic approaches, and treatment outcomes of ocular mets in an Israeli population. In our cohort, orbital mets were found to be a predictor of higher mortality. Back to TOC

SMSC-Derived Exosomes Convert Retinotoxic S100A9 Responses into Functional Enhancement in the Retina

Amanda Qarawani (1,2) Efrat Naaman (1), Shahaf Sigal-Dror (2), Shaked Golan (2), Tali Ben-Zur (3), Dani OLen (3), Shiri Zayit-Soudry (4)

(1) Clinical Research Institute, Rambam Health Care Campus, Haifa, Israel
(2) Ruth and Bruce Rappaport Faculty of Medicine, Technion Israel Institute of Technology, Haifa, Israel
(3) Department of Human Genetics and Biochemistry, School of Medicine, Felsenstein Medical Research Center, Tel Aviv University, Tel Aviv, Israel
(4) Department of Ophthalmology, Rabin Medical Center, Tel Aviv University, Tel Aviv, Israel

ABSTRACT

PURPOSE

S100A9, a major drusen component in eyes with age-related macular degeneration (AMD), is a pro-inflammatory calcium-binding protein that participates in diverse signaling processes and is intrinsically amyloidogenic *in vitro* and *in vivo*. We previously showed that the retinal eUects exerted by S100A9 are conformation-dependent, where native S100A9 had no impact on the retinal function *in vivo*, fibrillar S100A9 induced significant retinotoxicity. Notably, low-dose S100A9 fibrils produced paradoxical amplification of the ERG responses, associated with altered microglial activation. Here, we investigate whether mesenchymal stem cell derived-exosomes (MSC-exo) modulate these amyloid-mediated retinal eUects.

METHODS

Wild-type rats received intravitreal MSC-exo in the right eye, with vehicle-injected left eyes serving as internal controls. Five days later, fibrillar S100A9 was injected either unilaterally (right eye only) to evaluate functional enhancement compared to baseline, or bilaterally to determine MSC-exo-mediated protection. Retinal function was assessed by electroretinography (ERG) at baseline and longitudinally through 6 weeks post–S100A9 injection. ERG measures were compared between treated and control eyes at each timepoint. At the end of the functional follow-up, retinas were extracted for *ex vivo* analyses.

RESULTS

MSC-exo pretreatment unexpectedly converted the retinal response to fibrillar S100A9. Rather than inducing functional impairment, the high (otherwise retinotoxic) S100A9 fibrils dose produced paradoxical ERG amplification in MSC-exo pretreated eyes, resembling the augmented response previously observed with low-dose S100A9 fibrils alone. Immunolabeling of retinal sections revealed altered profiles of microglial activation consistent with this functional shift.

CONCLUSIONS

MSC-Exo pretreatment converted retinotoxic S100A9 responses to functional enhancement, demonstrating modulatory eUects on amyloid-mediated retinal pathology. As the development of MSC-exo-based therapies advances for retinal degeneration, understanding their interactions with the AMD-associated molecular environment may be critical for optimizing therapeutic outcomes.

Back to TOC

Microbead-induced glaucoma model in mice: EndoCoat prolongs IOP elevation and increases retinal ganglion cell loss

Mohammed Darawshe (1,2), Yael Nisgav (1), Shmuel Kagasov (1,2), Nitza Goldenberg-Cohen (3,4), Irit Bahar (1,2), Noa Geffen (1,2), Alon Zahavi (1,2)

(1) Ophthalmology Department and Eye Research Laboratory, FelsenstSein Medical Research Center, Rabin Medical Center, Petach Tikva, Israel
(2) Gray Faculty of Medical and Health Sciences, Tel Aviv University, Tel Aviv, Israel
(3) The Krieger Eye Research Laboratory, Bruce and Ruth Faculty of Medicine, Technion Institute of Technology, Haifa, Israel
(4) Ophthalmology Department, Bnai-Zion Medical Center, Haifa, Israel

ABSTRACT

PURPOSE

STo evaluate whether combining polystyrene microbeads with an ophthalmic viscoelastic (Healon EndoCoat) prolongs intraocular pressure (IOP) elevation and increases retinal ganglion cell (RGC) loss in a mouse model of glaucoma.

METHODS

A total of 38 C57BL/6 mice were divided into 4 groups for intracameral injections. Group A received fluorescent microbeads in saline (n=13); Group B received fluorescent microbeads mixed with Healon EndoCoat (n=13); Group C received the same mixture with the incision site sealed using fibrin glue (n=7); and Group D received saline as control (n=5). IOP was measured weekly for 4 weeks. Mice were euthanized, and retinal flat mounts were used for RGC quantification and calculation of RGC loss.

RESULTS

Microbeads delivered with Healon EndoCoat and sealed with fibrin glue produced the highest IOP elevation compared with microbeads in saline (ΔIOP 11.00 ± 12.51 mmHg vs 4.82 ± 3.23 mmHg, p=0.035). Microbeads were also identified on the retinal surface in several eyes, indicating posterior migration through the zonular region. Groups treated with EndoCoat demonstrated greater RGC loss in association with the prolonged IOP elevation.

CONCLUSIONS

Mixing microbeads with Healon EndoCoat instead of saline produces a longer and more stable ocular hypertensive response in mice and increases RGC damage. Adding fibrin glue further increases and extends the pressure elevation. The observation of beads on the retina has not been reported previously and may reflect posterior migration of beads from the anterior chamber through the zonular area. This modified model offers a more chronic and robust glaucoma phenotype and may improve the evaluation of neuroprotective strategies.

Back to TOC

Glial and neuronal responses following optic nerve crush in diabetic and non-diabetic mice

Sami Tuma (1,2), Talal Salti (1), Basel Obied (1,2), Irit Mann (1,2), Alon Zahavi (3,4), Nitza Goldenberg-Cohen (1,2)

(1) The Krieger Eye Research Laboratory, Bruce and Ruth Faculty of Medicine, Technion-Institute of Technology, Haifa, Israel
(2) Department of Ophthalmology, Bnai-Zion Medical Center, Haifa, Israel
(3) Department of Ophthalmology & Laboratory of Eye Research, FMRC, Rabin Medical Center, Petach Tikva, Israel
(4) Gray School of Medicine, Faculty of Medical and Health Sciences, Tel Aviv University, Tel Aviv, Israel

ABSTRACT

PURPOSE

Diabetes mellitus heightens the vulnerability of neural tissues to ischemic injury, and the optic nerve is particularly susceptible due to diabetes-related microvascular dysregulation. This study investigates whether diabetic conditions exacerbate structural and molecular damage following optic nerve crush (ONC), by comparing diabetic and non-diabetic mice.

METHODS

Forty C57BL/6 mice were assigned to two groups: streptozotocin-induced diabetic mice (confirmed by repeated glucose levels >250 mg/dL) and age-matched non-diabetic controls. ONC was performed in all mice. Ten animals per group were euthanized three weeks post-ONC for histological assessment. Retinal and optic nerve sections were analyzed using GFAP immunostaining to evaluate Müller cell/astrocytic activation, IBA1 to assess microglial response, and NeuN to quantify neuronal survival and retinal ganglion cell loss. For molecular analyses, tissues collected one day post-ONC from an additional ten mice per group were examined for gene and protein expression related to ischemia, inflammation, and apoptosis.

RESULTS

Diabetic mice exhibited significantly increased glial reactivity following ONC, with markedly elevated GFAP expression compared with non-diabetic controls. IBA1 staining revealed enhanced microglial activation and higher inflammatory cell density in the diabetic group. NeuN immunolabeling demonstrated a greater reduction in retinal ganglion cells in diabetic mice. Molecular profiling corroborated these findings, showing upregulation of ischemic, inflammatory, and apoptotic pathways in diabetic ONC retinas.

CONCLUSIONS

Chronic hyperglycemia substantially amplifies both glial and neuronal injury following ONC. Diabetic mice show heightened glial activation, stronger inflammatory responses, and increased retinal ganglion cell loss relative to non-diabetic controls. These effects are likely driven by diabetes-associated microvascular dysfunction.

Back to TOC

NGLY1 Deficiency Disrupts Aqueous and Lipid Homeostasis in the Eye: Evidence from a Zebrafish Model

Aviv Mesika (1), Golan Nadav (2), Hadas Pizem (3), David Karasik (1), Tzipora C. Falik-Zaccai (1)

(1) Azrieli Faculty of Medicine, Bar Ilan University, Safed, Israel
(2) Institute of Human Genetics, Galilee Medical Center, Nahariya, Israel
(3) Department of Ophthalmology, Anterior segment unit, Hadassah Medical Center, Jerusalem, Israel.

ABSTRACT

PURPOSE

NGLY1 deficiency (NGLY1-CDDG) is a rare genetic disorder caused by bi-allelic pathogenic variants in *NGLY1*. Loss of NGLY1 function impairs deglycosylation of misfolded glycoproteins, disrupts proteostasis, mitochondrial function, and cellular signaling. The purpose of this study is to elucidate the pathophysiological mechanisms underlying the ocular abnormalities observed in NGLY1-CDDG, with a specific focus on alacrima and hypolacrima (deficiency or reduction in tear production), a prominent and characteristic clinical feature of the disorder.

METHODS

Zebrafish serve as a conserved model of ocular surface protection. We performed single-cell RNA sequencing (scRNA-seq) on dissected eyes from 5-days-old *ngly1*$^{(-/-)}$ and *ngly1*$^{(+/+)}$ zebrafish. Downstream analyses encompassed gene set enrichment analyses (GSEA), as well as RT-qPCR validation, western blotting, lipid staining, and lipidomic profiling.

RESULTS

scRNA-seq revealed a ~84% reduction in non-retinal ocular cell in *ngly1*$^{(-/-)}$ zebrafish, indicating a possible impaired development of the ocular surface. GSEA identified significant suppression of peroxisome proliferator-activated receptor (PPAR) signaling, including downregulation of pparab, the zebrafish homolog of human PPARα. Reduced pparab expression was associated with higher levels of triglycerides and phosphatidylcholines in *ngly1*$^{(-/-)}$ eyes compared with *ngly1*$^{(+/+)}$. Additionally, we documented downregulation of aqp1a.1 (zebrafish homolog of human Aquaporin-1) in the *ngly1*$^{(-/-)}$ eyes.

CONCLUSIONS

We report for the first time reduction of non-retinal ocular cells and downregulation of pparab and aqp1a.1 in NGLY1 deficiency model. The abnormal expression of pparab and aqp1a.1 is associated with damage to the conserved ocular surface protection in an NGLY1-deficient animal model.
Elevated levels of triglycerides and phosphatidylcholines, together with reduced aqp1a.1 expression in *ngly1*$^{(-/-)}$ eyes, indicate a possible dual disruption of aqueous and lipid homeostasis. This pattern supports a pathophysiology that combined fat-accumulative and evaporative defects underlying the dry eye disease observed in NGLY1-CDDG patients. Back to TOC

Assessing Coenzyme Q10 as a Neuroprotectant in Chronic Cobalt Intoxication: A TEM-Based Study

Basel Obied (1,2), Talal Salti (1), Alon Zahavi (3,4), and Ni<a Goldenberg Cohen (1,2)

(1) The Krieger Eye Research Laboratory, Bruce and Ruth Faculty of Medicine, Technion – Israel Institute of Technology, Haifa, Israel
(2) Department of Ophthalmology, Bnai Zion Medical Center, Haifa, Israel
(3) Department of Ophthalmology and Laboratory of Eye Research, Felsenstein Medical Research Center, Rabin Medical Center, Petach Tikva, Israel
(4) Gray Faculty of Medicine, Tel Aviv University, Tel Aviv, Israel

ABSTRACT

PURPOSE

Cobalt intoxication is associated with mitochondrial dysfunction and chronic ischemic injury, particularly in tissues with high metabolic demand such as the optic nerve. Coenzyme Q10 (CoQ10), a key component of the mitochondrial respiratory chain, and its synthetic analog Idebenone have been proposed as potential neuroprotective agents due to their antioxidant and bioenergetic properties. This study aimed to assess the protective effect of CoQ10 against chronic low-dose cobalt-induced ultrastructural damage in the mouse optic nerve.

METHODS

A murine model of cobalt toxicity was induced by daily low-dose cobalt injections for one month. Ten mice were included; five received oral CoQ10 via daily gavage during the first week of exposure. Optic nerves were harvested and analyzed by transmission electron microscopy (TEM). Structural metrics, including myelin integrity, mitochondrial morphology, and axonal caliber, were evaluated qualitatively and quantitatively.

RESULTS

CoQ10 supplementation did not confer detectable neuroprotection in cobalt-exposed mice. Myelin architecture, mitochondrial features, and axonal dimensions were comparable between treated and untreated groups. Persistent cobalt-induced ultrastructural abnormalities were observed regardless of CoQ10 administration.

CONCLUSIONS

In this model, short-term CoQ10 administration did not provide neuroprotection against chronic low-dose cobalt toxicity. The findings suggest that either higher or prolonged dosing may be required, or that alternative mitochondrial support strategies should be explored. These results provide a foundation for optimizing therapeutic approaches in toxin-induced optic neuropathies.
Back to TOC

Alström Syndrome modeling based on human pluripotent stem cells as a tool to understand the visual symptoms of the disease

Elie Frank (1,2,5,6), Camille Geiger (1,2,3), Natacha Perrin (4), Christelle Monville (1,2), Karim Ben M'Barek (1,2,3)

(1) INSERM U861, I-Stem, AFM, Institute for Stem Cell Therapy and Exploration of Monogenic Diseases, 91100 Corbeil-Essonnes, France
(2) U861, I-Stem, AFM, Université Paris-Saclay, Université d'Evry, 91100 Corbeil-Essonnes, France
(3) Centre d'Etude des Cellules Souches, 91100 Corbeil-Essonnes, France
(4) Centre de Nanosciences et de Nanotechnologies (C2N), CNRS UMR 9001, Université Paris-Saclay, 91120 Palaiseau, France

ABSTRACT

PURPOSE

Alström Syndrome (AS) is a rare monogenic recessive multisystemic disease caused by mutations in *ALMS1*, characterized by hearing and vision loss, obesity, type II diabetes, cardiomyopathy, and progressive liver and kidney failure. Visual symptoms develop within the first weeks after birth and ultimately lead to complete blindness. As no curative treatment currently exists, therapeutic approaches aim only at alleviating symptoms. The goal of this study was to establish hiPSC-based models of AS to investigate the cellular and molecular mechanisms underlying retinal defects and to identify potential therapeutic targets.

METHODS

hiPSC lines carrying either pathological or de novo *ALMS1* mutations were generated using CRISPR/Cas9-mediated genome editing. Clones were characterized at the pluripotent stage by assessing standard molecular and phenotypic markers and compared with patient-derived hiPSCs. Mutant and wild-type hiPSC lines were then differentiated into retinal pigment epithelium (RPE) cells and neuro-retinal organoids. RPE cells were analyzed by immunofluorescence and morphological assessment. Neuro-retinal organoids were evaluated by immunofluorescence to assess cell identity, opsin expression, and cell viability.

RESULTS

ALMS1 mutations were successfully introduced or reproduced without affecting hiPSC pluripotency characteristics. Both hiPSCs and RPE cells displayed a loss or reduction of ALMS1 expression at the primary cilium, but no additional phenotype was detected at these stages. In contrast, neuro-retinal organoids derived from *ALMS1*-mutant hiPSCs exhibited a marked reduction or absence of cone- and rod-specific opsin expression, together with increased cell death compared with control organoids. These results indicate that *ALMS1* dysfunction impairs photoreceptor differentiation and survival during organoid development.

SCONCLUSIONS

Our hiPSC-based models of Alström Syndrome recapitulate essential pathological features of the disease, particularly photoreceptor degeneration. These models provide a valuable platform for dissecting *ALMS1*-related retinal mechanisms and for supporting the development of future therapeutic and screening strategies targeting retinal degeneration. Back to TOC

Assessment of Visual Functions and Pupil Light Reflex in Fragile X Carriers

Lea Zelianodjevo Engel (1, 2, 5), Dima Shbita (1,2), Shai Elizur, (3, 5), Lital Kalich-Philosoph (4), Omer Bar Yosef (4, 5), Ifat Sher (1, 2), Ygal Rotenstreich (1, 2)

(1) The Goldschleger Eye Institute, Sheba Medical Center, Tel-HaShomer, Israel
(2) Department of Ophthalmology, Gray Faculty of Medicine and Health Sciences, Tel Aviv University, Israel
(3) IVF Unit and the Endometriosis Center, Sheba Medical Center, Tel-HaShomer, Israel
(4) The Research Center at the Child Development Institute, Sheba Medical Center, Tel-HaShomer, Israel
(5) Faculty of Medicine, Tel Aviv University, Israel.

ABSTRACT

PURPOSE

This study aims to characterize color vision, and rod-, cone-, and melanopsin-mediated pupil light response (PLR) in Fragile X carriers.

METHODS

12 Fragile X carriers (all females, Age: 52.3 ± 16.5 YO) and 36 healthy controls (all females, Age: 48.0 ± 21.5 YO) were enrolled. The PLR responses to red and blue stimuli (0.43°) presented at central (4.2°) and peripheral (21°) retinal locations were assessed in FXCs and age-matched healthy controls using a Chromatic Pupilloperimeter. Ophthalmic evaluations included color vision testing, best-corrected visual acuity (BCVA), refraction, and Spectral-Domain Optical Coherence Tomography (SD-OCT). In addition, the fragile X carriers underwent the Montreal Cognitive Assessment (MoCA).

RESULTS

Fragile X carriers exhibited a significant reduction in maximum contraction velocity (MCV) in response to blue light stimuli compared to controls, in both eyes. Specifically, in the right eye, MCV was significantly slower in patients (12.7 ± 7.2 pixel/sec vs. −20.4 ± 9.1 pixel/sec, $p = 7.3\times10^{-16}$). A similar, though slightly less pronounced, difference was observed in the left eye (−17.4 ± 10.0 pixel/sec vs. −22.9 ± 8.7 pixel/sec, $p = 2.9\times10^{-7}$). No significant differences were observed in the PLR recorded in response to red light stimuli. Pupil responses driven by melanopsin were comparable between the carriers and controls in both eyes.

CONCLUSIONS

SOur results show a selective impairment in the rod-mediated magnocellular pathway, while the cone-mediated parvocellular pathway remains relatively unaffected. The reduction in blue-light–induced MCV, combined with preserved red-light responses, suggests that the rod-mediated PLR could serve as an objective marker for disease-related dysfunction in this group. Although the test cannot explicitly differentiate between magnocellular and parvocellular pathways, it is currently the only non-invasive functional measure available that can distinguish between rod-and cone-driven contributions to the pupillary response.

Back to TOC

Towards high-acuity vision restoration: Hybrid retinal prosthesis composed of a high-density multielectrode array integrated with glutamatergic cells

Nairouz Farah (1,2), Amos Markus (1,2), Gal Shpun (1,2), Yoav Chemla (1,2), Erel Lasnoy (1,2), Tamar Azrad-Leibovitch (1,2), Fikre Fentahon (1,2), Zeev Zalvesky (2,3), Yossi Mandel (1,2).

(1) Faculty of Life Sciences, School of Optometry & Visual Science, Bar Ilan University
(2) Bar Ilan Institute for Nanotechnology & Advanced materials (BINA), Bar Ilan University
(3) The Alexander Kofkin Faculty of Engineering, Bar Ilan University

ABSTRACT

PURPOSE

Retinal prostheses offer a promising approach for vision restoring in patients with degenerative retinal diseases. However, current devices remain limited by their low spatial resolution, non-selective retinal circuit activation, and unnatural pulsatile stimulation. To overcome these limitations, this work introduces a novel device in the form of a Hybrid Retinal Implant (HRI). Here we present the through characterization of this implant and in-vitro performance

METHODS

The Hybrid Retinal Implant concept relies on a high-density electrode array integrated with glutamatergic neurons (human embryonic stem cell-derived photoreceptor precursors, hESC-PRPs). The electrodes are designed to create a tight neuron-electrode coupling through a 3D microwell-shaped design, thereby confining and amplifying the induced electric fields. To validate our concept, finite element modelling was performed to characterize the electrical field distribution and estimate activation thresholds of cells sealed in the micro-well structures. Furthermore, activation threshold reduction was verified using an in-vitro implant protype with patch clamp recoding of cells seeded to investigate the activation threshold. Finally, the device with seeded cells was implanted in the subretinal space of rats and the integration of the cells was investigated using histological studies.

RESULTS

Our computer modelling revealed both the confinement and amplification of the electrical field around the glutamatergic neurons when a micro-well configuration is used. The simulation suggested a significant increase in spatial resolution, down to at least 10µm, while eliminating the electrode crosstalk. Furthermore, our simulations indicated a three-order-of-magnitude reduction in the activation threshold in neurons and photoreceptors, reaching the picocoulomb (pC) level, a finding validated using an in-vitro prototype of the hybrid retina. Finally, implantation of the device in the subretinal space of rats with retinal degeneration reveals the survival of the hESC-PRP cells within the microwells. Furthermore, the device-integrated cells exhibit axonal sprouting toward the host bipolar cells and form putative synapses with the host retina.

CONCLUSIONS

Our promising results pave the way for the realization of a novel concept putatively facilitating vision restoration at an unrivaled visual acuity while mimicking natural vision. Back to TOC

High-density lipoprotein cholesterol levels and risk of age-related macular degeneration

Itay Nitzan (1), Shlomit Jaskoll (1,2), Adi Kramer (1), Or Shmueli (1), Jaime Levy (1), Itay Chowers (1)

(1) The Faculty of Medicine, Department of Ophthalmology, Hadassah-Hebrew University Medical Center, The Hebrew University of Jerusalem, Jerusalem, Israel
(2) Faculty of Medicine, Department of Military Medicine and "Tzameret", Hebrew University of Jerusalem, Jerusalem, Israel, and Medical Corps, Israel Defense Forces, Ramat Gan, Israel

ABSTRACT

PURPOSE

To evaluate the association between high-density lipoprotein cholesterol (HDL-C) levels and incident age-related macular degeneration (AMD) in a large, multi-institutional cohort.

METHODS

This retrospective cohort study used real-world electronic health records from 70 U.S. healthcare organizations within the TriNetX US Collaborative Network (September 1, 2005 to August 28, 2025). A total of 373,493 adults with at least two HDL-C measurements taken three months apart or more were included and classified into high HDL-C (all values ≥60 mg/dL) or low HDL-C (all values ≤39 mg/dL) groups. Cohorts were matched 1:1 for demographics, comorbidities, lipid-lowering therapy, laboratory indices, and healthcare utilization. The index date was defined as the second qualifying HDL-C measurement. Follow-up extended for up to 10 years. Incident non-exudative and exudative AMD were evaluated using Kaplan–Meier survival analyses and Cox proportional hazards models. Robustness was examined through nested, subgroup, and sensitivity analyses, and specificity was confirmed with positive and negative control outcomes. The primary outcomes were hazard ratios for non-exudative and exudative AMD by HDL-C category.

RESULTS

During 1.29 million person-years of follow-up, high HDL-C was associated with an increased risk of non-exudative AMD (HR = 1.53; 95% CI, 1.32–1.78) and exudative AMD (HR = 1.37; 95% CI, 1.09–1.73). For non-exudative AMD, risk was elevated across early (HR = 1.55; 95% CI, 1.26–1.91), intermediate (HR = 1.82; 95% CI, 1.42–2.33), and advanced atrophic stages (HR = 1.85; 95% CI, 1.16–2.97). Findings for non-exudative AMD remained consistent after a 360-day washout period, across 3-, 5-, and 20-year follow-up intervals, and after excluding deaths. For exudative AMD, associations were directionally positive across sensitivity analyses, although statistical significance was inconsistent. Results persisted in stepwise matching models. Positive and negative control outcomes supported the specificity and internal validity of the associations.

CONCLUSIONS

High HDL-C levels were associated with an increased risk of non-exudative AMD and with a weaker, less consistent risk of exudative AMD. Findings were robust across model specifications and sensitivity analyses, supporting HDL-C as a potential biomarker in AMD risk stratification.
Back to TOC

Chronic Proton Pump Inhibitor Use Is Associated with Increased Risk of Diabetic Retinopathy: A Real-World Cohort Study

Nir Zontag 2, Natan Lishinsky-Fischer 1,2*, Shoham Kubovsky 1,2, Jaime Levy 1,2

(1) Faculty of Medicine, Hebrew University of Jerusalem
(2) Ophthalmology Department, Hadassah Medical Center, Jerusalem, Israel

*These authors contributed equally

ABSTRACT

PURPOSE

To investigate the association between chronic use of proton pump inhibitors (PPIs) and the incidence of diabetic retinopathy (DR) among patients with type 2 diabetes mellitus (T2D), using a large global electronic medical records network.

METHODS

A retrospective cohort analysis was conducted using the TriNetX Global Collaborative Network. Adults with T2D were stratified into two cohorts: those who received chronic PPI therapy (DM +PPIs) and those who did not (DM -PPIs). Patients with pre-existing DR or retinal diseases were excluded. Propensity score matching (PSM) was applied to balance demographic and clinical variables. The primary outcome was the development of DR over a 10-year follow-up. Survival analysis and hazard ratios were calculated using Kaplan–Meier methods and Cox proportional hazards models.

RESULTS

After 1:1 PSM, each cohort included 444,329 patients. Diabetic retinopathy occurred in 13,949 patients in the DM +PPIs group and 10,446 in the DM -PPIs group. PPI use was associated with a significantly increased risk of DR (hazard ratio 1.15, 95% CI [1.12, 1.18; $p < 0.001$). This association remained consistent across DR subtypes, including mild, moderate, and severe nonproliferative DR and proliferative DR.

CONCLUSION

Chronic PPI use was associated with a modest but significant increase in the risk of DR in patients with T2D. Prospective studies are needed to confirm these findings and explore the mechanisms linking PPI use to retinal microvascular damage.

Back to TOC

Retinal Ischemic Events Following Cardiovascular Procedures: Temporal Patterns and Clinical Characteristics

Or Gil, MD,[1] Avner Hostovsky, MD,[1] Noah Benjamin Nagar, MD, Shalev Fried, MD,[1] Iris Moroz, MD,[1] Gabriel Katz, MD,[1] Ari Leshno, MD,[1] Miri Fogel Levin, MD[1]

(1) Goldschleger Eye Institute, Sheba Medical Center, Tel-Hashomer, Israel

ABSTRACT

PURPOSE

To characterize retinal ischemic events following cardiovascular procedures and identify timing patterns and clinical features.

METHODS

We retrospectively reviewed acute retinal ischemia cases confirmed by optical coherence tomography (OCT) at a tertiary center (2015–2024). Patients who underwent cardiovascular procedures within 30 days prior to symptom onset were included.

RESULTS

13 eyes of 13 patients were included. All patients had cardiovascular risk factors. Procedures included cardiac catheterization (n=4), valve replacement (n=3), carotid interventions (n=3), heart transplant (n=1), aortic surgery (n=1), and peripheral vascular intervention (n=1). Nine patients (69.2%) developed branch retinal artery occlusion (BRAO), 1 (7.7%) central retinal artery occlusion (CRAO) and 3 patients (25%) developed paracentral acute middle maculopathy (PAMM). Three timing presentations were observed: immediate onset (day 0, n=4), early onset (days 2-7, n=5) characterized by absence of visible emboli, and delayed onset (days 8-28, n=4) with visible emboli in all cases. Neuroimaging revealed cerebral ischemia in 7 of 10 patients (70%).

CONCLUSIONS

SSRetinal ischemic events can occur from immediately to 28 days following cardiovascular procedures. The timing of onset may suggest different mechanisms, such as procedural release of emboli, perioperative hypoperfusion, or delayed evolving embolic sources such as new onset atrial fibrillation, thrombus, or vegetation.

Back to TOC

Retinal Microvascular Changes After a 26-Hour On-Call Shift in Medical Residents

Hadas Pizem (1), Javier Gonzales (2), Daniella Monge (2), Adir Sommer (2), Dror Ben Ephraim Noyman (2), Luis Filipe Nakayama (4), Ben Gofrit (3), Estel Saiman (5), Jonathan Fhima (3), Joachim Behar (3), Eytan Blumenthal (2), Nitsan Duvdevan-Strier (2)

(1) Department of Ophthalmology, Hadassah Ein Kerem Medical Center, Jerusalem, Israel
(2) Department of Ophthalmology, Rambam Health Care Campus, Haifa, Israel
(3) Faculty of Biomedical Engineering, Technion – Israel Institute of Technology, Haifa, Israel
(4) Department of Ophthalmology, São Paulo Federal University (UNIFESP), São Paulo, Brazil
(5) Department of Neurology, Rambam Health Care Campus, Haifa, Israel

ABSTRACT

PURPOSE

Sleep deprivation is associated with endothelial dysfunction and increased cardiovascular risk, yet its effects on the retinal microvasculature are not well characterized. On-call hospital shifts offer a unique real-world setting to study the physiological consequences of prolonged sleep deprivation, providing an opportunity to capture real-world data on its vascular effects. Epidemiological and clinical studies show that changes in retinal vascular parameters are associated with systemic conditions, hence the eye provides a non-invasive window to assess the systemic impact of extended sleep deprivation through fundus imaging. In this study, deep-learning–based analysis was used to extract quantitative structural vascular biomarkers from retinal images, enabling objective assessment of sleep-related microvascular alterations.

METHODS

Prospective observational comparative study including 22 residents and two control groups: 17 young attendings and 18 medical students. Residents underwent fundus imaging twice (post-call and after three nights of regular sleep), while controls were imaged once. Demographics, sleep parameters, stimulant use, and PSQI scores were collected. Retinal microvasculature was segmented using a deep-learning model with specialist validation, and comparisons were performed between post-call and rested states and across groups.

RESULTS

Preliminary quantitative analysis showed retinal microvascular alterations in post-call residents, specifically arterial. Central Retinal Artery Equivalent (CRAE), representing the average caliber of the retinal arterioles, decreased from 14.62 ±1.16 μm (rested) to 13.85± 1.54 μm post-call ($p = 0.02$). Arterial vessel area and length were reduced as well ($p < 0.01$ and $p = 0.01$, respectively). Arterio-Venous Ratio (AVR) declined from 0.65 ± 0.06 to 0.63 ± 0.06 ($p < 0.01$).

CONCLUSIONS

On-call shifts may transiently affect the retinal microvasculature in medical residents, and deep-learning vascular biomarkers may offer a non-invasive way to monitor these changes. Reductions in CRAE, AVR, and arterial area and length suggest early microvascular alterations that may reflect endothelial dysfunction and possibly greater cardiovascular susceptibility. These changes may also contribute to pathways linking sleep deprivation with cognitive, emotional, and HPA-axis disturbances described in similar cohorts. Back to TOC

Retinal hemorrhage in AMD patients - Systemic comorbidities or antithrombotic therapy?

Raz Tshuva-Bitton (1,2), Efrat Naaman (1,2,3), Erez Bibi (1), Maya Nimri-Distelfeld (5), Roee Arnon (1,4), Yariv Keshet (1,4), Assaf Dotan (1,4), Orly Gal-Or (1,2,4), Gilad Rabina (1,4), Alon Tiosano (1,2,4)

(1) Department of Ophthalmology, Rabin Medical Center, Petah Tikva, Israel
(2) Gray Faculty of Medical & Health Sciences, Tel Aviv University, Tel Aviv, Israel
(3) Genetics Department, Harvard Medical School, Boston, MA, USA
(4) Ophthalmology Artificial Intelligence Center, Rabin Medical Center, Petah Tikva, Israel
(5) Ruth and Bruce Rappaport Faculty of Medicine, Technion – Israel Institute of Technology, Haifa, Israel

ABSTRACT

PURPOSE

To investigate whether systemic use of anticoagulant or antiplatelet agents is associated with retinal hemorrhage in patients with age-related macular degeneration (AMD), and whether systemic comorbidities are more prevalent among patients who develop retinal hemorrhage.

METHODS

This retrospective study included 99 AMD patients who experienced retinal hemorrhage and 90 AMD patients without hemorrhage, all treated at a single tertiary medical center. Clinical data were extracted from electronic medical records, including demographic characteristics, systemic comorbidities, and detailed documentation of systemic antithrombotic therapy (anticoagulants, antiplatelets, or direct oral anticoagulants). The prevalence of each comorbidity and medication exposure was compared between groups.

RESULTS

There were no significant differences between groups in the use of systemic antithrombotic therapy, including anticoagulants (p = .62) and antiplatelet agents (p = .24). Patients with retinal hemorrhage were older and demonstrated a higher prevalence of systemic comorbidities. Hypertension was significantly more common in the hemorrhage group compared with controls (60.6% vs 37.8%; p=.002), as were cerebrovascular disease (12.1% vs 2.2%; P = .011), congestive heart failure (12.1% vs 0%; P < .001), chronic obstructive pulmonary disease (11.1% vs 0%; P = .001), and chronic kidney disease (11.1% vs 2.2%; P = .02). Dyslipidemia was present in all patients in the hemorrhage group compared with 22.2% of controls (P < .001). No significant between-group differences were observed in the prevalence of diabetes mellitus (28.3% vs 23.3%; P = .51), ischemic heart disease (26.3% vs 20.0%; P = .39), atrial fibrillation (10.1% vs 3.3%; P = .09), or cancer (5.1% vs 7.8%; P = .56).

CONCLUSIONSS

Systemic use of antithrombotic therapy was not associated with an increased risk of retinal hemorrhage in AMD patients. Systemic comorbidities appear to contribute more significantly to hemorrhagic risk.

Back to TOC

Targeting Toll-Like Receptor 4 in a Mouse Model of Advanced AMD

Shmuel Kagasov (1,2), Yael Nisgav (1), Gil Ben-David (1,2), Tali Guetta (2,3), Edith Hochhauser (2,3), Alon Zahavi (1,2), Rita Ehrlich (2,4), Dahlia Palevski (1,2)

(1) Department of Ophthalmology and Eye Research Laboratory, Felsenstein Medical Research Center, Rabin Medical Center, Petah Tikva, Israel.
(2) Gray Faculty of Medical and Health Sciences, Tel Aviv University, Tel Aviv, Israel.
(3) Laboratory of Cardiac Research, Felsenstein Medical Research Center, Beilinson Hospital, Petah Tikva, Israel.
(4) Department of Ophthalmology, Wolfson Medical Center, Holon, Israel.

ABSTRACT

PURPOSE

To investigate the role of Toll-like receptor 4 (TLR4) in the pathogenesis of age-related macular degeneration (AMD) in a mouse model.

METHODS

An induced retinal degeneration model using intravenous sodium iodate (SI) injection was established. Mice with germline TLR4 knockout (KO) and wild-type (WT) controls underwent SI injection, leading to diffuse retinal pigment epithelium (RPE) cell damage. Fundus autofluorescence was performed on days 3, 7 and 21 post-injury. RPE and photoreceptor cell death was determined histologically using confocal microscopy. We assessed the inflammatory response through a combination of histological and molecular analyses, including detection of leukocyte and microglia recruitment, and inflammatory gene expression using real-time PCR.

RESULTS

SI injection caused widespread RPE damage, with hyper- and hypo-autofluorescent patches by day 2 that progressed to atrophy by day 21. Histological analysis showed RPE disorganization, migration and outer nuclear layer (ONL) thinning following injury. In WT mice, inflammatory mediators (IL-1β, IL-6, NFκB, NLRP3, ICAM1) rose >2-fold, while KO mice showed control-like levels after injection. Caspase-1, an apoptosis marker, remained markedly higher in WTs compared to TLR4-KO at day 7. TLR4-KO mice with SI demonstrated an increased, although insignificant, preservation of RPE compared to WTs ($p=0.42$) 7 days post-injury. Moreover, TLR4-KO mice exhibited increased numbers of microglia, with a significantly higher number of both active ($p=0.030$) and non-active ($p<0.001$) inflammatory cells compared to WTs after SI injection.

CONCLUSIONS

TLR4 plays a role in mediating the immune response following RPE damage in a mouse model of retinSSal degeneration. Modulating its activity could lead to novel insights and identify potential therapeutic targets in retinal degenerative diseases, such as AMD.

Back to TOC

Epidemiological Characterization of Intermediate uveitis: A Systematic review and Meta analysis

Tom Liba[1], Dr. Lily Masalha[2], Dr. Ron Eremenko[3], Alon Gorenshtein[1,2], Liron Leibovitch[1], Dr. Raz Gepstein [4]

[1] Azrieli Faculty of Medicine, Bar-Ilan University, Safed, Israel.

[2] Rambam Health Care Campus, Haifa, Israel.

[3] Ophthalmology department, Wolfson medical center.

[4] Department of Ophthalmology, Meir Medical Center, Kfar Sava and the Sackler School of Medicine, Tel Aviv University

Background:

To synthesize global evidence on the causes of intermediate uveitis (IU) and how they vary by region. We aimed to pool proportions of idiopathic IU and key infectious (tuberculosis, syphilis, toxoplasmosis) and non-infectious causes (sarcoidosis, multiple sclerosis) and compare regional patterns to guide diagnosis and management.

Methods:

Following the PRISMA guidelines, we searched PubMed/MEDLINE, Scopus, CENTRAL, and Web of Science (January 1, 2005–January 1, 2025). Data extraction focused on study characteristics, sample size, uveitis location, and reported causes. Random-effects models were used to pool proportions across studies, heterogeneity assessed by the I^2 statistic. Methodological quality was evaluated via the Newcastle–Ottawa Scale for cohort studies and the JBI Critical Appraisal Checklist for cross-sectional studies.

Results:

A total of 36 studies met the inclusion criteria. Idiopathic IU was the most frequently reported subtype, accounting for 68.96% (95% CI: 61.06%–76.02%) of cases. Among infectious causes, tuberculosis (TB) was the most prevalent, particularly in South Asia, with a pooled prevalence of 16.22% (95% CI: 10.10%–20.85%, $I^2 = 93.9\%$). Syphilis-related IU was reported in 2.22% (95% CI: 1.08%–5.60%) of cases, while toxoplasmosis-related IU was observed in 2.2% (95% CI: 1.44%–3.79%, $I^2 = 0\%$). Among non-infectious etiologies, sarcoidosis was most commonly reported in Europe and South America (6.92%, 95% CI: 5.67%–11.12%), while multiple sclerosis (MS)-related IU was more frequent in North America and Europe (3.37%, 95% CI: 2.26%–6.89%).

Conclusions:

This meta-analysis provides an updated epidemiological perspective on intermediate uveitis (IU), emphasizing the predominance of idiopathic cases and the substantial geographic variability in etiology. Tuberculosis-related IU is most prevalent in South Asia, whereas multiple sclerosis-associated IU is more commonly observed in North America and Europe, highlighting the need for region-specific diagnostic and management strategies.

Table 2. Meta-analysis of Differences in Intermediate Uveitis Prevalence Across Various Conditions

Condition	No. of studies	Sample size	Prevalence	Proportion (95% CI)	p-value	Heterogeneity (I^2%)
Infection						
TB	21	2,702	438 (16.22%)	0.1548 [0.1010; 0.2085]	< 0.0001	93.90%
Syphilis	8	1,220	27 (2.22%)	0.0248 [0.0108; 0.0560]	< 0.0001	79.50%
Toxocariasis	2	375	43 (11.47%)	0.0654 [0.0050; 0.4957]	< 0.0001	94.90%
Non-infection						
Sarcoidosis	25	2,995	207 (6.92%)	0.0798 [0.0567; 0.1112]	< 0.0001	77.90%
Multiple_sclerosis	12	1,605	54 (3.37%)	0.0398 [0.0226; 0.0689]	< 0.0001	75.50%
Behçet's disease	12	1,321	22 (1.67%)	0.0307 [0.0161; 0.0578]	0.0092	55.90%
pars_planitis	7	1,109	303 (27.33%)	0.4704 [0.1577; 0.8082]	< 0.0001	98.20%
Lymphoma	3	198	7 (3.54%)	0.0573 [0.0051; 0.4181]	0.0003	87.50%
Spondyloarthropathy	3	224	6 (2.68%)	0.0474 [0.0076; 0.2451]	0.0215	73.90%
VKH	3	332	3 (0.91%)	0.0153 [0.0026; 0.0847]	0.0913	58.20%
Idiopathic	34	3,205	2210 (68.96%)	0.6903 [0.6106; 0.7602]	< 0.0001	92.00%

Back to TOC

Fig.4 TB

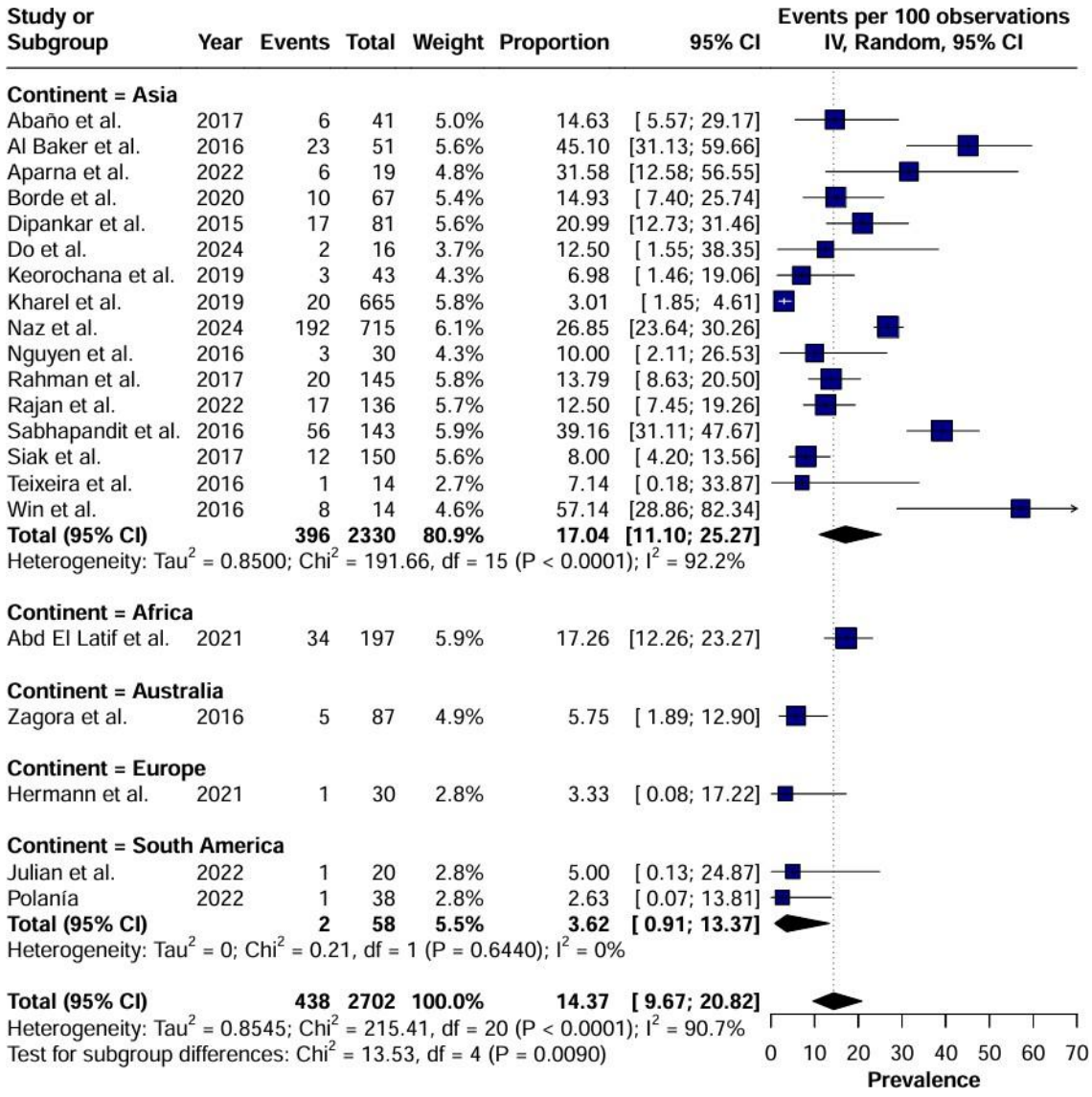
Study or Subgroup
Year
Events
Total
Weight
Proportion
95% CI
Events per 100 observations
IV, Random, 95% CI
Continent = Asia
Abaño et al. 2017 6 41 5.0% 14.63 [5.57; 29.17]
Al Baker et al. 2016 23 51 5.6% 45.10 [31.13; 59.66]
Aparna et al. 2022 6 19 4.8% 31.58 [12.58; 56.55]
Borde et al. 2020 10 67 5.4% 14.93 [7.40; 25.74]
Dipankar et al. 2015 17 81 5.6% 20.99 [12.73; 31.46]
Do et al. 2024 2 16 3.7% 12.50 [1.55; 38.35]
Keorochana et al. 2019 3 43 4.3% 6.98 [1.46; 19.06]
Kharel et al. 2019 20 665 5.8% 3.01 [1.85; 4.61]
Naz et al. 2024 192 715 6.1% 26.85 [23.64; 30.26]
Nguyen et al. 2016 3 30 4.3% 10.00 [2.11; 26.53]
Rahman et al. 2017 20 145 5.8% 13.79 [8.63; 20.50]
Rajan et al. 2022 17 136 5.7% 12.50 [7.45; 19.26]
Sabhapandit et al. 2016 56 143 5.9% 39.16 [31.11; 47.67]
Siak et al. 2017 12 150 5.6% 8.00 [4.20; 13.56]
Teixeira et al. 2016 1 14 2.7% 7.14 [0.18; 33.87]
Win et al. 2016 8 14 4.6% 57.14 [28.86; 82.34]
Total (95% CI) 396 2330 80.9% 17.04 [11.10; 25.27]
Heterogeneity: Tau² = 0.8500; Chi² = 191.66, df = 15 (P < 0.0001); I² = 92.2%
Continent = Africa
Abd El Latif et al. 2021 34 197 5.9% 17.26 [12.26; 23.27]
Continent = Australia
Zagora et al. 2016 5 87 4.9% 5.75 [1.89; 12.90]
Continent = Europe
Hermann et al. 2021 1 30 2.8% 3.33 [0.08; 17.22]
Continent = South America
Julian et al. 2022 1 20 2.8% 5.00 [0.13; 24.87]
Polanía 2022 1 38 2.8% 2.63 [0.07; 13.81]
Total (95% CI) 2 58 5.5% 3.62 [0.91; 13.37]
Heterogeneity: Tau² = 0; Chi² = 0.21, df = 1 (P = 0.6440); I² = 0%
Total (95% CI) 438 2702 100.0% 14.37 [9.67; 20.82]
Heterogeneity: Tau² = 0.8545; Chi² = 215.41, df = 20 (P < 0.0001); I² = 90.7%
Test for subgroup differences: Chi² = 13.53, df = 4 (P = 0.0090)
0 10 20 30 40 50 60 70
Prevalence

Abstract title: Mitochondria transplantation protects RGCs from diabetic retinopathy

Authors: Ziv Rotfogel [1,2], Keren Ben-Yaakov [1], Arie L Marcovich [1,2], Avital Eisenberg-Lerner [1]

Institutes:

[1] Ophthalmology Research Laboratory, Department of Ophthalmology, Kaplan Medical Center, Rehovot, Israel

[2] Faculty of Medicine, Hadassah Medical School, The Hebrew University of Jerusalem, Israel

Purpose: Retinal ganglion cells (RGCs) are highly energy-dependent neurons, relying on mitochondrial ATP production to sustain their function and survival. In diabetic retinopathy, oxidative stress and elevated glucose-derived metabolites damage mitochondrial function, disrupting the electron transport chain and decreasing ATP generation. Dysfunctional mitochondria in RGCs trigger pro-apoptotic signaling pathways, leading to cell death and contributing to the neurodegenerative component of DR. Additionally, mitochondrial impairment can promote pathological VEGF secretion, further driving retinal vascular abnormalities. Targeting mitochondrial health in RGCs may therefore represent a promising approach to prevent both neurodegeneration and vascular pathology in DR. We tested mitochondrial transplantation as a therapeutic approach to protect DR-associated retinal damage.

Methods: C57BL/6 mice were rendered diabetic using streptozotocin (STZ) and subsequently received intravitreal injections of isolated mitochondria. Retinal thickness were monitored over time using optical coherence tomography (OCT) and histology to assess the effects of mitochondrial transplantation on retinal integrity.

Results: STZ-induced diabetes led to significant retinal thinning, accompanied by marked loss of retinal ganglion cells, consistent with neurodegeneration observed in diabetic retinopathy. Notably, intravitreal transplantation of healthy mitochondria effectively prevented these structural changes, preserving overall retinal thickness and RGC density.

Conclusion: These findings indicate that mitochondrial transplantation can protect retinal cells from diabetes-induced damage, highlighting mitochondrial transplantation as a potential neuroprotective strategy in DR.

Back to TOC

Optimizing hiPSCs Sources for Retinal Organoids and Retinal Implant Integration

Diana Merezhko (1,2), Shelly Yakubovich (1,2), Ohad Cohen (1), Ran Ben Cnaan (1,2), Igal Leibovitch (1,2), Olivier Goureau (3), Adiel Barak (1,2), Maxim Bez (1,2)

(1) Ophthalmology Department, Tel Aviv Sourasky Medical Center, Tel-Aviv
(2) Gray Faculty of Medical and Health Sciences, Tel-Aviv University, Tel-Aviv
(3) Institute De La Vision, Sorbonne University, Paris

Purpose

Age-related macular degeneration (AMD) is a degenerative disease of the macula and the leading cause of visual disability in older adults worldwide. In the atrophic form, geographic atrophy (GA), a progressive loss of photoreceptors (PR), retinal pigment epithelium (RPE), and choriocapillaris leads to vision decline with no available curative therapy. Many current cell replacement studies rely on human induced pluripotent stem cells (hiPSCs) as a promising autologous source for retinal cell replacement. Although fibroblasts and peripheral blood cells are commonly used for hiPSC generation, orbital adipose-derived stem cells (OASCs) provide a minimally invasive, autologous alternative that potentially retains epigenetic memory of its developmental origin, making them highly relevant for retinal regeneration. A recent study in our laboratory demonstrated the feasibility of assembling a three-layer retinal implant using immortalized cell lines. Building on this framework, this study aims to determine if the specific anatomical depot of OASCs influences reprogramming efficiency and subsequent differentiation into autologous human RPE and PR cells derived from OASC-derived hiPSCs for future integration into bio-fabricated retinal implants.

Methods

Nasal and central orbital fats were surgically obtained from healthy donors. OASCs were isolated, validated by flow cytometry for mesenchymal stem cell (MSCs) markers, and assessed for multipotency through adipogenic and osteogenic differentiation, evaluated by lipid and calcium deposition staining and quantitative optical density analysis. Neurogenic differentiation was induced in both groups and analyzed by RT-PCR for neurogenic marker expression. To evaluate the impact of somatic cell origin, reprogrammed OASC-derived hiPSCs, alongside ectoderm-derived hiPSCs (controls), were differentiated toward retinal lineages using a defined 3D organoid protocol. Self-forming retinal vesicles were manually isolated at week 4 to generate retinal organoids, while RPE monolayers were obtained from the adherent culture. Developing organoids were analyzed at multiple time points using immunofluorescence for lineage-specific markers.

Results

Our results confirmed that while both orbital fat-derived cells expressed MSC markers, distinct functional dichotomies emerged between nasal and central derived cells. Nasal-derived OASCs, consistent with their presumed neural crest origin, demonstrated significantly stronger adipogenic and neurogenic differentiation capacities, whereas central-derived OASCs showed a qualitative trend toward enhanced osteogenic potential. Ectoderm-derived hiPSCs reliably generated self-forming retinal vesicles, and immunostaining of early organoids confirmed the emergence of retinal ganglion cells and retinal progenitors. Crucially, nasal OASC-derived hiPSCs exhibited superior propensity for neuro-retinal induction compared to central depot counterparts. Initial RPE regions developed characteristic pigmentation and morphology.

Conclusions

Nasal and central orbital fat provide distinct OASC populations with differing differentiation capacities driven by their embryonic lineage. Nasal OASCs can be efficiently reprogrammed into hiPSCs and preferentially directed toward retinal fates, supporting their superior potential as an autologous cell source for retinal repair. These findings suggest that OASC-derived hiPSCs can generate functional retinal progenitors, forming the basis for personalized retinal implants for treating advanced AMD.

Back to TOC

Early detection of retinal Beta-Amyloid accumulation in 5XFAD Alzheimer mice using Immunohistochemistry and Advanced Imaging.

Maha Othman Afifi (1), Talal Salti (1), Irit Mann (1), Basel Obied (1), Nitza Goldenberg-Cohen (1,2)

1. Krieger Eye Research Laboratory, Rappaport Faculty of Medicine, Technion – Israel Institute of Technology, Haifa.
2. Ophthalmology Department, Bnai Zion Medical Center, Haifa

Purpose: Beta-amyloid (Aβ) accumulation is a key biomarker of Alzheimer's disease (AD), traditionally characterized by its progressive deposition in the brain. Recent evidence suggests that Aβ aggregates may appear earlier in the retina, offering a potential window for early diagnosis. This study aimed to detect and characterize retinal Aβ accumulation in 5XFAD transgenic mice across a broad age range.

Methods: 5XFAD transgenic mice aged 3–24 months were evaluated. Retinas and brains were harvested and processed using classical immunohistochemistry (IHC) and advanced three-dimensional imaging. Retinas were flat-mounted and stained with anti-Aβ antibodies, followed by fluorescence microscopy for visualization and comparative quantification.

Results: Retinal Aβ accumulation was clearly detectable as early as 3 months of age using slide-based IHC. Fluorescent staining of flat-mounted retinas confirmed the presence of Aβ deposits, with a progressive increase observed in older mice. In parallel, age-associated Aβ deposition was evident in brain regions classically implicated in AD pathology, including the hippocampus and amygdala.

Conclusions: These findings demonstrate that Aβ accumulation in the retina precedes its deposition in the brain in 5XFAD mice. Flat-mounted retinal immunohistochemistry provides a robust and accessible method for detecting early retinal Aβ pathology. This supports the emerging concept that retinal imaging may serve as a non-invasive biomarker for early detection of Alzheimer's disease.

Back to TOC

Sex-based differences in subretinal and intraretinal fluid Absorption dynamics in age-related macular degeneration: a longitudinal real-world study.

Michal Kaminer Abargel (1,2), Shlomit Jaskoll (1,2), Adi Kramer (2), Liran Tiosano (2), Jaime Levi (2), Sandro De Zanet (3), Stefanos Apostolopoulos (3), Carlos Ciller (3), Itay Chowers (2)

(1) Department of Military Medicine and "Tzameret", Faculty of Medicine, Hebrew University of Jerusalem, Jerusalem, Israel, and Medical Corps, Israel Defense Forces, Israel
(2) Department of Ophthalmology, Hadassah-Hebrew University Medical Center, and the Faculty of Medicine, The Hebrew University of Jerusalem, Jerusalem, Israel
(3) RetinAI Medical AG, Freiburgstrasse 3, CH-3010, Bern, Switzerland.

ABSTRACT

PURPOSE

To evaluate sex-based differences in subretinal fluid (SRF) and intraretinal fluid (IRF) absorption in age-related macular degeneration (AMD) patients using long-term real-world OCT data.

METHODS

This retrospective cohort included OCT images from 1,209 AMD patients (2,400 eyes) obtained between 2009–2024. Absorption was defined as follow-up fluid volume minus baseline (nL/month). For each month, mean absorption was computed, and period-specific absorption (0–24, 24–48, 0–48 months) was obtained by averaging monthly values to yield mean ± SD. Cumulative absorption was quantified using trapezoidal area-under-the-curve (AUC, nL x month). Scans with intra-visit segmentation variability >0.1 SD were excluded. Mixed-effects models included, baseline fluid volume, age, and follow-up duration, with a random intercept for inter-eye correlation.

RESULTS

Mean age was 75.7 ± 9.5 years; 59.7% were female. Baseline SRF and IRF volumes were comparable between sexes. From 0–24 months, females showed slightly greater SRF absorption (−91.15 ± 30.55 vs −89.19 ± 32.31nL/month; AUC 2245.45 vs 2198.74 nL x month; $p < 0.001$). From 24–48 months, males demonstrated stronger SRF absorption (−93.04 ± 21.41 vs−52.29 ± 35.36 nL/month; AUC 2244.13 vs 1275.68 nL x month; $p < 0.001$), resulting in higher 0–48 SRF absorption (−91.74 ± 27.10 vs −71.84 ± 38.52 nL/month; AUC 4442.87 vs 3521.14 nL x month. Across the full cohort, IRF remained mostly below baseline, indicating net reduction, with males showing slightly greater long-term absorption (−43.5 ± 27.1 vs −30.3 ± 32.0 nL/month) and higher cumulative IRF AUC (2178.38 vs 1811.03 nL x month).In the 0–48-month SRF mixed-effects model, the time-by-sex interaction was significant (β= 1.152 nL/month; 95% CI 0.073–2.232; $p = 0.036$), indicating divergent long term trajectories. baseline fluid volume was strongly associated with both SRF and IRF absorption in all models ($p < 0.001$)

CONCLUSIONS

Females exhibited faster early SRF absorption, whereas males showed more sustained long-term reduction, confirmed by AUC and mixed-effects modeling. IRF behavior was more variable and treatment-dependent, with injected females showing periods above baseline. Sex may represent a relevant biological factor in OCT-based fluid interpretation and could help guide more individualized monitoring strategies in AMD, although these findings should be interpreted cautiously and require validation in further studies.

Back to TOC

The risk of retinal vein occlusion among patients with neovascular age related macular degeneration: a large-scale cohort study

Orly Weinstein # 1 2, Mouhammad Kridin # 3, Khalaf Kridin 4, Oran Mann 1, Arnon D Cohen 1 2, Ofira Zloto 5 6

1 Clalit Health Services, Tel-Aviv, Israel.

2 Faculty of Health Sciences, Ben-Gurion University of the Negev, Ben-Gurion Ave, Beer Sheva, Israel.

3 Sackler Faculty of Medicine, Tel-Aviv University, Tel-Aviv, Israel.

4 Lübeck Institute of Experimental Dermatology, University of Lübeck, Lübeck, Germany.

5 Sackler Faculty of Medicine, Tel-Aviv University, Tel-Aviv, Israel.

6 Goldschleger Eye Institute, Sheba Medical Center, Tel-Hashomer, Israel.

#Contributed equally.

Abstract

PURPOSE

To examine the risk for retinal-vein-occlusion (RVO) in patients with neovascular age-related-macular-degeneration (AMD) as compared to age- and sex-matched controls.

METHOD

This is a population-based, cohort study. The study encompassed 24,578 consecutive patients with neovascular AMD and 66,129 control subjects. Multivariate cox regression analysis was utilized to detect the risk of RVO among patients with neovascular AMD. Predictors of RVO in patients with neovascular AMD were identified using multivariate logistic regression analysis. Mortality of patients was assessed using Kaplan-Meier method.

RESULTS

The incidence rate of RVO was estimated at 1.25 (95% CI, 1.06-1.45) per 1000 person-years among patients with neovascular AMD and 0.25 (95% CI, 0.20-0.31) per 1000 person-years among controls. Patients with neovascular AMD were associated with an increased risk of RVO (adjusted HR, 4.35; 95% CI, 3.34-5.66; P < 0.001). Among patients with neovascular AMD, older age (≥79.0 years) was associated with a decreased risk of RVO (adjusted OR, 0.50; 95% CI, 0.37-0.70; P < 0.001), whilst a history of glaucoma increased the likelihood of RVO (adjusted OR, 2.66; 95% CI, 1.94-3.65; P < 0.001). Patients with neovascular AMD and comorbid RVO had a comparable risk of all-cause mortality relative to other patients with neovascular AMD (HR, 0.90; 95% CI, 0.67-1.22; P = 0.500).

CONCLUSION

An increased risk of RVO was found among patients with neovascular AMD. Younger age and glaucoma predicted the development of RVO in patients with neovascular AMD. Awareness of this comorbidity is of benefit for clinicians as patients with neovascular AMD might be carefully examined for RVO signs and complications.

Back to TOC

From Risk to Progression: Genetic Insights into Atrophy Progression in AMD

Shlomit Jaskoll (1,2), Adi Kramer (1), Liran Tiosano (1), Jaime Levi (1), Sandro De Zanet (3), Stefanos Apostolopoulos (3), Carlos Ciller (3), Itay Chowers(1)

(1) Department of Ophthalmology, Hadassah-Hebrew University Medical Center, and the Faculty of Medicine, The Hebrew University of Jerusalem, Jerusalem, Israel

(2) Department of Military Medicine and "Tzameret", Faculty of Medicine, Hebrew University of Jerusalem, Jerusalem, Israel.

(3) RetinAI Medical AG, Freiburgstrasse 3, CH-3010, Bern, Switzerland

Purpose: Age-related macular degeneration (AMD) is the leading cause of irreversible visual loss in older adults. Although genome-wide association studies (GWAS) have identified multiple susceptibility loci, their impact on macular atrophy (MA) progression remains unclear. We examined whether AMD-associated genetic variants modulate progression rates in macular atrophy.

Methods: We analyzed 632 patients (1,131 eyes) with MA by optical coherence tomography (OCT). Deep learning segmentation (1) quantified photoreceptor (PR) and retinal pigment epithelium (RPE) atrophy. Linear mixed-effects models tested 113 variants as the primary fixed effect of interest.

Results: Mean age was 87.4 ± 9.2 years, and 59.7% were female. Variants in RDH5/CD63 (β = –0.03 mm/year, CI –0.05 to –0.005, p=0.01) and TGFBR1 (β = –0.02 mm/year, CI –0.05 to –0.002, p=0.03) loci were associated with slower PR atrophy, with similar RPE trends. In contrast, variants in CETP, PLA2G12A, COL10A1, ARHGAP21, and VARS loci, involved in lipid metabolism, collagen regulation, visual cycle, and protein synthesis, were linked to faster RPE atrophy (β: 0.04–0.09 mm/year; p: 0.001–0.02). A known association at ARMS2, one of the strongest risk alleles for AMD onset, was replicated (β = 0.04 mm/year, CI 0.02–0.06, p=0.001). Other variants were not significant, supporting distinct genetic architecture for atrophy versus disease onset.

Conclusions: This large-scale genotype-phenotype analysis reveals that certain AMD loci are associated with atrophy progression beyond initial disease susceptibility.
Identifying these progression-associated variants provides a genetic framework for patient stratification and therapeutic targeting, bridging molecular risk to clinical trajectory in AMD.

(1) RetinAI Discovery; Ikerian AG, Bern, Switzerland

Back to TOC

Skin Carotenoid Levels in Israeli Patients With Age-Related Macular Degeneration

Tzippora Greenberg [1] Itay Chowers [2]

[1] The Faculty of Medicine, Department of Ophthalmology, Hadassah-Hebrew University Medical Center, The Hebrew University of Jerusalem, Jerusalem, Israel.

[2] Ophthalmology Department, Faculty of Medicine, Hadassah Medical Center, Hebrew University, POB 12000, Jerusalem, 91120, Israel

Purpose:

Carotenoids such as lutein and zeaxanthin support retinal health through antioxidant and blue-light filtering effects and are concentrated in the macula. Skin carotenoid levels can be measured using the Veggie Meter, a device that assesses carotenoids in the skin through reflection spectroscopy. These measurements correlate strongly with serum carotenoid levels and provide a simple, noninvasive marker of carotenoid levels. This pilot study aims to characterize skin carotenoid levels in Israeli AMD patients and to evaluate whether demographic or health factors are associated with carotenoid status.

Methods:

Twenty-eight AMD patients (mean age 79.96 ± 10.1 years, 64 percent female) from Hadassah underwent skin carotenoid assessment using the Veggie Meter, which uses pressure-mediated reflection spectroscopy through a fingertip scan with no radiation exposure. The device reports scores on a 0-800 scale. Three consecutive measurements were obtained and averaged for each participant. The device was calibrated hourly, and room temperature and humidity were recorded to ensure measurement stability. Participants completed a brief questionnaire covering age, sex, height, weight, smoking status, chronic diseases, and supplement use. Veggie Meter scores were compared with published population data from Japan and the United States using Welch's t-test.

Results:

Veggie Meter scores in the AMD cohort showed substantial variation among patients (mean 338.4 ± 84.8, range 107-508). To contextualize these values, scores were compared with published cohorts. Relative to a Japanese cohort, using the subset of 660 adults aged 55 and older to match our age range, Israeli AMD patients had significantly lower skin carotenoid levels (Japanese mean 417.05 ± 144, $p < 0.0001$). In contrast, compared with a U.S. cohort of 54 adults over age 60 from the Washington DC area, Israeli AMD patients had significantly higher Veggie Meter scores (U.S. mean 275.6 ± 98.88, $p = 0.0039$).

Conclusions:

This pilot study provides the first characterization of skin carotenoid levels in Israeli AMD patients. Given the established associations between skin carotenoids, serum carotenoid concentrations, and macular pigment density, these findings support the potential utility of the Veggie Meter as a practical, noninvasive biomarker of nutritional status relevant to retinal health and AMD risk.

Back to TOC